

Title	ポリオール類の化学品への選択酸化反応のための不均一系触媒としての白金ナノ粒子のグリーン調製法の開発に関する研究
Author(s)	Tongsakul, Duangta Miss
Citation	
Issue Date	2014-09
Type	Thesis or Dissertation
Text version	ETD
URL	http://hdl.handle.net/10119/12310
Rights	
Description	Supervisor:海老谷 幸喜, マテリアルサイエンス研究科, 博士

**Studies on the Development of Platinum-Based
Nanoparticles by a Green Synthetic Method as
Heterogeneous Catalyst for Selective Oxidation of
Polyols into Value-Added Chemicals**

DUANGTA TONGSAKUL

Japan Advanced Institute of Science and Technology

Studies on the Development of Platinum-Based
Nanoparticles by a Green Synthetic Method as
Heterogeneous Catalyst for Selective Oxidation of
Polyols into Value-Added Chemicals

by

DUANGTA TONGSAKUL

Submitted to

Japan Advanced Institute of Science and Technology

In partial fulfillment of requirements

For the degree of

Doctor of Philosophy

Supervisor: **Professor Dr. Kohki Ebitani**

School of Materials Science

Japan Advanced Institute of Science and Technology

September 2014

Referee-in-chief : **Professor Dr. Kohki Ebitani**
Japan Advanced Institute of Science and Technology

Referees : **Professor Dr. Minoru Terano**
Japan Advanced Institute of Science and Technology

Professor Dr. Noriyoshi Matsumi
Japan Advanced Institute of Science and Technology

Associate Professor Dr. Kazuaki Matsumura
Japan Advanced Institute of Science and Technology

Associate Professor Dr. Tetsuya Shishido
Kyoto University

ACKNOWLEDGEMENTS

First of all, I wish to express my deep and sincere gratitude to my supervisor Professor Dr. Kohki Ebitani for very kind assistance, generous guidance, and encouragement throughout the course of this research.

Secondly, I would like to express my appreciation to Assistant Prof. Dr. Shun Nishimura and Professor Dr. Shinya Maenosono, who provided me a lot of valuable support. I also wish to express gratitude to my committee: Professor Dr. Minoru Terano, Professor Dr. Noriyoshi Matsumi, Professor Dr. Tetsuya Shishido and Associate Professor Dr. Kazuaki Matsumura for all their valuable discussion and suggestion.

I am profoundly grateful to Professor Dr. Masayuki Yamaguchi for provided me a lot of valuable support throughout my sub-theme research. Further, I would like to show my best gratitude to my supervisor at Chulalongkorn University, Associate Professor Dr. Sanong Ekgasit for his help and valuable advice during my completion sub-theme research. Appreciation is also extended to my co-supervisors, Associate Professor Chuchaat Thammacharoen for their kind suggestion and discussion in this work.

Acknowledgements

I would like to thanks all present and former members in Ebitani Laboratory for their friendly assistance. Finally, I would like to express my special gratitude to my parents, family members for their inspiration, understanding, great support and encouragement throughout the entire my course of study.

Duangta Tongsakul

September 2014

CONTENTS

CHAPTER 1. GENERAL INTRODUCTION

1. Background	
1.1 The world economic growth and the energy crisis.....	1
1.2 The alternative energy and chemical production based on renewable resources.....	2
1.3 Biofuel and glycerol production.....	4
1.4 Transformation of glycerol and glycerol-derived product to value- added chemicals.....	6
1.5 Green chemistry and sustainability.....	9
1.6 Nanotechnology.....	11
1.6.1 Definition of nanotechnology.....	11
1.6.2 Nanocatalysts.....	14
1.7 Oxidation reaction of alcohol.....	18
1.7.1 Selective oxidation of glycerol and 1,2-propanediol.....	21
1.7.2 Importance parameter for the catalytic performance of glycerol and 1,2-propanediol oxidation.....	29
1.7.3 Ligand effect on the performance of catalyst.....	32
1.8 Soluble starch.....	35
2. Purposes of this Thesis.....	36
3. Outline of the Thesis.....	36

4. References..... 39

**CHAPTER 2. DEVELOPMENT OF NOVEL STARCH-STABILIZED
SUPPORTED PLATINUM NANOPARTICLES AS
HETEROGENEOUS AND REUSABLE CATALYST FOR
SELECTIVE GLYCEROL OXIDATION**

1. Introduction..... 59

2. Experiment..... 63

 2.1 Chemicals..... 63

 2.2 Preparation of supported-Pt NPs catalysts..... 63

 2.2.1 Impregnation method..... 63

 2.2.2 Immobilization method..... 64

 2.3 Characterization..... 65

 2.4 Catalytic activity for glycerol oxidation..... 66

3. Results and Discussion..... 67

 3.1 Screening of Green synthesis methods and supporting materials..... 67

 3.2 An investigation of the immobilization method for Pt NPs/HT
 catalysts..... 72

 3.2.1 Characterization of Catalysts..... 62

 3.2.2 Oxidation of glycerol over Pt NPs/HT..... 75

 3.2.2.1 Influence of initial concentration of glycerol..... 77

 3.2.2.2 Influence of glycerol/metal ratio..... 78

 3.2.2.3 Influence of oxygen flow rate..... 79

3.2.2.4 Influence of reaction temperature.....	80
3.2.2.5 Reaction time profile under optimum conditions.....	81
3.2.3 Detection of leached Pt NPs in the solution.....	82
3.2.4 Catalyst recycling.....	83
4. Conclusion.....	87
5. References.....	89

CHAPTER 3. PROBING THE EFFECT OF POLYMER

STABILIZED-PLATINUM NANOPARTICLES

1. Introduction.....	
2. Experiment.....	96
2.1 Chemicals.....	99
2.2 Preparation of hydrotalcite supported-Pt NPs catalysts.....	99
2.3 Characterization.....	100
2.4 Catalytic activity for 1,2-propanediol oxidation.....	101
3. Results and discussion.....	102
3.1 Preparation of HT supported–Pt NPs with same diameter using three polymers	103
3.2 Oxidation of 1,2-propanediol.....	103
3.3 Electronic structure of Pt–polymer NPs	105
3.4 Water wettability of the Pt-polymer/HT	107
4. Discussion.....	110
4.1 Effect of polymer on the Pt–polymer/HT and their catalytic activity	111

4.2 Proposal mechanism for aerobic oxidation of PG over Pt–polymer/HT in aqueous solution.....	111
5. Conclusion.....	115
6. References.....	117
	118
CHAPTER 4. EVOLUTION OF STARCH STABILIZED SUPPORTED PLATINUM-BASED BIMETALLIC CATALYSTS FOR SELECTIVE AND AQUEOUS POLYOLS OXIDATION USING MOLECULAR OXYGEN	
1. Introduction.....	126
2. Experiment.....	129
2.1 Chemicals.....	129
2.2 Preparation of hydrotalcite supported Pt-based bimetallic catalysts.....	130
2.2.1 Fast co-reduction method (FCR).....	130
2.2.2 Slow co-reduction method (SCR).....	132
2.3 Catalytic activity for polyols oxidation.....	133
2.4 Characterization.....	133
3. Results and Discussion.....	134
3.1 Preparation of Pt-based bimetallic heterogeneous catalysts.....	134
3.2 Improvement of the synthetic method for preparation of Pt _x Au _y NPs/HT.....	137
3.2.1 Glycerol and 1,2-propanediol oxidation.....	137
3.2.2 Characterization of catalysts.....	139

3.3 An investigation of the immobilization method for the PtAu NPs/HT catalysts.....	140
3.3.1 Glycerol oxidation.....	140
3.3.2 1,2-Propanediol (PG) oxidation.....	143
3.3.3 Polyols oxidation in the presence of a radical scavenger.....	145
3.3.4 Catalyst recycling.....	146
3.3.5 Characterization of PtAu NPs/HT catalysts.....	148
3.3.6 Oxidation mechanism	155
4. Conclusion.....	157
5. References.....	158
CHAPTER 5. GENERAL CONCLUSION.....	168
ACHIEVEMENTS.....	173
MINOR RESEARCH THEME.....	177

Chapter 1

GENERAL INTRODUCTION

This chapter comprehends recent issues about science and technology including energy and biomass utilization, Green chemistry, nanotechnology and catalytic oxidations of polyols. Purpose and outline of this thesis are also described.

1. Background

1.1 The world economic growth and the energy crisis

The technology progress and the economic growth cause impact not only on the environment but also human and animal. One of the most widely discussed environmental problems which may have a long term effect on economic growth is global warming resulting from the greenhouse effect.^[1] Furthermore, the economic growth goes together with growing energy needs on a global scale, bring about the world energy crisis in the era of society's almost total dependence on fossil resources (oil, gas and coal). Since, the fossil energy is almost consumed in the industrial and transportation (Figure 1), and there are limit and will come to an end during the twenty-first century.^{[2]-[4]} To overcome the progressive depletion of fossil resources,

the alternative energy based on renewable and sustainable resources have been developed.^{[3],[5]}

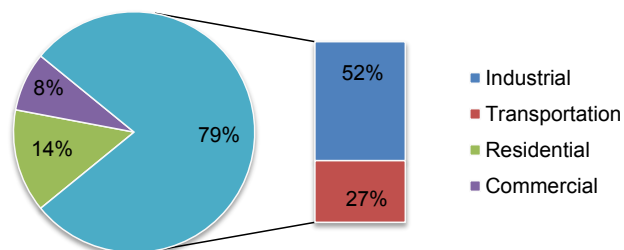


Figure 1 World energy consumption by sector 2012.^[2]

1.2 The alternative energy and chemical production based on renewable resources

For energy use, there are several options of renewable resources (Figure 2) including wind, water, solar and nuclear as well as biomass, however, non-fossil option is only biomass for the organic chemical production (Figure 3).^[4]

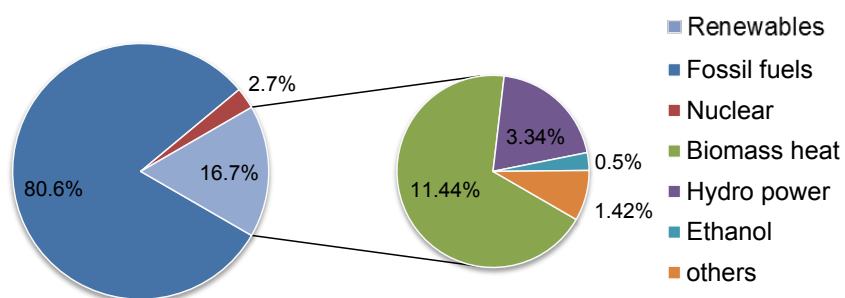


Figure 2 Total world energy consumption by source (2010).^[6]

Biomass is biological material derived from living, or recently living organism which is renewable overtime. The availability of diverse biomass resources, such as agricultural lignocellulosic residues and edible and non-edible crops, has resulted in significant advancements in the conversion of biomass into renewable fuels and chemicals through the implementation of different technologies capable of utilizing specific biomass feedstock constituents (Figure 3).^[7] In addition, the biomasses are sustainable feedstock which low net greenhouse gas emissions despite CO₂ emissions, because the carbon in the biomass is sourced from the atmosphere as CO₂ during plant growth thus the carbon cycle of bioenergy is closed.^{[7],[8]}

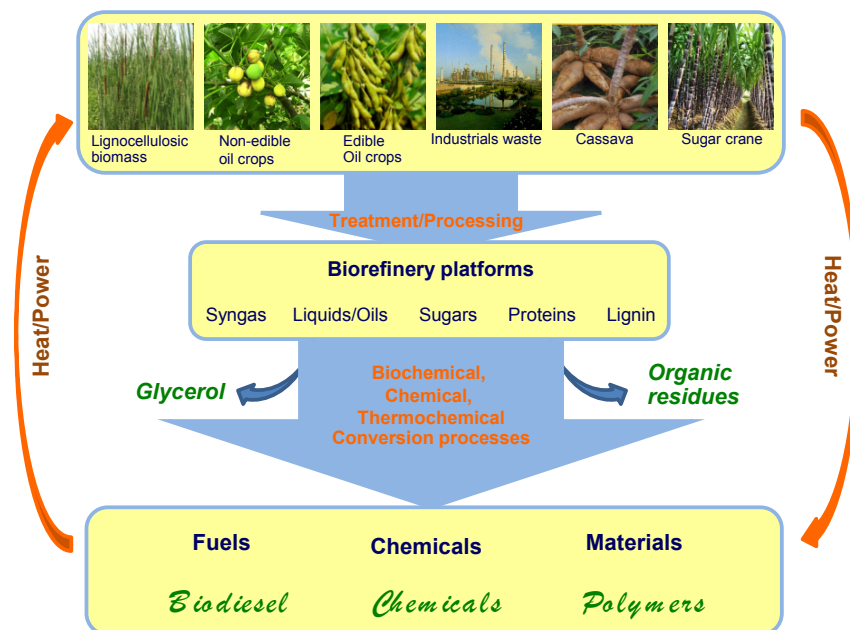
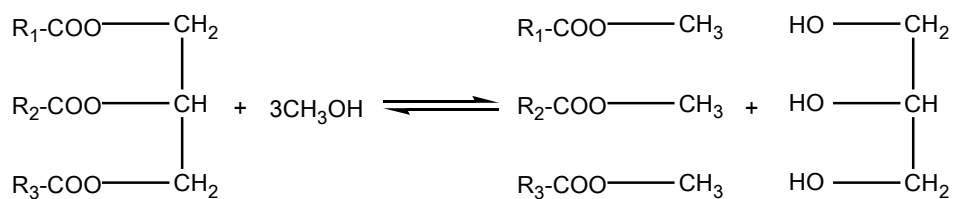


Figure 3 Generalized schematic of material and process integration within a biorefinery.^[7]

1.3 Biofuel and glycerol production

Biofuel is the biomass-derived fuels which have the potential to meet the challenges of sustainable and green energy systems.^[5] Biodiesel is also one of the biofuel which has proved its value as a fuel for diesel engines which current uses in industrial and transportation section.^[9] As mentioned above that almost of the energy is consumed in industrial and transportation. Therefore the past decade, biodiesel has been gaining worldwide popularity and research interest in utilization in vehicle engines and other kinds of internal combustion engines as an alternative energy source to petro-diesel.^[9] Biodiesel is produced from vegetable oils and is therefore non-toxic and biodegradable. In order to convert the raw oils into biodiesel, transesterification technology is used. The oil is reacted with a low molecular weight alcohol (e.g., methanol and ethanol) in the presence of sodium or potassium hydroxide as a base catalyst to form the fatty acid ester and glycerol (GLY) (see Scheme 1).^{[4],[9],[10]} One ton of biodiesel yield produces about 110 kg of crude GLY or about 100 kg of pure GLY. In addition, GLY can be obtained from the saponification and hydrolysis of fats and oils, including to the commercial production by the fermentation of sugars such as glucose and fructose, either directly or as a by-product.^[11] The global estimate of GLY production and price chart of crude GLY for Asia were shown in Figure 4.^{[9],[12]}



Scheme 1. Overall reaction for production of GLY from biodiesel industry.^[9]

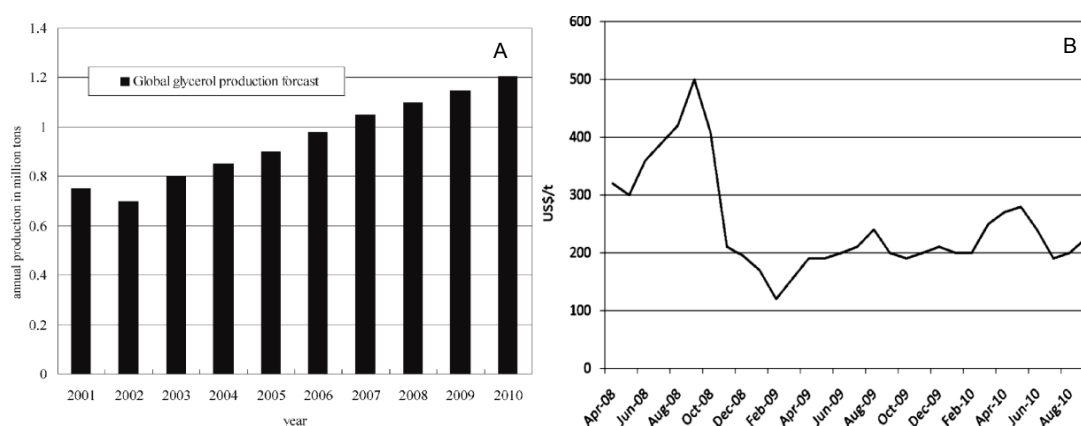


Figure 4 The global projection estimates by Procter & Gamble of GLY production to 2010 (A) and price chart of crude GLY for Asia (B).^{[9],[12]}

As there is an increase in biodiesel production, the GLY from their process has also been produced in large quantities. There are interesting from industrial point of view to investigate the value-added products from the GLY. Since, the alternative of an entirely new downstream process and product chain using renewable raw materials, there will be more focused on that of oxohydrocarbons (particularly carbohydrates) rather than hydrocarbons. Therefore, GLY which possess three hydroxyl groups, is classified as the top sugar-derived potential intermediates on which down-stream chemical process as shown in Figure 5.^{[11],[13]}

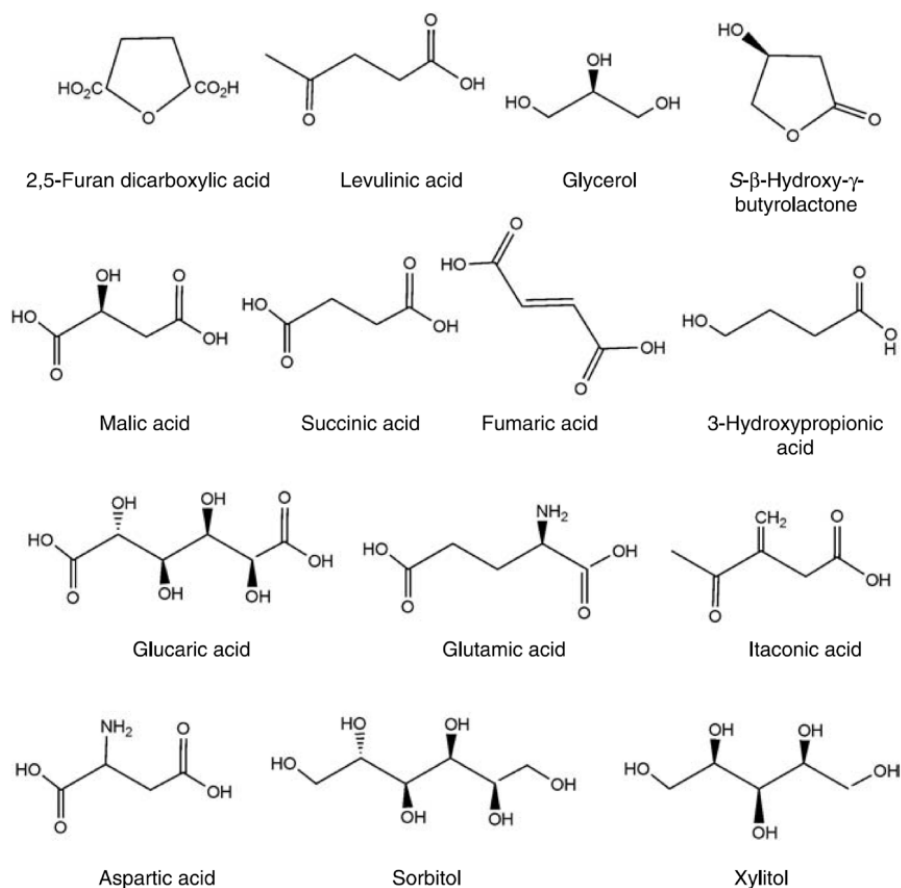


Figure 5 Top sugar-derived potential key intermediate identified by the US National Renewable Energy Laboratory.^{[11],[13]}

1.4 Transformation of glycerol and glycerol-derived product to value-added chemicals

GLY is non-toxic, biosustainable and biodegradable compound, abundant industrial waste and low price (0.23 USD/1 kg) (see also Figure 4). The transformation of GLY with several different reaction pathway can be produced many useful and value-added chemicals as shown in Figure 6. For instance, the oxidation of the primary hydroxyl groups of GLY produces glyceraldehyde, which

can further oxidation produces carboxylic acids, like glyceric acid (GA: 6,720 USD/kg) which is high value compound. The application of GA can be used for treatment of skin disorders, pharmaceuticals, biodegradable fabric softener and an anionic monomer of packaging material for volatile agents.^{[12],[14]-[16]}

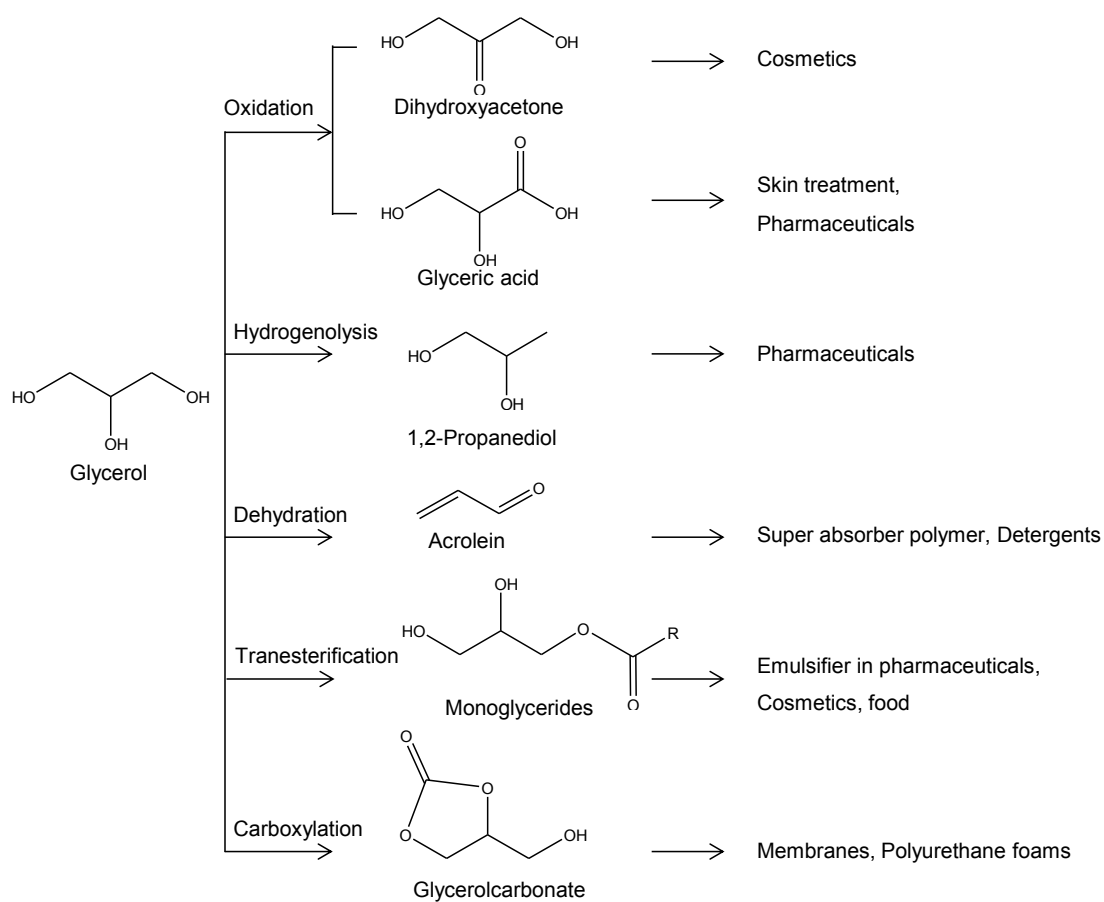


Figure 6 Process of catalytic conversion of GLY into useful chemicals.^[9]

In addition, GLY-derived products can be further serves as a substrate for the manufacture of high-end chemicals. For instance, 1,2-propanediol (PG) which is the product of GLY hydrogenolysis, is a crucial starting material for the chemical synthesis of lactic acid (2-hydroxypropanoic acid) (Figure 7). Lactic acid (LA: 15,000 USD/kg) was used in the industrial field of food, beverage, personal-care and pharmaceutical products.^[13]

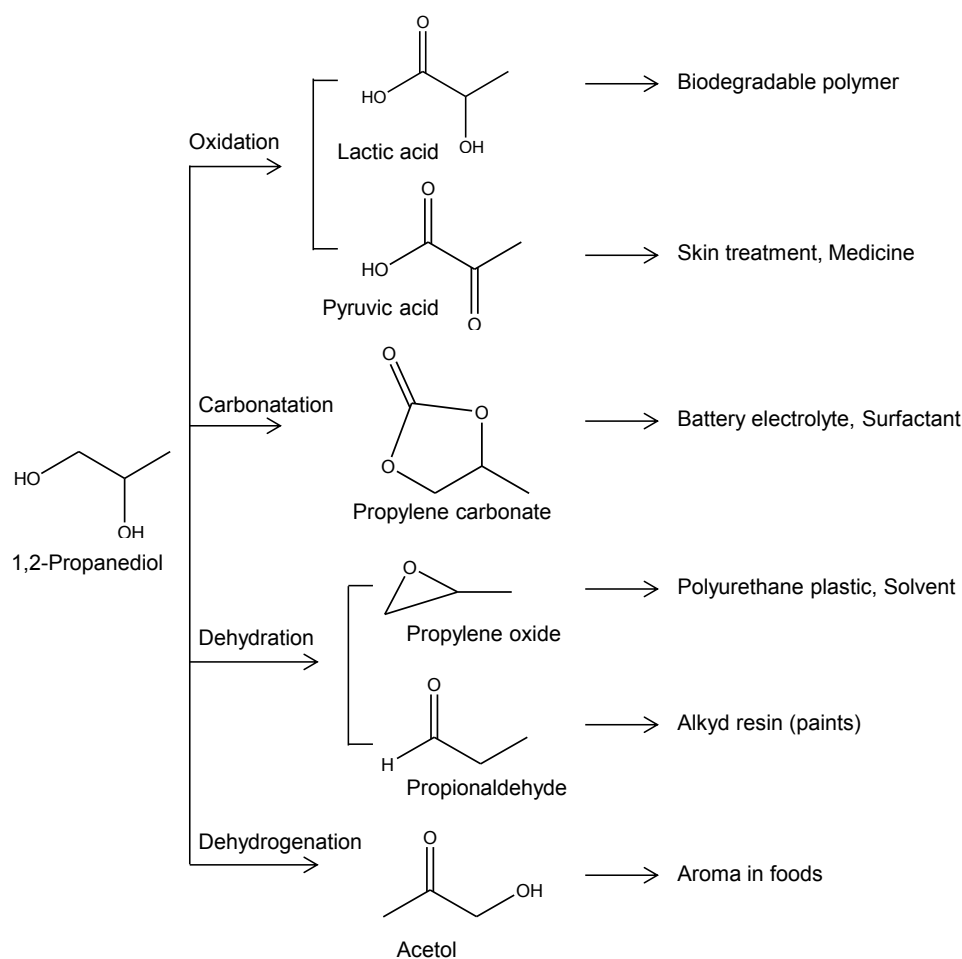


Figure 7 Process of catalytic conversion of PG into useful chemicals.^{[9],[17],[18]}

1.5 Green chemistry and sustainability

Sustainability focuses on the integration of ecological integrity, societal responsibility and economic viability.^[11] The tremendous economic growth leading to the parallel competition of chemicals manufacture. The production under the competitive pricing results in inefficient processes which unacceptable levels of pollution and hazardous operations. Presently, the industry effort to solves the problem using environmentally sustainable and economically viable manufacturing which responds to demanding of economic growth. Sustainable chemical production for the new century can be realized through a reassessment of the entire chemical product life-cycle from resources, to manufacturing and production, through to product use and ultimate fate.^[11] An increasing use of biomass for energy, chemicals and materials supply is one of the key issues of sustainable development because biomass resources are renewable and CO₂ neutral in contrast with fossil fuels. The molecules extracted from biomass resources already contain functional groups so that the synthesis of chemicals generally requires a lower number of steps than from fossil resource.^[19]

Green chemistry is defined as the efficiently utilizes (preferably renewable) raw materials, eliminates waste and avoids the use of toxic and/or hazardous reagents and solvents in the manufacture and application of chemical products.^[11] Anastas and Warner defined the twelve principles for guiding the designation of environmentally benign products and processes. The 12 green chemistry principles are summarized in Table 1.

Table 1 12 Green chemistry principles.^{[20],[21]}

<i>Green chemistry principles</i>	<i>Design to greener nanomaterial and production method</i>
1. Prevent waste	design to prevent waste than to treat or clean up waste after it has been created
2. Atom economy	design to maximize all of the materials use in the synthetic process to final product
3. Less hazardous chemical synthesis	design to a little use or generate the hazardous substance
4. Designing safer chemicals	design the desire product with minimizing their toxicity
5. Safer solvents/reaction media	design to make a necessary use of substances (e.g., solvents)
6. Design for energy efficiency	design to minimize energy using.
7. Renewable feed stocks	design to used renewable raw material or feedstock
8. Reduce derivatives	design to minimize or avoid the using of unnecessary derivative (e.g., protection group)
9. Catalysis	design to use the catalytic reagent which as selective as possible
10. Design for degradation/ design for end of life	design to gain the product which non-toxic and environmentally benign
11. Real-time monitoring and process control	design to develop the real-time analysis for prevention of the formation of hazardous substances
12. Inherently safer chemistry	design to use the potential substance for minimizing of an accident

1.6 Nanotechnology

1.6.1 Definition of nanotechnology

Nanotechnology is the ability to observe, measure, manipulate and manufacture things at the nanometer scale. The definition of nanotechnology only if it involves all of the following:

- ✓ Research and technology development at the atomic, molecular, or macromolecular levels, in the length scale of approximately 1 to 100 nanometer range.

- ✓ Creating and using structures, devices and systems that have novel properties and functions because of their small and/or intermediate size.

- ✓ Ability to control or manipulate on the atomic scale. It should be to note that the nanotechnology is not only merely the study of small things but also the research and development of materials, devices and systems that exhibit physical, chemical and biological properties. These properties can be different from those found at larger scales, those that are more than 100 nanometers.^[22]

The nanotechnology has come to play an important role for the development of nano-size of metal. Since, the metallic nanoparticles (NPs) are attractive for use, particularly as catalysts because of their high surface-to-volume ratios which can minimize the costs associated with their usage.^[23] In addition, metallic NPs also exhibit distinct properties (optical, electronic, magnetic and so on) from those of individual atoms or their bulk counterparts due to the quantum-size and surface

effects.^[24] The properties of NPs are usually depend on size and structure, reveal the attractive tremendous research and extensive use in various applications.

There are two methods involved in nanomaterial synthesis and fabrication of nanostructures; top down and bottom up approaches.

Top down approach, attrition or milling, is a typical top-down method in making NPs such as etching of thin film.

Bottom up approach, is to build material from bottom: atom by atom, molecule, or cluster by cluster.

Both these approaches play an important role in modern industry and most likely in nanotechnology as well, however there are advantage and disadvantages in both type of approach. Bottom up approach offers a better chance to obtain nanostructures with less defects and more homogeneous chemical composition. This is because the bottom up approach is driven mainly by the reduction of Gibb free energy, such that nanostructure and nanomaterials produced are close to thermodynamic equilibrium. On the contrary, top down approach most likely introduces internal stress, in addition to surface defects and contaminations. Therefore, bottom up approach is more popular in synthesis of NPs and is synthesized by homogeneous nucleation from liquid or vapor or by heterogeneous nucleation on substrate.^[25]

The formation mechanism of monodisperse NPs is often used the LaMer model in which particle formation is separated into three stages: generation of atoms, nucleation and growth (Figure 8).^[23] Once the concentration of atoms reaches a point

of, the atoms start to aggregate into small clusters (i.e., nuclei, self-nucleation). These nuclei then grow in an accelerated manner and the concentration of metal atoms in solution drop. If the concentration of atoms drops quickly below the level of minimum supersaturation, no additional nucleation events will occur. However, if metal atoms continuous supply, the nanocrystals will grow and increase in size until an equilibrium state reaching between the atoms on the surface of the nanocrystal and the atoms in the solution. Besides growth via atomic addition, the nuclei and nanocrystals can directly merge into larger objects via agglomeration.^[23]

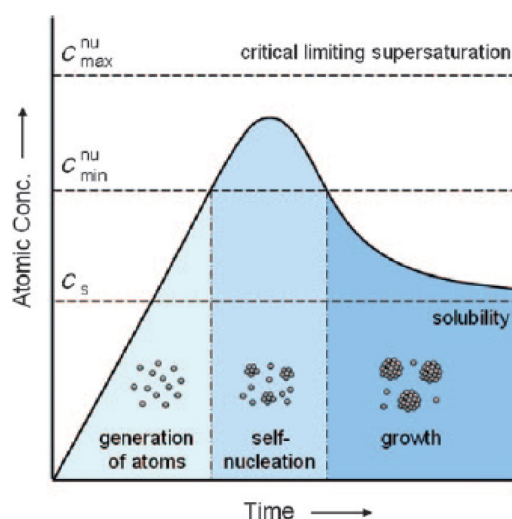


Figure 8 Plot of atomic concentration against time, illustrating the generation of atoms, nucleation and subsequent growth.^[23]

1.6.2 Nanocatalysts

Heterogeneous catalysis has received a tremendous amount of interest, both from a scientific and an industrial perspective.^[26] It has an enormous impact on the world economy, since more than 90% of chemical manufacturing processes utilize catalysts.^[27] The efficient, controlled and cost-effective design of catalysts is thus a goal of great importance. Nanocatalysis is one area of catalysis which is developing at a rapid pace. Novel catalytic properties including greatly enhanced reactivities and selectivities have been reported for NPs catalysts as compared to their bulk counterparts. Many experimental studies on nanocatalysts have focused on correlating catalytic activity with particle size. While particle size is an important consideration, many other factors such as geometry, composition, oxidation state and chemical/physical environment can play a role in determining NPs reactivity.^[26]

Size effect

Haruta *et al.*^[28] found that the dramatic enhancement of the catalytic activity and selectivity of highly dispersed Au particles (<5 nm) supported on reducible metal oxides, considerable efforts have been dedicated to the investigation of the influence of NP size.^{[29]-[35]} Cuenya *et al.* explained that it is not a single, unique cause which results in the enhanced catalytic activity and selectivity observed for small NPs, but rather, several of the above mentioned factors acting in parallel.^[26] For instance, with decreasing NPs size, the surface to volume ratio increases, resulting in a larger number of low-coordinated atoms available for interaction with chemical adsorbates. The distinct electronic properties of such sites are also expected to play a role in

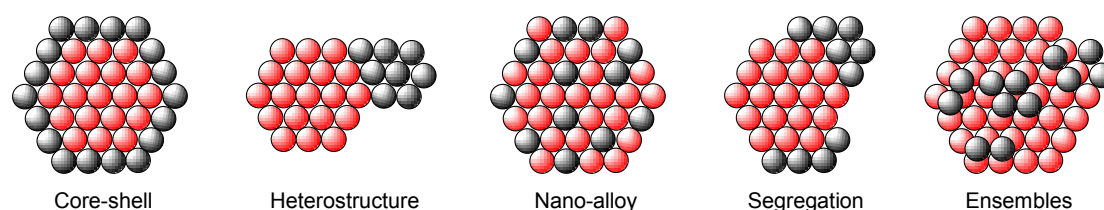
chemical reactivity, for example, by facilitating the dissociation of reactants or by stabilizing intermediate reaction species. In addition, the particle size also plays an important role in the stability of surface oxides on clusters. This can affect the reactivity of certain NPs, since several metal oxides (e.g., RuO₂) have been proven more active than the pure metals.^{[26],[36]}

Shape effect

Xia *et al.* reported that both the reactivity and selectivity of a catalyst can be tailored by controlling the shape of a nanocrystal.^[23] As a first approximation, shape determines which crystal facets comprise the surface of a nanocrystal. For example, consider a tetrahedron and a cube made of an fcc metal: all the exposed facets of a tetrahedron are {111} and all the exposed facets of a cube are {100}. Such a difference can give rise to different catalytic activity and selectivity. For example, from studies with single crystals, the Pt(111) surface was found to be three to seven times more active than the Pt(100) surface for aromatization reactions.^{[37],[38]} Also, shape determines the number of atoms located at the edges or corners, which can have a profound effect on catalytic performance.^[39] El-Sayed *et al.* studied the effect shape had on the catalytic performance of Pt nanocrystals.^[40] When used as catalysts, they found that the average rate constant increased exponentially as the percentage of surface atoms at corners and edges increased.

Composition effect

Heterometallic NPs composed of more than one metal in nanostructures which can range from bimetallic heterostructures, to core-shell structures, alloys and intermetallic as shown in Scheme 2.^{[41],[42]} Due to the positive effects arising from the cooperative interactions between the (two) metals which electronic and geometric structures are tailored. For instance, bimetallic NPs, the difference in electronic affinity between first metal (M1) and second metal (M2), and thus M1 can suffer an electronic density increase or a decrease depending on whether M2 has a lower or higher electronic affinity. In this case phenomena such as adsorption/desorption of reagents/reaction intermediates/products can be strongly affected and consequently activity and selectivity. Therefore, bimetallic NPs are widely employed in many fields of catalysis.^{[42]-[45]} For instance, single phase bimetallic Au-Pd/AC showed high activity attributed to the synergistic effect between Au and Pd in the selective liquid-phase oxidation of GLY towards glycerate.^{[46]-[49]} Hutchings *et al.* prepared Au-Pd alloy NPs with different methods which showed synergistic effects in redox catalysis.^{[50]-[52]} Currently, there had been reported that Pt alloying with another metals (such as Au, Ru, Pd, etc.) is an alternative increasing the resistance to poisoning of polymer electrolyte membrane fuel cells.^{[53]-[59]}



Scheme 2 Examples of bimetallic NPs structures.^[42]

Oxidation state effect

The traditionally view of the oxidation as a process leading to reduced catalytic performance.^[60] Recently, there has reported that the oxidation of a metal surface subsequent role in promoting reactivity of the surface, however, their role in catalysis is still not fully understood and likely need to be investigated on a case-by-case basis.^[26] In addition, Croy *et al.* have observed that the size,^[61] the catalyst pretreatment,^[62] the support^[63] and the secondary metal^[64] of mono- and bimetallic Pt catalyst can influence the type of oxide formed (PtO and PtO₂) as well as the stability of the metal-oxide shell present on catalysts under realistic reaction conditions. Some experimental evidence that metal oxides, such as RuO₂ is already a thorough understanding of the nature of their enhanced reactivity, and superior catalytic performance over their metallic counterparts is generally agreed upon but the same cannot be said for other important catalytically active metals such as Pt.^{[26],[60],[65],[66]} In case of Pt, there is an ongoing debate in the current literature as to whether Pt oxides are beneficial or detrimental to the catalytic performance of Pt particles. Gastgeier *et al.* have attributed the decay in the performance of fuel cell electrodes to the formation of PtO.^[67] Thus, the resistance to oxidation that can be achieved by alloying Pt with noble metals could be of advantage for this system. Metallic Pt species were also reported to be the most active species for C₃H₈ combustion^[65] and NO₂ decomposition.^[68] As an example, Dam *et al.* reported that Pt dissolution in fuel cells reaches a saturation level due to the presence of a protective Pt oxide layer.^[69]

1.7 Oxidation reaction of alcohol

For the classical chemistry, the waste generated in the organic compounds manufacture consists of inorganic salts which are a direct consequence of the use of stoichiometric inorganic reagents in production process. Especially, fine chemicals and pharmaceuticals industries are refractory with antiquated ‘stoichiometric’ technologies. Example of common stoichiometric reagents are stoichiometric reductions with metals (Na, Mg, Zn, Fe) and metal hydride reagents (LiAlH₄, NaBH₄), oxidations with permanganate, manganese dioxide and chromium(VI) reagents and a wide variety of reactions, e.g., sulfonations and nitrations. To overcome the using of classical stoichiometric methodologies, the cleaner catalytic alternatives had been developed. For example, development of chemical production processes based on H₂, O₂, H₂O₂, CO, CO₂ and NH₃ as the direct source of H, O, C and N. Catalytic hydrogenation, oxidation and carbonylation are good examples of highly atom efficient, low-salt processes (Figure 9).^[70]

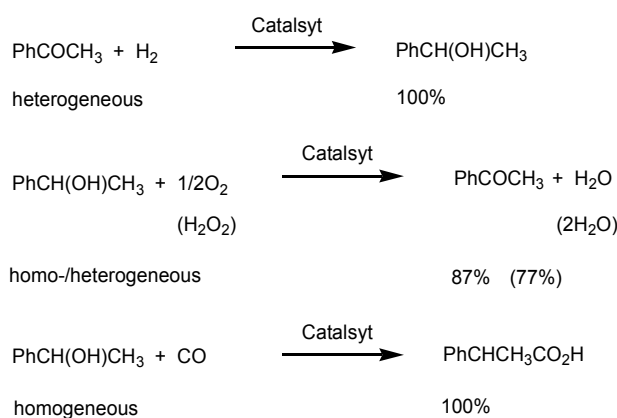
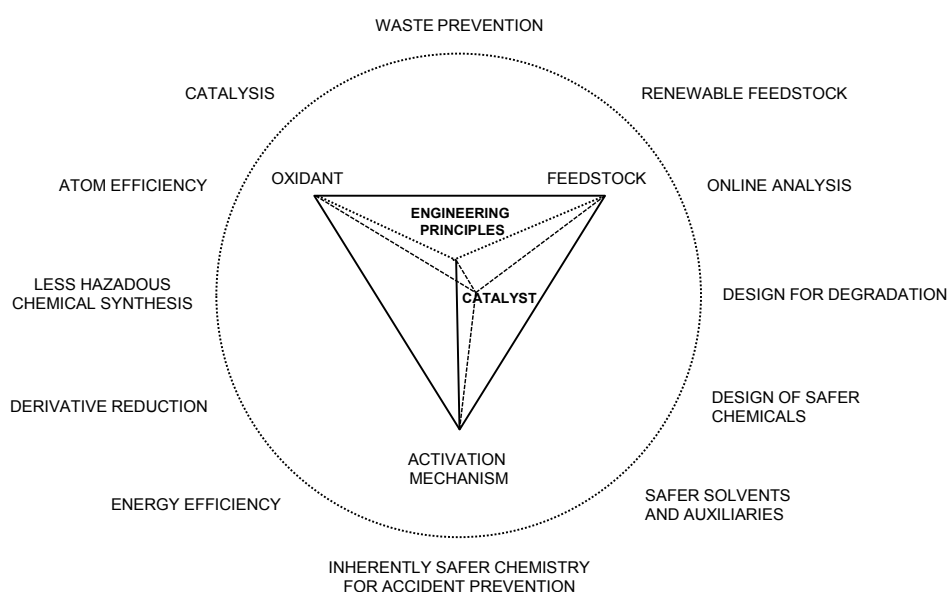


Figure 9 Atom efficient catalytic processes.

Catalysis offers advantages over stoichiometric reactions in terms of both selectivity and energy minimization. The specificity of a catalyst for each reaction is applied for driving the reaction to a preferred product, the amount of undesired by-products is decreased, thereby reducing waste generated. The amount of energy required for a given transformation is also reduced as the catalyst decreases the activation energy of the reaction.^[71] Both of monometallic and heterometallic NPs are essential form for catalysis. Today it is estimated that 90% of the chemicals used catalyst at some stage in their manufacture, come into contact with a catalyst. The range is truly broad from bulk chemicals such as acetic acid and ammonia to consumer products, such as detergents and vitamins. Virtually all major bulk chemical and refining processes employ catalysts.^[4]

Selective oxidation processes represent a large class of organic reactions where the development of clean and efficient green chemistry processes can have a significant positive economic and environmental impact.^[72] Especially, the oxidations of primary and secondary alcohol to the corresponding carbonyl compounds play a center role in organic synthesis.^[73] In the classical oxidation processes, stoichiometric reagents such as chromate (CrO_3) and permanganate (KMnO_4) which large harmful impacts for environment were employed as oxidant.^{[74],[75]} Hence, the modern oxidation process prefers using either molecular oxygen (O_2) or hydrogen peroxide (H_2O_2) as a green stoichiometric reagents that were consumed by the reaction. In addition, these oxidants are inexpensive and produce water as a by-product. Nowadays, many researches tend to make environmentally-friendly method for preparation of metal catalyst. Therefore, the simplification of the catalyst

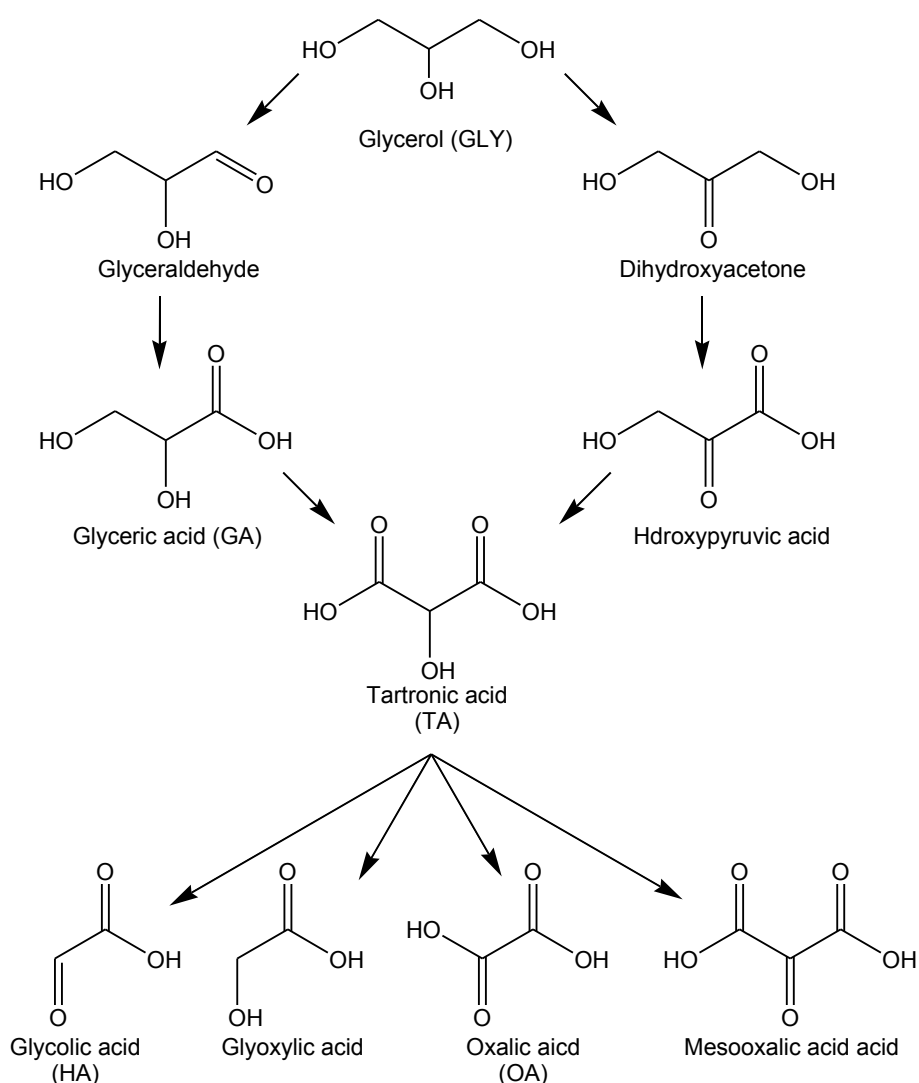
development in term of optimizing atom and energy efficiencies was referred to green technology to overall process design the reaction or choose the environmental benign reagent. In order to design the green oxidation reaction, the key design parameter for selective oxidation catalysis was adapted from green chemistry principle as shown in Scheme 3.^[76]



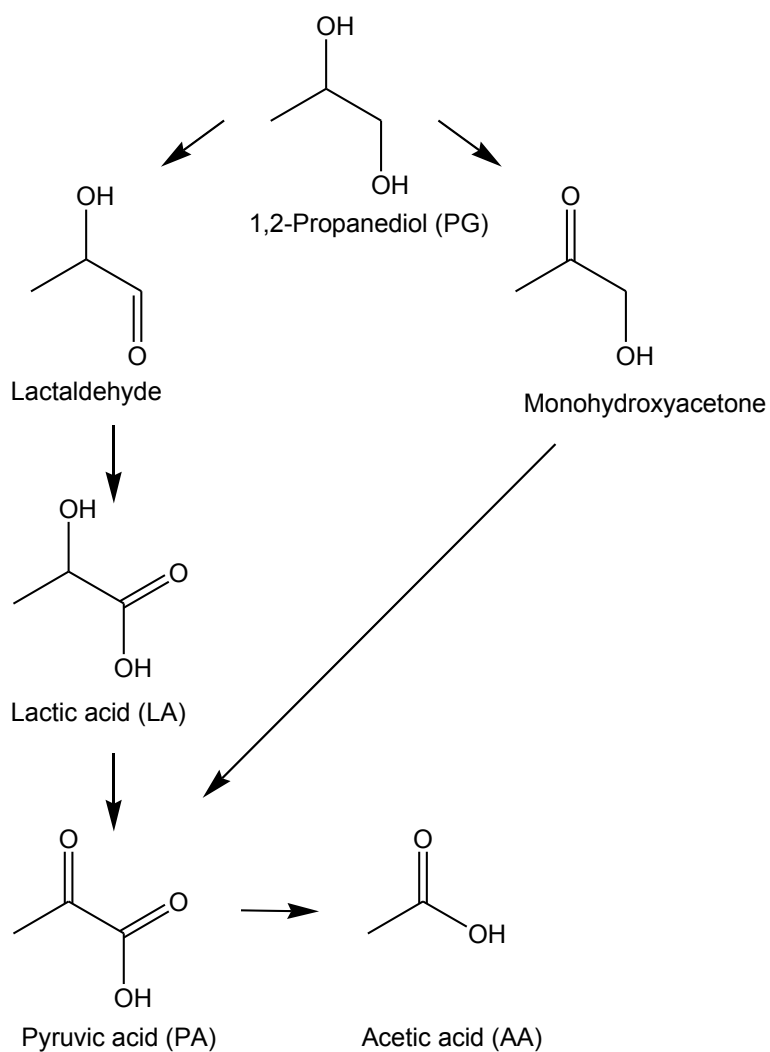
Scheme 3 Key design parameter for selective oxidation catalysis.^[76]

1.7.1 Selective oxidation of glycerol and 1,2-propanediol

As mentioned above, the partial oxidation of GLY and PG produced value-added products. However, GLY and PG compose of both primary and secondary hydroxyl group in their structure, which may lead to poor selective to target product. The general oxidation scheme of GLY and PG were shown in Schemes 4 and 5.



Scheme 4 Oxidation product of GLY.^[12]



Scheme 5 Oxidation product of PG.^[76]

Therefore, the metal-based catalysts such as Pt, Pd and Au had been used for control the oxidation reaction. The high cost and scarce availability of noble metals make industrialization very difficult.^{[77],[78]} The utilization of the low cost catalyst with less noble metal or non-noble metal affords to overcome this problem. There had been reported of heterometallic NP catalyst (e.g., bi- and tri-metallic catalyst) of noble metal with non-noble and two non-noble metals such as PtCu, PtBi, AuCu,

NiCu and FeNi. However, until now the noble metals (e.g., Pt, Au, Pd) are also attractive catalysts, especially for GLY and GLY derivative oxidation. Since, Pt and Pd catalysts have been reported as highly active for the oxidation of polyols even under acidic and basic conditions. Au catalyst was found to be high resistance to oxygen poisoning; however the oxidation reaction over Au catalyst never proceeds under base-free condition.^[12]

The reviews of the chemoselective oxidation at primary hydroxyl group of GLY and PG toward GA and LA, respectively over mono- and bimetallic catalysts were summarized in Tables 2–4. Most of publications required the basic condition, temperature at least 333 K and pressurized oxygen for carrying out the oxidation reaction of GLY and PG. It is hardly to compare the true rate and selectivity from each literature according to the difference in reaction conditions and metal particle size.

Table 2 Selective oxidation of GLY to GA over monometallic catalysts

Catalysts	Size (nm)	Temp. (K)	pO_2 (atm)	NaOH/GLY (mol/mol)	Conv. GLY (%)	Sel. GA (%)	TOF (h^{-1})	Ref
1% Au/AC	-	333	3	1	56	100	-	[79]
5% Pt/C	2.3	333	3	2	56	69	-	[80]
1% Au/C	6	303	3	4	100	92	-	[81]
1% Au/G	-	303	3	4	25	81	26	[82]
1% Pd/G	-	303	3	4	25	83	54	
1% Au/C	2.5	323	3	4	50	65	1090	[83]
0.75% Au/C	3.7	333	10	2	75	100	-	[84]
1% Pt/C	2.5	323	3	4	80	61	332	[85]
1% Pd/C	5.6	323	3	4	90	80	28	[86]
1.5% Au/TiO ₂	4	323	3	4	90	60	203	[87]
1% Au/CeO ₂	10.2	333	1	pH=12	-	38	-	[88]
1% Au/C	3.7	333	10	2	-	-	4.8 ^c	[89]
1% Au/C	4.3	333	1	pH=12	50	45	-	[91]
Au powder	-	333	10	2	50	-	2.5 ^d	[92]
1.47% Au/TiO ₂	3.7	308	10	2	51	-	1.7 ^d	[93]
0.5% Au/C	7.3	333	10	2	50	82	1 ^d	[94]
2.9% Pd/C	2.9	333	10	2	50	65	17 ^d	
1% Au/TiO ₂	3.5	373	5	0.1	-	-	-	[95]
1% Au/Fe ₂ O ₃	3.5	373	5	0.1	-	-	-	
5% Pt/ MWCNTs	6.7	333	flow ^a	-	70	70	0.87 ^e	[95]
5% Pt/C	3.6	398	flow ^b	pH = 4	20	-	238	[97]

AC = Activated carbon. C = Carbon. G = graphite. MWCNTs = Multi-wall carbon nanotubes. ^a150 mL·min⁻¹. ^b300 mL·min⁻¹. ^cTOF (s⁻¹) (Calculated by Ref. [90]). ^dTOF (s⁻¹). ^eTOF (min⁻¹).

Table 2 (continue) Selective oxidation of GLY to GA over monometallic catalysts

Catalysts	Size (nm)	Temp. (K)	pO_2 (atm)	NaOH/GLY (mol/mol)	Conv. GLY (%)	Sel. GA (%)	TOF (h^{-1})	Ref
5% Pt/C	3.2	333	flow ^a	-	50	47	223	[98]
1.6 Au/TiO ₂	3.5	333	10	2	35	58	4.1 ^c	[99]
5% Au/C	4.7	333	10	2	60	63	75	[100]
5% Pd/C	6.3	333	10	2	44	65	55	
0.8% Au/C	10.5	333	11	2	7	67	6.1 ^c	[101]
3% Pd/C	3	333	11	2	29	83	4.9 ^c	
3% Pt/C	2.3	333	11	2	18	70	2.2 ^c	
0.5% Pt/AC	3.8	333	3	2	25	62	-	[102]
0.65% Pd/AC	2	333	3	2	25	61	-	
0.74% Rh/AC	1.3	333	3	2	25	61	-	
0.59% Au/C	6.8	333	10	2	40	59	-	[103]
5% Pt/ MWCNTs	2.1	333	flow ^a	-	90	68	336	[104]
0.5% Pt/CS	5	343	10	0.8	66	82	645	[105]
0.6% Au/G	7.7	333	5	2	25	63	1280	[106]
1.1 % Au/AC	13.3	333	5	2	25	25	438	
1% Au/C	3.5	323	3	4	73	68	-	[107]
5% Ru/AC	3	323	3	4	<1	-	-	
0.64% Pt/HT	2.1	333	flow ^b	-	52	46	-	[108]
Au/MWCNTs	3.2	333	flow ^a	-	50	59	-	[109]
Au/Al ₂ O ₃	-	333	10	6.7 ^d	5	4	7	[110]
Au/TiO ₂	-	333	10	6.7 ^d	3	17	5	
Au/ZrO ₂	-	333	10	6.7 ^d	3	14	4	
Au/NiO	-	333	10	6.7 ^d	11	5	20	

C = Carbon. G = Graphite. AC = Activated carbon. HT = hydrotalcite. MWCNTs = Multi-wall carbon nanotubes. ^a150 mL·min⁻¹. ^b10 mL·min⁻¹. ^cTOF (s⁻¹). ^dpH.

Table 3 Selective oxidation of GLY to GA over bimetallic catalysts

Catalysts	Size (nm)	Temp. (K)	pO_2 (atm)	NaOH/GLY (mol/mol)	Conv. GLY (%)	Sel. GA (%)	TOF (h^{-1})	Ref
1% Pd@Au/G	-	323	3	4	90	55	505	
1% Au+Pd/G	-	323	3	4	90	56	675	[82]
1% Au@Pd/G	-	323	3	4	90	54	528	
1% Pd@Au/C	2.5–3	323	3	4	79	71	3261 ^a	[111]
1% Pt@Au/C		323	3	4	88	61	3455 ^a	
1% Pd@Au/C	3–4	323	3	4	90	77	6435 ^a	[47]
1% Au-Pd/C	-	353	3	-	25	48 ^b	-	[112]
1% Au-Pt/C	-	353	3	-	80	60 ^b	-	
1% Au-Pd/C	3.4	323	3	4	40	77	1891 ^a	[113]
1% Au-Pd/TiO ₂	3.8	333	10	2	100	53	500	[100]
1% Pt-Cu/C	-	333	flow ^c	-	48	62	-	
3% Pt-Cu/C	3.5	333	flow ^c	-	82	67	-	[114]
5% Pt-Cu/C	5	333	flow ^c	-	86	71	-	
1% AuPd(1:3)/MgO	2	333	3	-	15	74	-	
1% AuPt(1:3)/MgO	2	333	3	-	43	72	-	[74]
1% AuPd(1:3)/MgO	2	296	3	-	43	85	-	
1% AuPt(1:3)/MgO	2	296	3	-	30	67	-	
1% Ru@Au/AC	4.3	323	3	4	99	57	-	[107]
1% Au@Ru/AC	4.2	323	3	4	26	43	-	

G = Graphite. C = Carbon. AC = Activated carbon. ^aTOF (h^{-1}). ^bGA+TA. ^c150 mL·min⁻¹.

Table 3 (continue) Selective oxidation of GLY to GA over bimetallic catalysts

Catalysts	Size (nm)	Temp. (K)	p_{O_2} (atm)	NaOH/GLY (mol/mol)	Conv. GLY (%)	Sel. GA (%)	TOF (h^{-1})	Ref
Au/C	4.1	333	120 ^a	4	-	-	445	
10 sc%	-	333	120 ^a	4	-	-	809	
30 sc%	-	333	120 ^a	4	-	-	1582	
50 sc%	-	333	120 ^a	4	-	-	3036	
60 sc%	4.2	333	120 ^a	4	-	-	4038	[115]
80 sc%	-	333	120 ^a	4	-	-	6076	
100 sc%	-	333	120 ^a	4	-	-	4915	
150 sc%	4.2	333	120 ^a	4	-	-	4084	
300 sc%	-	333	120 ^a	4	-	-	4254	
Pd/C	4.2	333	120 ^a	4	-	-	424	
<hr/>								
0.6%Pt0.6%Pd/ Al ₂ O ₃	-	333	1	1.5	97	-	33	
1.2%Pt-1.2%Pd/ Al ₂ O ₃	-	333	1	1.5	100	-	42	
2.5%Pt-2.5%Pd/ Al ₂ O ₃	-	333	1	1.5	91	-	41	[116]
2.5%Pt/Al ₂ O ₃	-	333	1	1.5	69	-	49	
2.5%Pd/Al ₂ O ₃	-	333	1	1.5	74	-	66	
<hr/>								
Au-Pd/TiO ₂	2.242	373	3	2	37	30	38	
Pd-Pt/TiO ₂	2.32	373	3	2	39	64	210	
Au-Pt/TiO ₂	1.19	373	3	2	-	-	-	[117]
Au-Pd-Pt/TiO ₂	2.03	373	3	2	37	55	378	

C = Carbon. sc = surface coverages. ^amL·min⁻¹.

Table 4 Selective oxidation of PG to LA over mono- and bimetallic catalysts

Catalysts	Size (nm)	Temp. (K)	pO_2 (atm)	NaOH/GLY (mol/mol)	Conv. PG (%)	Sel. LA (%)	TOF (h^{-1})	Ref
1% Au/C	-	363	1	pH=8	30	30	-	
5% Pd/C	-	343	1	pH=8	46	5	-	[118]
5% Pt/C	-	343	1	pH=8	56	18	-	
1% Au/C	7.8	363	2	1	80	100	780	
5% Pd/C	-	343	2	1	80	90	720	[119]
5% Pt/C	-	343	2	1	80	89	650	
1% Au/G	-	333	6	1	32	100 ^a	-	[79],
0.5% Au/G	-	333	6	1	53	71 ^a	-	[120]
0.25% Au/G	-	333	6	1	28	65 ^a	-	
1% Au/BP	2–5	353	1	pH=12	100	64	-	[9]
1% Au/CeO ₂	2–5	353	1	pH=12	98	55	-	
Pd black	-	368	H ₂ O ₂	pH=1.5	35	26	-	[121]
1% Au/TiO ₂	3.5	373	5	0.1	98	72	-	[95]
1% Au-Pd/TiO ₂	-	333	10	2	94	96	1880	[122]
1% Au-Pd/TiO ₂	-	333	H ₂ O ₂	2	10	96	66	
1.4% Au/Mg(OH) ₂		333	3	2	97	84	-	[123]
2.8% Au/Mg(OH) ₂		333	3	2	86	53	-	
0.5% Pt/CS	100 ^b	343	10	0.8	91	93	852	[105]
1% Au/CeO ₂		373	3	0.1 ^c	13 ^d	75	-	
1% Au-Pd/CeO ₂	2–7	373	3	0.1 ^c	31 ^d	76	-	[124]
1% Pd/CeO ₂		373	3	0.1 ^c	56 ^d	54	-	
5% Pd/C	-	338	10	0.7	62	-	-	[125]
0.5%Au+ 0.5%Pt/KB-B	2.1	298	air	1	38	81	-	[126]

C = Carbon. G = Graphite. BP = Carbon black pearl. CS = Carbon spherule. KB-B = Activated carbon. ^aMono acid. ^bMicron. ^cNaOMe. ^dMethyl lactate.

1.7.2 Importance parameter for the catalytic performance of glycerol and 1,2-propanediol oxidation

Particle size Effect

Pt and Pd catalysts have been described as highly active for the oxidation of polyols in the liquid phase while Au based catalysts were found highly active in the oxidation of diols.^{[1],[118]} Liang *et al.* studied the influence of the particle size on the catalytic performances by preparation a series of carbon-supported Pt catalysts (Pt/C) with particle sizes ranging from 1.2 to 26.5 nm.^[98] The activity increased for particle size of less than 6 nm while the catalytic activity dropped as the particle size larger than 6 nm, which was ascribed to the lower metallic surface area. Dimitratos *et al.* showed that increasing the particle size (2 nm to 16 nm) of Pd/C catalysts decreases the catalytic activity (TOF), but increases the selectivity to GA.^[87] Porta *et al.* also reported the influence of the particle size (6–20 nm) on the catalytic performances over Au/C.^[81] They found that the small particle size of 6 nm showed an about 10 times higher catalytic activity which was ascribed to the higher surface exposition of the metal. Whereas, the bigger particles (>15 nm) were less active but maintained constant selectivity until full conversion of GLY. The author explain the effect of the particle size on the selectivity to GA as a competition between the increase in the particle size and the density of the (111) planes.^[1]

pH effect

It is well known that the catalysis for alcohol oxidation strongly dependent on the basicity of the reaction medium. Pt and Pd based catalysts can also be used either in acidic or basic conditions, whereas Au limits the reaction conditions to the basic media.^{[9],[87]} Many studies have been performed using Pd/C catalysts for GLY oxidation which generally carried out at pH = 11 in order to increase the activity of the catalysts.^{[112],[[127]-[129]} The main oxidation product is always GA. Garcia *et al.* reported that the initial rates of GLY oxidation are pH dependent over 5%Pt/C with GA was identified as the main product.^[130] Hutchings *et al.* demonstrated the selective oxidation of GLY to glycerate over supported Au NPs using alkaline condition. They proposed that the role of NaOH was essential for the initial dehydrogenation pathway, since in the presence of base the hydrogen is readily abstracted from one of the primary hydroxyl groups of GLY.^{[79],[131]}

Support Effect

Tuning the catalyst support is an important parameter to build highly active catalysts for liquid phase GLY oxidation.^[1] Demirel *et al.* studied the influence of the nature of the support and chose titania and active carbon as comparative examples.^[88] They found that carbon supported-Au was the best system to achieve selective GLY oxidation. Nowadays, most of the catalysts for GLY oxidation use carbon-type compounds as supports, and especially active carbon, which are well recognized in industrial chemistry for being stable in acidic or basic conditions. Furthermore, they offer the possibility of an easy recovery of Au by burning off the support.^[132] A

completely different approach was recently reported by Villa *et al.* who used several MgAl_2O_4 -spinels as supports for Au catalysts in order to show that the Au-catalyzed reaction could be tuned *via* the interaction of the Au NPs with the support.^{[11],[133]} Therefore, the authors propose a correlation between the Al/Mg ratio and thereby the basicity of the support and the selectivity to glycerate and tartronate. This influence of the Al/Mg ratio on the catalytic performances was recently confirmed by Tsuji *et al.* for Pt/hydrotalcite (HT).^[108] In addition, the latter case, the reaction can be performed in base-free conditions.

As described above, the catalysis for alcohol oxidation strongly dependent on the basicity of the reaction medium, consequently, salt of products were being form, then the obtained products required the additional neutralization.^[98] Therefore, in advanced research, oxidation reaction have been performed with metal species supported on basic materials, they will permit a base-free oxidation producing the free carboxylic acid product rather than salt form. HT (Mg-Al-CO_3) is basic and layered double hydroxide, which is frequently used as a support for Pd,^[134] Ru,^{[135],[136]} Pt^[137] and Au^[137] species. HT model structure was shown in Figure 10. The HT denoted by $\text{Mg}_6\text{Al}_2(\text{OH})_{16}\text{CO}_3 \cdot n\text{H}_2\text{O}$ (Mg-Al-CO_3) consists of a positively charged two-dimensional Brucite-like layers with anionic species in the interlayer to form a neutral material, and which possesses basicity derived from OH^- and/or HCO_3^- on their surface.^[138]

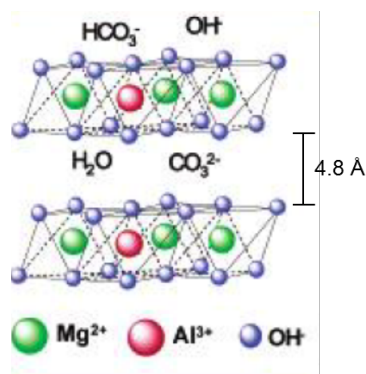


Figure 10 Structure model of hydrotalcite.

1.7.3 Ligand effect on the performance of catalyst

As referred above, particle size, shape, composition and electronic state determine the efficiency of catalyst. The selection of nanocatalysts, the stability of NPs and the capping agents on their surfaces are also important factor.^[23] In many cases, the surface atoms of nanocatalysts are so active that their size and shape change during the catalytic reaction.^[139] Such changes can drastically alter their performance and lifetime. Additionally, capping agents might deactivate catalytic sites, with recent work demonstrating that Pt NPs prepared with tetradecyltrimethylammonium bromide exhibit much higher activity than poly(vinyl pyrrolidone) (PVP)-capped Pt nanocrystals.^{[140],[141]} Zhang *et al.* reported that Au/Pt/Ag trimetallic NPs (TNPs) showed higher activity than that of Au NPs with nearly same particle size for the aerobic glucose oxidation, since the negative charge on the Au surface due to electron donation from Ag neighboring atoms and PVP.^[142] Borodko *et al.* probed the interaction between PVP and Pt nanocrystals by UV-Raman and FT-IR, and concluded that PVP adheres to the NPs through a charge-transfer interaction between the pyrrolidone rings and surface Pt atoms.^[143] The

reviews of the effect of stabilizer on the properties of metal NPs were summarized in Table 5. Therefore, the selection of the suitable stabilizer has an important to improve catalytic properties of metal nanoclusters.

Table 5 Effect of stabilizer on the properties of metal NPs

Catalysts	Stabilizer/ Capping agent	Particle size (nm)	Binding energy (eV)	Remark
Au NPs	Dendrimer	2.0	-	- Dendrimers stabilized-Au gain 5d electrons (weakly interacting)
	Dodecanethiol	2.1	-	- Thiol stabilized-Au lose 5d electrons (strongly interacting) ^[144]
Pt NPs	PVP	< 7	70.6	- Charge transfer from carbonyl group in PVP to Pt NPs
	PVP	> 25	70.9	- Charge transfer from Pt metal to polymer side chain of PVP ^[145]
Au clusters	PVP	-	-	- PVP-Au ₁₃ enhances the negative charge density on Au ₁₃ cluster - Negatively charged surface Au ₁₃ -PVP promote the generation of anionic O ₂ ^[146]
Au clusters	PVP	1.1±0.2	82.7	Aerobic oxidation catalysis of alcohol: PVP-Au clusters show higher activity than PAA-Au cluster ^[147]
	PAA	1.4±0.4	83.2	
Au/C	PVA	3.0±0.6	84/87.6	Electrocatalysis of Au NPs and their derived Pt-on-Au (Pt ^o /Au) nanostructure depends on the nature of stabilizers ^[143]
	PVP	3.2±0.5	83/86.5	
	Citrate	10±1.2	84/87.6	

Dendrimer: starburst poly(amidoamine) dendrimer. PVP: poly(vinyl pyrrolidone). PAA: poly(allylamine). PVA: poly(vinylalcohol). Bulk Au4f: 84 eV and 87.7 eV. Bulk Pt4f: 71 eV and 74.4 eV.

Table 5 (continue) Effect of stabilizer on the properties of metal NPs

Catalysts	Stabilizer/ Capping agent	Particle size (nm)	Remark
Pd NPs	PVP	-	- PAMAM-G3-Pd NPs and PVP-Pd NPs are found to be efficient catalysts for the Suzuki reactions between phenylboronic acid and iodobenzene
	PAMAM-G2	3.6	
	PAMAM-G3	1.4	
	PAMAM-G4	1.4	
	Block-copolymer	3.0	
Au sols	PVA	2.5	The Au _{THPC} showed a high activity for the liquid phase oxidation of glycerol in comparison to Au _{PVA} and Au _{Citrate} [142]
	THPC	2.0	
	Citrate	9.8	
Pt/Silica	TTAB	1.5	Amine (OA) capping exhibited a detrimental influence on the catalytic properties and low activity were observed for ethylene hydrogenation and CO oxidation [149]
	PVP	1.5	
	OA	1.5	

PVP: poly(vinyl pyrrolidone). PAMAM: poly(amido-amine) (5 Pd²⁺ ions per dendrimer (G2-OH(Pd²⁺)₅; 10 Pd²⁺ ions per dendrimer, Gn-OH(Pd²⁺)₁₀, n = 3 and 4). Block copolymer: polystyrene-block-poly(sodium acrylate). THPC: tetrakis(hydroxypropyl)phosphonium chloride. OA: oleylamine. TTAB: trimethyl tetradecyl ammonium bromide.

1.8 Soluble starch

Soluble starch is the amylose component of starch that is a linear polymer formed by the α -(1 \rightarrow 4) linkages between D-glucose units and adopts a left-handed helical conformation in aqueous solution as shown in Figure 11.^[150] Soluble starch has been used for the synthesis and stabilization of NPs such as Ag,^[150] Pt^[151] and Au^[152] due to its inexpensiveness and renewability as well as with numerous applications. The hydroxyl groups of starch possibly facilitate metal ions by electrostatic binding in the helical structure of polysaccharide and, therefore, prevent the metal NPs from aggregation.^[153] Furthermore, the aldehyde terminus of the starch molecule obtained from the degradation of polysaccharides under alkaline conditions can reduce the metal ions to its atomic state.^{[150],[154],[155]}

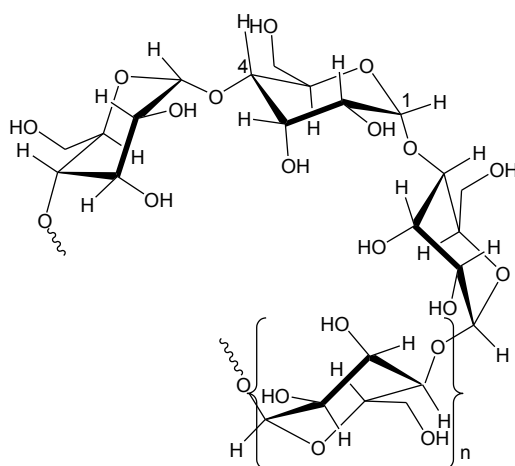


Figure 11 Soluble starch structure.

2. Purposes of this Thesis

- 2.1 Study on the development of novel green method for preparation of Pt-based NPs heterogeneous catalysts, and utilize as catalytic oxidation of polyols.
- 2.2 Study on the effect of polymer stabilized-Pt NPs and the effect on the catalytic property.
- 2.3 Modify the structures and properties of Pt-based NPs heterogeneous catalysts by the synthesis of heterometallic NPs, and clarify the reaction mechanism for the catalytic oxidation of polyols.

3. Outline of the Thesis

This thesis manipulates with studies on the development of Pt-based NPs heterogeneous catalysts by a green method, in order to enhance selective polyols oxidation into value-added chemicals under mild reaction conditions.

Description in Chapter 2 is the development of novel green method for the preparation of Pt NPs heterogeneous catalysts. Pt NPs/HT catalysts were successfully prepared by the immobilization method, in which Pt NPs were pre-generated by the reduction of $\text{H}_2\text{PtCl}_6 \cdot 6\text{H}_2\text{O}$ precursor with soluble starch as a reducing and a stabilizing agent under alkaline treatment, and were further immobilized on the HT support. The method resulted in the reproducible particle size distribution which can be controlled by the reduction times. The catalysts showed high activity and selectivity toward GA formation for the aerobic oxidation of GLY in base-free aqueous solution under atmospheric pressure of molecular oxygen and mild

conditions. After the reaction, the catalyst was easily removed by hot filtration and no Pt leaching was detected in the solution. The catalyst retained high activity in recycling experiments.

In Chapter 3, the effect of polymer stabilized-Pt NPs/HT on catalytic oxidation is explored. The efficiencies of different polymers, i.e., soluble starch, PVP and PVA stabilized-Pt NPs/HT catalysts for the aerobic PG oxidation in base-free aqueous solution under atmospheric pressure of molecular oxygen at room temperature are discussed. The structural investigation of polymer stabilized-Pt NPs/HT catalysts with keeping the same particle size (2.2 nm) on the same basic HT support showed that starch has strong electron donation power to create negatively-charged Pt surface atoms. In addition, the polymer structure also effect on the catalytic activity by made the different wettibility of stabilized-Pt NPs/HT in the water solution. Anionic Pt surface atoms, formed by starch ligand, may transfer electrons to oxygen molecule to form adsorbed O_2^- species. This step is proposed to be a crucial in the aerobic oxidation of PG in water at room temperature. Therefore, soluble starch is found to be suitable ligand for creating negatively-charged Pt surface atoms with low coverage to facilitate O_2 activation for PG oxidation at room temperature.

Chapter 4 explains the modification of developed technique from Chapter 2 for the preparation of Pt-based bimetallic NPs heterogeneous catalysts (fast co-reduction method). The aerobic oxidation of PG over Pt_xM_y NPs/HT (M = Ru, Ag, Pd, Au) catalysts exhibited the selectivity toward LA. Especially, PtAu NPs/HT was most selective in base-free aqueous solution under atmospheric pressure of molecular

oxygen at 353 K. Further development of synthetic method (slow co-reduction method) explored the very active PtAu NPs/HT which is able to oxidize polyols (GLY and PG) to produce GA and LA in base-free aqueous solution under atmospheric pressure of molecular oxygen at room temperature (298 K). The investigations on catalyst structure by XRD, TEM and XAFS revealed that negative charge on both Au and Pt atoms, in which starch ligand donates electrons, and the excess charge on Au atoms can also transfer to Pt atoms. The negatively-charged Pt atoms cause enhancement of the oxygen absorption and generate anionic O₂ like superoxo or peroxy oxygen to oxidize polyols. Therefore, it is concluded that the geometric and electronic changes of the catalytically active surface Pt sites by adjacent Au atoms and the starch ligand lead to improvement of the activity and selectivity to target products.

Finally, in Chapter 5, I summarize overall conclusions of the thesis. The scope of the research is also described.

4. References

- [1] O. Eismont, Economic growth with environmental damage and technical progress, *Environ. Resour. Econ.*, 1994, **4**, 241–249.
- [2] <http://www.iea.org/stats/index.asp>.
- [3] http://coriolis-energy.com/wind_energy/fossil_fuels.html#top
- [4] M. Lancaster, Green chemistry: An introductory text, The Royal Society of Chemistry, **2002**.
- [5] S. Fernando, S. Adhikari, C. Chandrapal and N. Murali, Biorefineries: current status, challenges, and future direction, *Energ. Fuel*, 2006, **20**, 1727–1737.
- [6] http://en.wikipedia.org/wiki/File:Total_World_Energy_Consumption_by_Source_2010.png.
- [7] J. M. Clomburg¹ and R. Gonzalez, Anaerobic fermentation of glycerol: a platform for renewable fuels and chemicals, *Trends Biotechnol.*, 2012, **31**, 20–28.
- [8] <http://www.sustainability.vic.gov.au>
- [9] C.-H. (Clayton) Zhou, J. N. Beltramini, Y.-X. Fan and G. Q. (Max) Lu, Chemoselective catalytic conversion of glycerol as a biorenewable source to valuable commodity chemicals, *Chem. Soc. Rev.*, 2008, **37**, 527–549.
- [10] J. Xuan, M. K. H. Leung, D. Y. C. Leung and M. Ni, A review of biomass-derived fuel processors for fuel cell systems, *Renew. Sust. Energ. Rev.*, 2009, **13**, 1301–1313.

- [11] M. A. Abraham, J. Clark and N. Winterton, Green chemistry metrics: measuring and monitoring sustainable processes, Blackwell Publishing Ltd., **2009**.
- [12] A. Behr, J. Eilting, K. Irawadi, J. Leschinski and F. Lindner, Improved utilisation of renewable resources: new important derivatives of glycerol, *Green Chem.*, 2008, **10**, 1-30.
- [13] T. Werpy and G. Peterson, Top value-added chemicals from biomass, Pacific northwest national laboratory and national renewable energy laboratory, US, **2004**.
- [14] R. F. Stockel, Method of treating dermatological conditions, U.S. Patent 2007/086 977 A1, April 19, 2007.
- [15] S. K. Gupta, Novel hydroxyl acid complexes for antiaging and skin renovation, U.S. Patent 2007/092 461 A1, April 26, 2007.
- [16] A. Corma, S. Iborra, and A. Velty, chemical routes for the transformation of biomass into chemicals, *Chem. Rev.*, 2007, **107**, 2411-2502.
- [17] Z. Yu, L. Xu, Y. Wei, Y. Wang, Y. He, Q. Xia, X. Zhang and Z. Liu, A new route for the synthesis of propylene oxide from bio-glycerol derivated propylene glycol, *Chem. Commun.*, 2009, 3934-3936.
- [18] E. D. Silva, W. Dayoub, G. Mignani, Y. Raoul and M. Lemaire, Propylene carbonate synthesis from propylene glycol, carbon dioxide and benzonitrile by alkali carbonate catalysts, *Catal. Commun.*, 2012, **29**, 58-62.
- [19] P. Gallezot, Catalytic routes from renewables to fine chemicals, *Catal. Today*, 2007, **121**, 76-91.

- [20] J. A. Dahl, B. L. S. Maddux and J. E. Hutchison, Toward greener nanosynthesis, *Chem. Rev.*, 2009, **107**, 2228–2269.
- [21] P. T. Anastas and J. C. Warner, Green chemistry theory and practice, New York: Oxford University Press, **1998**.
- [22] J. Mongillo, Nanotechnology 101, Greenwood Press, **2007**.
- [23] Y. Xia, Y. Xiong, B. Lim and S. E. Skrabalak, Shape-controlled synthesis of metal nanocrystals: simple chemistry meets complex physics?, *Angew. Chem. Int. Ed.*, 2009, **48**, 60–103.
- [24] A. Zecchina, E. Groppo and S. Bordiga, Selective catalysis and nanoscience: an inseparable pair, *Chem. Eur. J.*, 2007, **13**, 2440–2460.
- [25] H. Lee, S. E. Habas, S. Kweskin, D. Butcher, G. A. Somorjai and P. Yang, Morphological control of catalytically active platinum nanocrystals, *Angew. Chem.*, 2006, **118**, 7988–7792.
- [26] B. R. Cuenya, Synthesis and catalytic properties of metal nanoparticles: Size, shape, support, composition, and oxidation state effects, *Thin Solid Films*, 2010, **518**, 3127–3150.
- [27] J. M. Thomas, Principles and practice of heterogeneous catalysis, VCH, Weinheim, **1997**.
- [28] S. Yamamuro and K. Sumiyama, Why do cubic nanoparticles favor a square array? Mechanism of shape-dependent arrangement in nanocube self-assemblies, *Chem. Phys. Lett. A*, 2006, **418**, 166–169.
- [29] M. Haruta, Size- and support-dependency in the catalysis of gold *Catal. Today*, 1997, **36**, 153–166.

- [30] M. Haruta, *J. New Mater.* Nanoparticulate gold catalysts for low-temperature CO oxidation, *Electrochem. Syst.*, 2004, **7**, 163–172.
- [31] M. Valden, X. Lai and D. W. Goodman, Onset of catalytic activity of gold clusters on titania with the appearance of nonmetallic properties, *Science*, 1998, **281**, 1647–1650.
- [32] T. F. Jaramillo, S. H. Baeck, B. R. Cuenya and E. W. McFarland, Catalytic activity of supported Au nanoparticles deposited from block copolymer micelles, *J. Am. Chem. Soc.*, 2003, **125**, 7148–7149.
- [33] C. T. Campbell, S. C. Parker and D. E. Starr, The effect of size-dependent nanoparticle energetics on catalyst sintering, *Science*, 2002, **298**, 811–814.
- [34] S. Lee, C. Fan, T. Wu and S. Anderson, CO oxidation on Au_n/TiO₂ catalysts produced by size-selected cluster deposition, *J. Am. Chem. Soc.*, 2004, **126**, 5682–5683.
- [35] S. K. Shaikhutdinov, R. Meyer, M. Naschitzki, M. Baumer and H. J. Freund, Size and support effects for CO adsorption on gold model catalysts, *Catal. Lett.*, 2003, **86**, 211–219.
- [36] H. Over, Y. D. Kim, A. P. Seitsonen, S. Wendt, E. Lundgren, M. Schmid, P. Varga, A. Morgante and G. Ertl, Atomic-scale structure and catalytic reactivity of the RuO₂(110) surface, *Science*, 2000, **287**, 1474–1476.
- [37] G. A. Somorjai and D. W. Blakely, Mechanism of catalysis of hydrocarbon reactions by platinum surfaces, *Nature*, 1975, **258**, 580–583.
- [38] G. A. Somorjai, *Chemistry in two dimensions: surfaces*, Cornell University Press, **1981**.

- [39] G. C. Bond, Small particles of the platinum metals, *Platin. Metals Rev.*, 1975, **19**, 126–134.
- [40] R. Narayanan and M. A. El-Sayed, Catalysis with transition metal nanoparticles in colloidal solution: nanoparticle shape dependence and stability, *J. Phys. Chem. B*, 2005, **109**, 12663–12676.
- [41] H.-L. Jiang and Q. Xu, Recent progress in synergistic catalysis over heterometallic nanoparticles, *J. Mater. Chem.*, 2011, **21**, 13705–13725.
- [42] V. D. Santo, A. Gallo, A. Naldoni, M. Guidotti and R. Psaro, Bimetallic heterogeneous catalysts for hydrogen production, *Catal. Today*, 2012, **197**, 190–205.
- [43] K. An, S. Alayoglu, T. Ewers and G. A. Somorjai, Colloid chemistry of nanocatalysts: a molecular view, *J. Colloid Interf. Sci.*, 2012, **373**, 1–13.
- [44] H. Zhang and N. Toshima, Glucose oxidation using Au-containing bimetallic and trimetallic nanoparticles, *Catal. Sci. Technol.*, 2013, **3**, 268–278.
- [45] M. Yamada, M. Maesaka, M. Kurihara, M. Sakamoto and M. Miyake, Novel synthetic approach to creating PtCo alloy nanoparticles by reduction of metal coordination nano-polymers, *Chem. Commun.*, 2005, 4851–4853.
- [46] D. Wang, A. Villa, F. Porta, D. Su and L. Prati, Single-phase bimetallic system for the selective oxidation of glycerol to glycerate, *Chem. Commun.*, 2006, 1956–1958.
- [47] L. Prati, A. Villa, F. Porta, D. Wang and D. Su, Single-phase gold/palladium catalyst: the nature of synergistic effect, *Catal. Today*, 2007, **122**, 386–390.

- [48] A. Villa, C. Campione and L. Prati, Bimetallic gold/palladium catalysts for the selective liquid phase oxidation of glycerol, *Catal. Lett.*, 2007, **115**, 133–136.
- [49] D. Wang, A. Villa, F. Porta, L. Prati and D. Su, Bimetallic gold/palladium catalysts: correlation between nanostructure and synergistic effects, *J. Phys. Chem. C*, 2008, **112**, 8617–8622.
- [50] G. Li, D. I. Enache, J. Edwards, A. F. Carley, D. W. Knight and G. J. Hutchings, Solvent-free oxidation of benzyl alcohol with oxygen using zeolite-supported Au and Au–Pd catalysts, *Catal. Lett.*, 2006, **110**, 7–13.
- [51] P. J. Miedziak, Z. Tang, T. E. Davies, D. I. Enache, J. K. Bartley, A. F. Carley, A. A. Herzing, C. J. Kiely, S. H. Taylor and G. J. Hutchings, Ceria prepared using supercritical antisolvent precipitation: a green support for gold–palladium nanoparticles for the selective catalytic oxidation of alcohols, *J. Mater. Chem.*, 2009, **19**, 8619–8627.
- [52] G. Li, J. Edwards, A. F. Carley and G. J. Hutchings, Direct synthesis of hydrogen peroxide from H₂ and O₂ using zeolite-supported Au-Pd catalysts, *Catal. Today*, 2007, **122**, 361–364.
- [53] D. Mott, J. Luo, P. N. Njoki, Y. Lin, L. Wang and C.-J. Zhong, Synergistic activity of gold-platinum alloy nanoparticle catalysts, *Catal. Today*, 2007, **122**, 378–385.
- [54] W. Tang, S. Jayaraman, T. F. Jaramillo, G. D. Stucky and E. W. McFarland, Electrocatalytic activity of gold–platinum clusters for low temperature fuel cell applications, *J. Phys. Chem. C*, 2009, **113**, 5014–5024.

- [55] M. D. Obradovic, A. V. Tripkovic and S. L. Gojkovic, The origin of high activity of Pt–Au surfaces in the formic acid oxidation, *Electrochim. Acta.*, 2009, **55**, 204–209.
- [56] M. Mirdamadi-Esfahani, M. Mostafavi, B. Keita, L. Nadjo, P. Kooyman and H. Remita, Bimetallic Au-Pt nanoparticles synthesized by radiolysis: application in electro-catalysis, *Gold Bull.*, 2010, **43**, 49–56.
- [57] S. Zhang, Y. Shao, H.-G. Liao, J. Liu, I. A. Aksay, G. Yin and Y. Lin, Graphene decorated with PtAu alloy nanoparticles: facile synthesis and promising application for formic acid oxidation, *Chem. Mater.*, 2011, **23**, 1079–1081.
- [58] Y. Gu, G. Wu, X. F. Hu, D. A. Chen, T. Hansen, H.-C. zur Loye and H. J. Ploehna, PAMAM-stabilized Pt–Ru nanoparticles for methanol electro-oxidation, *J. Power Sources*, 2010, **195**, 425–434.
- [59] S.-H. Chang, W.-N. Su, M.-H. Yeh, C.-J. Pan, K.-L. Yu, D.-G. Liu, J.-F. Lee and B.-J. Hwang, Structural and electronic effects of carbon-supported Pt_xPd_{1-x} nanoparticles on the electrocatalytic activity of the oxygen-reduction reaction and on methanol tolerance, *Chem. Eur. J.*, 2010, **16**, 11064–11071.
- [60] H. Over and A. P. Seitsonen, Oxidation of metal surfaces, *Science*, 2002, **297**, 2003–2005.
- [61] J. R. Croy, S. Mostafa, J. Liu, Y. Sohn and B. R. Cuenya, Size dependent study of MeOH decomposition over size-selected Pt nanoparticles synthesized via micelle encapsulation, *Catal. Lett.*, 2007, **118**, 1–7.

- [62] J. R. Croy, S. Mostafa, H. Heinrich and B. R. Cuenya, Size-selected Pt nanoparticles synthesized via micelle encapsulation: effect of pretreatment and oxidation state on the activity for methanol decomposition and oxidation, *Catal. Lett.*, 2009, **131**, 21–32.
- [63] J. R. Croy, S. Mostafa, J. Liu, Y. Sohn, H. Heinrich and B. R. Cuenya, Support dependence of MeOH decomposition over size-selected Pt nanoparticles, *Catal. Lett.*, 2007, **119**, 209–216.
- [64] J. R. Croy, S. Mostafa, L. Hickman, H. Heinrich and B. R. Cuenya, Bimetallic Pt/Metal catalysts for the decomposition of methanol: effect of secondary metal on the oxidation state, activity, and selectivity of Pt, *Appl. Catal. A-Gen.*, 2008, **350**, 207–216.
- [65] H. Over, Y. D. Kim, A. P. Seitsonen, S. Wendt, E. Lundgren, M. Schmid, P. Varga, A. Morgante and G. Ertl, Atomic-scale structure and catalytic reactivity of the RuO₂(110) surface, *Science*, 2000, **287**, 1474–1476.
- [66] D. R. Rolison, P. L. Hagans, K. E. Swider and J. W. Long, Role of hydrous ruthenium oxide in Pt–Ru direct methanol fuel cell anode electrocatalysts: the importance of mixed electron/proton conductivity, *Langmuir*, 1999, **15**, 774–779.
- [67] H. A. Gastgeiger, S. S. Kocha, B. Sompalli and F. T. Wagner, Activity benchmarks and requirements for Pt, Pt-alloy, and non-Pt oxygen reduction catalysts for PEMFCs, *Appl. Catal. B-Environ.*, 2005, **56**, 9–35.

- [68] L. Olsson and E. Fridell, The influence of Pt oxide formation and Pt dispersion on the reactions $\text{NO}_2 \rightleftharpoons \text{NO} + 1/2 \text{O}_2$ over Pt/Al₂O₃ and Pt/BaO/Al₂O₃, *J. Catal.*, 2002, **210**, 340–353.
- [69] V. A. T. Dam and F. A. de Bruijn, The stability of PEMFC electrodes platinum dissolution vs potential and temperature investigated by quartz crystal microbalance, *J. Electrochem. Soc.*, 2007, **154**, B494–B499.
- [70] R. A. Sheldon, I. Arends and U. Hanefeld, Green chemistry and catalysis, WILEY-VCH Verlag GmbH & Co. KGaA, **2007**.
- [71] P. T. Anastas, L. B. Bartlett, M. M. Kirchhoff and T. C. Williamson, The role of catalysis in the design, development, and implementation of green chemistry, *Catal. Today*, 2000, **55**, 11–22.
- [72] N. R. Shiju and V. V. Guliants, Recent developments in catalysis using nanostructured materials, *Appl. Catal. A-Gen.*, 2009, **356**, 1–17.
- [73] I. W. C. E Arends and R. A. Sheldon, Modern oxidation methods, WILEY-VCH Verlag GmbH & Co. KGaA, **2010**.
- [74] G. L. Brett, Q. He, C. Hammond, P. J. Miedziak, N. Dimitratos, M. Sankar, A. A. Herzing, M. Conte, J. A. Lopez-Sanchez, C. J. Kiely, D. W. Knight, S. H. Taylor and G. J. Hutchings, Selective oxidation of glycerol by highly active bimetallic catalysts at ambient temperature under base-free conditions, *Angew. Chem. Int. Ed.*, 2011, **50**, 10136–10139.
- [75] N. Dimitratos, J. A. Lopez-Sanchez, J. M. Anthonykuty, G. Brett, A. F. Carley, R. C. Tiruvalam, A. A. Herzing, C. J. Kiely, D. W. Knight and G. J.

- Hutchings, Oxidation of glycerol using gold–palladium alloy-supported nanocrystals, *Phys. Chem. Chem. Phys.*, 2009, **11**, 4952–4961.
- [76] C. P. Vinod, K. Wilson and A. F. Lee, Recent advances in the heterogeneously catalysed aerobic selective oxidation of alcohols, *J. Chem. Technol. Biotechnol.*, 2011, **86**, 161–171.
- [77] <http://www.kitco.com/charts/historicalgold.html>
- [78] S. Lux, P. Stehring and M. Siebenhofer, *Separ.* Lactic acid production as a new approach for exploitation of glycerol, *Sci. Technol.*, 2010, **45**, 1921–1927.
- [79] S. Carrettin, P. McMorn, P. Johnston, K. Griffin and G. J. Hutchings, Selective oxidation of glycerol to glyceric acid using a gold catalyst in aqueous sodium hydroxide, *Chem. Commun.*, 2002, 696–697.
- [80] S. Carrettin, P. McMorn, P. Johnston, K. Griffin, C. J. Kiely and G. J. Hutchings, Oxidation of glycerol using supported Pt, Pd and Au catalysts, *Phys. Chem. Chem. Phys.*, 2003, **5**, 1329–1336.
- [81] F. Porta and L. Prati, Selective oxidation of glycerol to sodium glycerate with gold-on-carbon catalyst: an insight into reaction selectivity, *J. Catal.*, 2004, **224**, 397–403.
- [82] N. Dimitratos, F. Porta and L. Prati, Au, Pd (mono and bimetallic) catalysts supported on graphite using the immobilisation method: synthesis and catalytic testing for liquid phase oxidation of glycerol, *Appl. Catal. A-Gen.*, 2005, **291**, 210–214.

- [83] C. L. Bianchi, P. Canton, N. Dimitratos, F. Porta and L. Prati, Selective oxidation of glycerol with oxygen using mono and bimetallic catalysts based on Au, Pd and Pt metals, *Catal. Today*, 2005, **102**, 203–212.
- [84] S. Demirel-Gülen, M. Lucas and P. Claus, Liquid phase oxidation of glycerol over carbon supported gold catalysts, *Catal. Today*, 2005, **102–103**, 166–172
- [85] N. Dimitratos, C. Messi, F. Porta, L. Prati and A. Villa, Investigation on the behaviour of Pt(0)/carbon and Pt(0),Au(0)/carbon catalysts employed in the oxidation of glycerol with molecular oxygen in water, *J. Mol. Catal., A*, 2006, **256**, 21–28.
- [86] N. Dimitratos, J. A. Lopez-Sanchez, D. Lennon, F. Porta, L. Prati and A. Villa, Effect of particle size on monometallic and bimetallic (Au,Pd)/C on the liquid phase oxidation of glycerol, *Catal. Lett.*, 2006, **108**, 147–153.
- [87] N. Dimitratos, A. Villa, C. L. Bianchi, L. Prati and M. Makkee, Gold on titania: effect of preparation method in the liquid phase oxidation, *Appl. Catal. A-Gen.*, 2006, **311**, 185–192.
- [88] S. Demirel, P. Kern, M. Lucas and P. Claus, Oxidation of mono- and polyalcohols with gold: comparison of carbon and ceria supported catalysts, *Catal. Today*, 2007, **122**, 292–300.
- [89] S. Demirel, M. Lucas, J. Wärnä, T. Salmi, D. Murzin and P. Claus, Reaction kinetics and modelling of the gold catalysed glycerol oxidation, *Top. Catal.*, 2007, **44**, 299–305
- [90] S. E. Davis, Ma. S. Ide and R. J. Davis, Selective oxidation of alcohols and aldehydes over supported metal nanoparticles, *Green Chem.*, 2013, **15**, 17–45.

- [91] S. Demirel, K. Lehnert, M. Lucas and P. Claus, Use of renewables for the production of chemicals: glycerol oxidation over carbon supported gold catalysts, *Appl. Catal. B-Environ.*, 2007, **70**, 637-643.
- [92] W. Ketchie, Y. Fang, M. Wong, M. Murayama and R. J. Davis, Influence of gold particle size on the aqueous-phase oxidation of carbon monoxide and glycerol, *J. Catal.*, 2007, **250**, 94-101.
- [93] W. C. Ketchie, M. Murayama and R. J. Davis, Promotional effect of hydroxyl on the aqueous phase oxidation of carbon monoxide and glycerol over supported Au catalysts, *Top. Catal.*, 2007, **44**, 307-317.
- [94] W. Ketchie, M. Murayama and R. J. Davis, Selective oxidation of glycerol over carbon-supported AuPd catalysts, *J. Catal.*, 2007, **250**, 264-273.
- [95] E. Taarning, A. T. Madsen, J. M. Marchetti, K. Egeblad and C. H. Christensen, Oxidation of glycerol and propanediols in methanol over heterogeneous gold catalysts, *Green Chem.*, 2008, **10**, 408-414.
- [96] J. Gao, D. Liang, P. Chen, Z. Hou and X. Zheng, Oxidation of glycerol with oxygen in a base-free aqueous solution over Pt/AC and Pt/MWNTs catalysts, *Catal. Lett.*, 2009, **130**, 185-191.
- [97] A. Brandner, K. Lehnert, A. Bienholz, M. Lucas and P. Claus, Production of biomass-derived chemicals and energy: chemocatalytic conversions of glycerol, *Top. Catal.*, 2009, **52**, 278-287.
- [98] D. Liang, J. Gao, J. Wang, P. Chen, Z. Hou and X. Zheng, Selective oxidation of glycerol in a base-free aqueous solution over different sized Pt catalysts, *Catal. Commun.*, 2009, **10**, 1586-1590.

- [99] B. N. Zope and R. J. Davis, Influence of reactor configuration on the selective oxidation of glycerol over Au/TiO₂, *Top. Catal.*, 2009, **52**, 269–277.
- [100] N. Dimitratos, J. A. Lopez-Sanchez, J. M. Anthonykutti, G. Brett, A. F. Carley, R. C. Tiruvalam, A. A. Herzing, C. J. Kiely, D. W. Knight and G. Hutchings, Oxidation of glycerol using gold–palladium alloy-supported nanocrystals, *Phys. Chem. Chem. Phys.*, 2009, **11**, 4952–4961.
- [101] B. N. Zope, D. D. Hibbitts, M. Neurock and R. J. Davis, reactivity of the gold/water interface during selective oxidation catalysis, *Science*, 2010, **330**, 74–78.
- [102] E.G. Rodrigues, S.A.C. Carabineiro, J.J. Delgado, X. Chen, M.F.R. Pereira, J.J.M. Órfão, Gold supported on carbon nanotubes for the selective oxidation of glycerol, *J. Cat.*, 2012, **285**, 83–91.
- [103] E. G. Rodrigues, M. F. R. Pereira, X. Chen, J. J. Delgado and J. J. M. Órfão, Influence of activated carbon surface chemistry on the activity of Au/AC catalysts in glycerol oxidation, *J. Catal.*, 2011, **281**, 119–127.
- [104] D. Liang, J. Gao, H. Sun, P. Chen, Z. Hou and X. Zheng, Selective oxidation of glycerol with oxygen in a base-free aqueous solution over MWNTs supported Pt catalysts, *Appl. Catal. B-Environ.*, 2011, **106**, 423–432.
- [105] Z. Huang, F. Li, B. Chen, F. Xue, Y. Yuan, G. Chen and G. Yuan, Efficient and recyclable catalysts for selective oxidation of polyols in H₂O with molecular oxygen, *Green Chem.*, 2011, **13**, 3414–3422.
- [106] S. Gil, M. Marchena, L. Sánchez-Silva, A. Romero, P. Sánchez and J. L. Valverde, Effect of the operation conditions on the selective oxidation of

- glycerol with catalysts based on Au supported on carbonaceous materials, *Chem. Eng. J.*, 2011, **178**, 423–435.
- [107] L. Prati, F. Porta, D. Wang and A. Villa, Ru modified Au catalysts for the selective oxidation of aliphatic alcohols, *Catal. Sci. Technol.*, 2011, **1**, 1624–1629.
- [108] A. Tsuji, K. T. V. Rao, S. Nishimura, A. Takaga and K. Ebitani, Selective oxidation of glycerol by using a hydrotalcite-supported platinum catalyst under atmospheric oxygen pressure in water, *ChemSusChem*, 2011, **4**, 542–548.
- [109] E. G. Rodrigues, S. A. C. Carabineiro, J. J. Delgado, X. Chen, M. F. R. Pereira and J. J. M. Órfão, Gold supported on carbon nanotubes for the selective oxidation of glycerol, *J. Catal.*, 2012, **285**, 83–91.
- [110] S.-S. Liu, K.-Q. Sun, B.-Q. Xu, Specific selectivity of Au-catalyzed oxidation of glycerol and other C₃-polyols in water without the presence of a base, *ACS Catal.*, 2014, **4**, 2226–2230.
- [111] L. Prati, A. Villa, C. Campione and P. Spontoni, Effect of gold addition on Pt and Pd catalysts in liquid phase oxidations, *Top. Catal.*, 2007, **44**, 319–324.
- [112] L. Prati, P. Spontoni and A. Gaiassi, From renewable to fine chemicals through selective oxidation: the case of glycerol, *Top. Catal.*, 2009, **52**, 288–296.
- [113] N. Dimitratos, A. Villa and L. Prati, Liquid phase oxidation of glycerol using a single phase (Au-Pd) alloy supported on activated carbon: effect of reaction conditions, *Cal. Lett.*, 2009, **133**, 334–340.

- [114] D. Liang, J. Gao, J. Wang, P. Chen, Y. Wei and Z. Hou, *Catal. Commun.*, 2011, **12**, 1059.
- [115] Z. Zhao, J. Arentz, L. A. Pretzer, P. Limpornpipat, J. M. Clomburg, R. Gonzalez, N. M. Schweitzer, T. Wu, J. T. Miller, M. S. Wong, Volcano-shape glycerol oxidation activity of palladium-decorated gold nanoparticles, *Chem. Sci.*, 2014 (DOI: 10.1039/c4sc01001a).
- [116] K. Dubencovs, S. Chornaja, E. Sproge, V. Kampars, D. Markova, L. Kulikova, V. Serga, A. Cvetkovs, Novel fine-disperse bimetallic Pt-Pd/Al₂O₃ catalysts for glycerol oxidation with molecular oxygen, *Mater. Sci. Eng.*, 2013, **49**, 012002.
- [117] S. A. Kondrat, P. J. Miedziak, M. Douthwaite, G. L. Brett, T. E. Davies, D. J. Morgan, J. K. Edwards, D. W. Knight, C. J. Kiely, S. H. Taylor, G. J. Hutchings, Base-free oxidation of glycerol using titania-supported trimetallic Au-Pd-Pt nanoparticles, *ChemSusChem*, 2014, **7**, 1326–1334
- [118] L. Prati and M. Rossi, *J. Catal.*, 1998, **176**, 552.
- [119] C. Bianchi, F. Porta, L. Prati and M. Rossi, *Top. Catal.*, 2000, **13**, 231.
- [120] S. Biella, G. L. Castiglioni, C. Fumagalli, L. Prati and M. Rossi, Application of gold catalysts to selective liquid phase oxidation, *Catal. Today*, 2002, **72**, 43–49.
- [121] R. S. Disselkamp, B. D. Harris and T. R. Hart, Hydroxy acetone and lactic acid synthesis from aqueous propylene glycol/hydrogen peroxide catalysis on Pd-black, *Catal. Commun.*, 2008, **9**, 2250–2252.

- [122] N. Dimitratos, J. A. Lopez-Sanchez, S. Meenakshisundaram, J. M. Anthonykutty, G. Brett, A. F. Carley, S. H. Taylor, D. W. Knight and G. J. Hutchings, Selective formation of lactate by oxidation of 1,2-propanediol using gold palladium alloy supported nanocrystals, *Green Chem.*, 2009, **11**, 1209–1216.
- [123] H. Ma, X. Nie, J. Y. Cai, C. Chen, J. Gao, H. Miao and J. Xu, Au/Mg(OH)₂: Highly efficient for selective oxidation of 1,2-propanediol to lactic acid with molecular oxygen, *Sci. China: Chem.*, 2010, **53**, 1497–1501.
- [124] G. L. Brett, P. J. Miedziak, N. Dimitratos, J. A. Lopez-Sanchez, N. F. Dummer, R. Tiruvalam, C. J. Kiely, D. W. Knight, S. H. Taylor, D. J. Morgan, A. F. Carley and G. J. Hutchings, Oxidative esterification of 1,2-propanediol using gold and gold-palladium supported nanoparticles, *Catal. Sci. Technol.*, 2012, **2**, 97–104.
- [125] S. Sugiyama, H. Tanaka, T. Bando, K. Nakagawa, K.-I. Sotowa, Y. Katou, T. Mori, T. Yasukawa and W. Ninomiya, Liquid-phase oxidation of propylene glycol using heavy-metal-free Pd/C under pressurized oxygen, *Catal. Today*, 2013, **203**, 116–121.
- [126] Y. Ryabenkova, Q. He, P. J. Miedziak, N. F. Dummer, S. H. Taylor, A. F. Carley, D. J. Morgan, N. Dimitratos, D. J. Willock, D. Bethell, D. W. Knight, D. Chadwick, C. J. Kiely, G. J. Hutchings, The selective oxidation of 1,2-propanediol to lactic acid using mild conditions and gold-based nanoparticulate catalysts, *Catal. Today*, 2013, **203**, 139–145.

- [127] H. Kimura and K. Tsuto, Selective oxidation of glycerol on a platinum-bismuth catalyst, *Appl. Catal. A-Gen.*, 1993, **96**, 217-228.
- [128] P. Gallezot, Selective oxidation with air on metal catalysts, *Catal. Today*, 1997, **37**, 405-418.
- [129] A. Villa, C. Campione and L. Prati, Bimetallic gold/palladium catalysts for the selective liquid phase oxidation of glycerol, *Catal. Lett.*, 2007, **115**, 133-136.
- [130] R. Garcia, M. Besson and P. Gallezot, Chemoselective catalytic oxidation of glycerol with air on platinum metals, *Appl. Catal. A-Gen.*, 1995, **127**, 165-176.
- [131] N. Dimitratos, J. A. Lopez-Sanchez and G. J. Hutchings, Selective liquid phase oxidation with supported metal nanoparticles, *Chem. Sci.*, 2012, **3**, 20-44.
- [132] E. Auer, A. Freund, J. Pietsch and T. Tacke, Carbons as supports for industrial precious metal catalysts, *Appl. Catal. A-Gen.*, 1998, **173**, 259-271.
- [133] A. Villa, A. Gaiassi, I. Rossetti, C. L. Bianchi, K. van Benthem, G. M. Veith and L. Prati, Au on MgAl₂O₄ spinels: the effect of support surface properties in glycerol oxidation, *J. Catal.*, 2010, **275**, 108-116.
- [134] K. Motokura, N. Fujita, K. Mori, T. Mizugaki, K. Ebitani, K. Jitsukawa and K. Kaneda, Environmentally friendly one-pot synthesis of α -alkylated nitriles using hydrotalcite-supported metal species as multifunctional solid catalysts, *Chem. Eur. J.*, 2006, **12**, 8228-8239.

- [135] K. Ebitani, K. Motokura, K. Mori, T. Mizugaki and K. Kaneda, Reconstructed hydrotalcite as a highly active heterogeneous base catalyst for carbon-carbon bond formations in the presence of water, *J. Org. Chem.*, 2006, **71**, 5440–5447.
- [136] K. Motokura, D. Nishimura, K. Mori, T. Mizugaki, K. Ebitani and K. Kaneda, A ruthenium-grafted hydrotalcite as a multifunctional catalyst for direct α -alkylation of nitriles with primary alcohols, *J. Am. Chem. Soc.*, 2004, **126**, 5662–5663.
- [137] K. Kaneda, T. Mitsudome, T. Mizugaki and K. Jitsukawa, Development of heterogeneous olympic medal metal nanoparticle catalysts for environmentally benign molecular transformations based on the surface properties of hydrotalcite, *Molecules*, 2010, **15**, 8988–9007.
- [138] K. Ebitani, K. Motokura, T. Mizugaki and K. Kaneda, Heterotrimetallic rnmnm species on a hydrotalcite surface as highly efficient heterogeneous catalysts for liquid-phase oxidation of alcohols with molecular oxygen, *Angew. Chem. Int. Ed.*, 2005, **44**, 3423–3426.
- [139] A. Zecchina, E. Groppo and S. Bordiga, Selective catalysis and nanoscience: an inseparable pair, *Chem. Eur. J.*, 2007, **13**, 2440–2460.
- [140] H. Lee, S. E. Habas, S. Kweskin, D. Butcher, G. A. Somorjai and P. Yang, Morphological control of catalytically active platinum nanocrystals, *Angew. Chem.*, 2006, **118**, 7988–7992.

- [141] H. Lee, S. E. Habas, S. Kweskin, D. Butcher, G. A. Somorjai and P. Yang, Morphological control of catalytically active platinum nanocrystals, *Angew. Chem. Int. Ed.*, 2006, **45**, 7824–7828.
- [142] A. Villa, D. Wang, D. S. Su and L. Prati, Gold sols as catalysts for glycerol oxidation: the role of stabilizer, *ChemCatChem*, 2009, **1**, 510–514.
- [143] G.-R. Zhang and B.-Q. Xu, Surprisingly strong effect of stabilizer on the properties of Au nanoparticles and Pt⁺Au nanostructures in electrocatalysis, *Nanoscale*, 2010, **2**, 2798–2804.
- [144] P. Zhang and T. K. Sham, Tuning the electronic behavior of Au nanoparticles with capping molecules, *Appl. Phys. Lett.*, 2002, **81**, 736–738.
- [145] L. Qiu, F. Liu, L. Z. Zhao, W. Yang and J. Yao, Evidence of a unique electron donor–acceptor property for platinum nanoparticles as studied by XPS, *Langmuir*, 2006, **22**, 4480–4482.
- [146] M. Okumura, Y. Kitagawa, T. Kawakami and M. Haruta, Theoretical investigation of the hetero-junction effect in PVP-stabilized Au₁₃ clusters. The role of PVP in their catalytic activities, *Chem. Phys. Lett.*, 2008, **459**, 133–136.
- [147] H. Tsunoyama, N. Ichikuni, H. Sakurai and T. Tsukuda, Effect of electronic structures of Au clusters stabilized by poly(*N*-vinyl-2-pyrrolidone) on aerobic oxidation catalysis, *J. Am. Chem. Soc.*, 2009, **131**, 7086–7093.
- [148] Y. Li and M. A. El-Sayed, The effect of stabilizers on the catalytic activity and stability of Pd colloidal nanoparticles in the suzuki reactions in aqueous solution, *J. Phys. Chem. B*, 2001, **105**, 8938–8943.

- [149] J. N. Kuhn, C.-K. Tsung, W. Huang and G. A. Somorjai, Effect of organic capping layers over monodisperse platinum nanoparticles upon activity for ethylene hydrogenation and carbon monoxide oxidation, *J. Catal.*, 2009, **265**, 209–215.
- [150] N. Vigneshwaran, R. P. Nachane, R. H. Balasubramanya and P. V. Varadarajan, A novel one-pot ‘green’ synthesis of stable silver nanoparticles using soluble starch, *Carbohydr. Res.*, 2006, **341**, 2012–2018.
- [151] D. Tongsakul, K. Wongravee, C. Thammacharoen and S. Ekgasit, Enhancement of the reduction efficiency of soluble starch for platinum nanoparticles synthesis, *Carbohydr. Res.*, 2012, **357**, 90–97.
- [152] T. K. Sarma and A. Chattopadhyay, Starch-mediated shape-selective synthesis of Au nanoparticles with tunable longitudinal plasmon resonance, *Langmuir*, 2004, **20**, 3520–3524.
- [153] S. Chairam, C. Poolperm and E. Somsook, Starch vermicelli template-assisted synthesis of size/shape-controlled nanoparticles, *Carbohydr. Polym.*, 2009, **75**, 694–704.
- [154] C. J. Knill and J. F. Kennedy, Degradation of cellulose under alkaline conditions, *Carbohydr. Polym.*, 2003, **51**, 281–300.
- [155] M. A. Clarke, L. A. Edye and G. Eggleston, *Advances in carbohydrate chemistry and biochemistry*, Academic Press, Washington, DC, **1997**.

Chapter 2

DEVELOPMENT OF NOVEL STARCH-STABILIZED SUPPORTED PLATINUM NANOPARTICLES AS HETEROGENEOUS AND REUSABLE CATALYST FOR SELECTIVE GLYCEROL OXIDATION

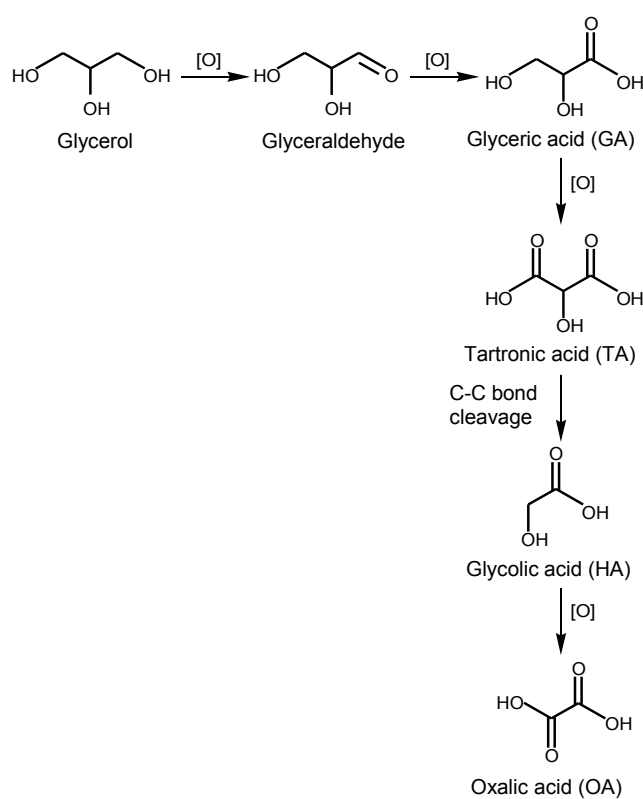
1. Introduction

Recently, many studies have used an eco-friendly method for synthesis of nanomaterials.^{[1]-[3]} It is well-known that a green synthesis method based on green chemistry principles not only involves production of environmentally friendly materials (e.g., reducing agent, stabilizing agent and solvent) but also design of the new reaction pathway (e.g., synthesis under atmospheric pressure).^{[3]-[5]} There are few reports that use the green method for synthesis of a metal catalyst, especially platinum (Pt)-based catalyst. For instance, Adlim *et al.* prepared chitosan-stabilized Pt NPs catalyst by reduction using methanol or NaBH₄.^[6] The results showed 99.99% selectivity and conversion of cyclooctene hydrogenation to cyclooctane as prepared by methanol reduction. Yang *et al.* reported a one-step preparation of Pt nanoparticles (NPs) using amino-functionalized dextran, which acts as a reducing and a protection agent.^[7] They showed good catalytic efficiency for the electron-transfer reaction

between hexacyanoferrate(III) and thiosulfate ions and also reported the synthesis of nanowire-like Pt nanostructures (NSs) in one step using dextran as a reducing agent. The immobilized nanowire-like Pt NSs on a glassy carbon electrode exhibited an excellent electrocatalytic activity for the reduction of oxygen, produced high specific current in the hydrogen region from -0.2 to 0.15 V.^[8] Johnson *et al.* synthesized carbon-supported Pt NPs using cellulose nanocrystals as a reducing agent.^[9] They showed high catalytic activity toward electrocatalysis for the oxygen reduction reaction. Upon scanning the potential in a positive direction a series of peaks due to desorption of hydrogen was observed between 0.0 V and 0.3 V.

Glycerol (GLY) is one of the byproducts from industries, especially from the biodiesel industry. As there is an increase in biodiesel production, the GLY from the process has also been produced in large quantities. Many researches have been conducted to the innovative utilizations of GLY. Possessing three hydroxyl groups, GLY is a potential starting material for several high-value fine chemicals, e.g., food, cosmetics and pharmaceutical industries.^{[10],[11]} It could be transformed into value-added chemicals by employing different chemical reactions^[12] such as hydrogenolysis,^{[13]-[15]} dehydration,^[16] and oxidation.^{[17],[18]} Because two primary hydroxyl groups in GLY have similar reactivity, they lead to poor selectivity. Therefore, a careful designing of the catalyst is required to achieve a high selectivity of the desired compounds. Pt-based metal has been reported to be an oxidation

catalyst, especially for the GLY oxidation. The oxidation reaction at the primary position of GLY can produce the carboxylic acids, such as glyceric acid (GA), tartronic acid (TA) and oxalic acid (OA) (Scheme 1). These acids are mainly converted into various market products, e.g., polymer and biodegradable emulsifiers, particularly GA that can be used for treatment of skin disorders, anionic monomer of packaging materials for volatile agent and biodegradable fabric softener.^{[19]-[22]}



Scheme 1 A reaction pathway of GLY oxidation.

Catalytic oxidation of GLY has been reported for both mono- and bimetallic catalyst.^{[18],[23]-[38]} Huang *et al.* developed Pt/carbon spherule catalyst, which gave GA (7.63 mmol) with 82% selectivity when 8 mmol of NaOH and 1.0 MPa oxygen pressure were applied.^[39] Liang *et al.* studied selective oxidation of GLY with

molecular oxygen over different functionalized MWNTs (multiwall carbon nanotubes) supported Pt catalysts.^[40] GA was formed with 68.3% selectivity (90.4% conversion of GLY) on Pt/S-MWNTs in base-free aqueous solution under oxygen flow ($150 \text{ cm}^3 \cdot \text{min}^{-1}$). Villa *et al.* reported the base-free aqueous-phase oxidation of GLY using AuPt NPs supported on the zeolite H-mordenite.^[41] It gave GA with a selectivity of 81% at full conversion under an oxygen pressure of 3 atm and temperature of 373 K. In the past decade, the transformation of GLY to value-added products tends to be performed under base-free conditions to allow free products rather than the salt form. However, pressured oxygen, large of flow rate (e.g., $150 \text{ mL} \cdot \text{min}^{-1}$) and/or high reaction temperature were required for the significant activity in the many works. Hence, the development of a highly efficient catalyst for the GLY oxidation in base-free and mild reaction conditions has been a challenging task.

In this chapter, I developed the hydrotalcite-supported platinum nanoparticles catalysts (Pt NPs/HT) for selective oxidation of GLY in base-free aqueous solution with molecular oxygen as an oxidant under atmospheric pressure. Very recently, I successfully found a Green synthesis method using soluble starch as a reducing and a stabilizing agent for the synthesis of Pt NPs.^[42] In this method, metal NPs were generated by the reduction of metal precursor with a reducing agent and then, they were immobilized on the support material. The advantages of this methodology are the reproducibility of particle size and control of particle size distribution. Therefore, the developed method was employed for the preparation of Pt NPs/HT catalyst. HT is layered double hydroxide which possesses basicity derived from OH^- and/or HCO_3^- on their surface.^{[43]-[46]} Hence, the oxidation reaction could occur in a base-free

condition when HT is used as the solid base support material. The objective of this chapter is to explore novel green synthesis of Pt-based heterogeneous catalysts, and utilize as catalyst for selective oxidation of GLY in aqueous solution using molecular oxygen at 333 K.

2. Experiment

2.1 Chemicals

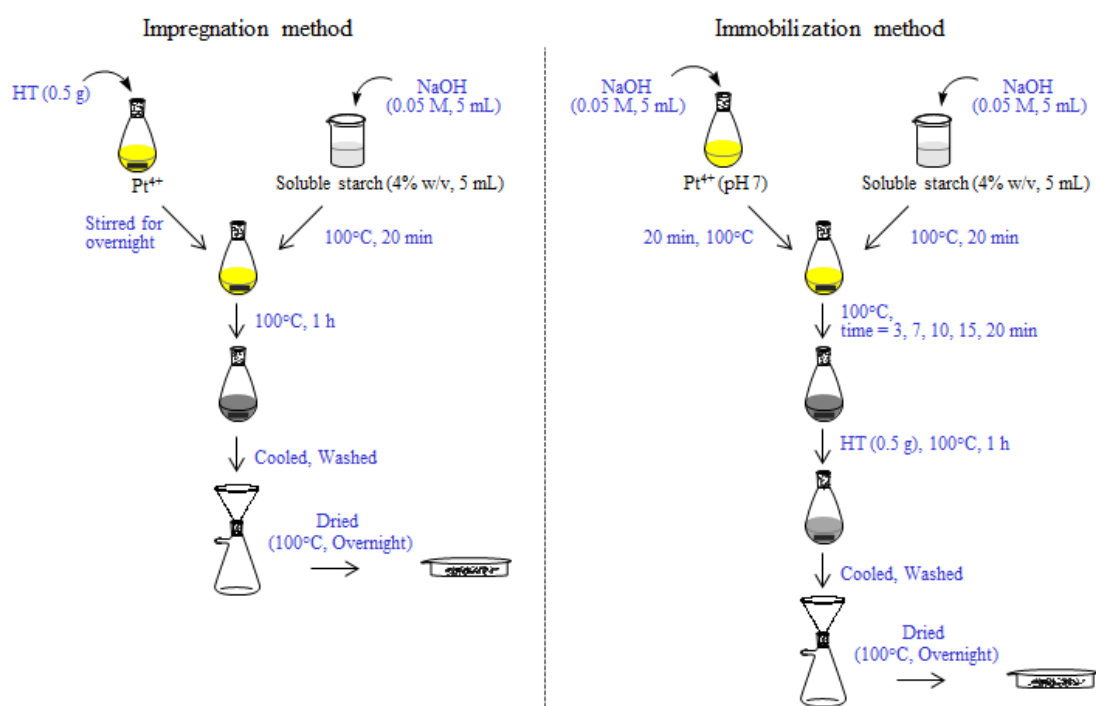
Hexachloroplatinic acid ($\text{H}_2\text{PtCl}_6 \cdot 6\text{H}_2\text{O}$, 99.9%; Cat. No: 089-05311) and soluble starch (Cat. No: 195-03961) were purchased from Wako Pure Chemicals Co, Ltd. (Japan). Sodium hydroxide (NaOH, 97%; Cat. No: 25012-31) was obtained from Kanto Chemicals Co, Ltd. GLY (99.9%; Cat. No: 17018-25) was provided from Nacalai Tesque. Hydrotalcite (HT, Mg/Al = 5, white powder; average particle size of 6.4 μm ; Cat. No: TOMITA-AD-550PF) was purchased from Tomita Pharmaceuticalm Co, Ltd. Platinum, 1 wt% on alumina (powder, Pt/Al₂O₃; Cat. No: 205966-25G), silica (granules, Pt/SiO₂; Cat. No: 52069-25G) and activated carbon (Pt/AC; Cat. No: 205923-5G) were received from Sigma-Aldrich.

2.2 Preparation of supported-Pt NPs catalysts

2.2.1 Impregnation method

Supported Pt catalysts were synthesized by the impregnation method using soluble starch as a reducing agent. Firstly, HT (0.5 g) was dispersed in an aqueous Pt (2.5 mM) solution which was prepared from $\text{H}_2\text{PtCl}_6 \cdot 6\text{H}_2\text{O}$ for overnight. A 4% w/v soluble starch solution was prepared by dissolving 4 g of soluble starch in hot water

(100 mL). After cooling, 5 mL fractions of starch solution were mixed with 5 mL of various concentrations (0.02–0.20 M) of NaOH. The Pt solution and the starch solution were heated at 373 K for 20 min before mixing under vigorous stirring and refluxed at 373 K for 1 h. Finally, the solution was cooled to room temperature, filtered and washed with deionized water. The solid catalyst was dried overnight at 373 K (see Scheme 2).



Scheme 2 Synthesis of Pt NPs/HT by a green synthesis method using starch as a reducing and a stabilizing agent in water.

2.2.2 Immobilization method

For the immobilization method, Pt NPs were synthesized using soluble starch as a reducing and a stabilizing agent.^[42] First, a defined volume of 2.5 mM Pt solution was prepared from $\text{H}_2\text{PtCl}_6 \cdot 6\text{H}_2\text{O}$. The pH of the solution was adjusted to neutral with

1 M NaOH. Separately, 5 mL fractions of the solution were individually pH adjusted with 5 mL of 0.05 M NaOH. A 4% w/v soluble starch solution was prepared by dissolving 4 g of soluble starch in hot water (100 mL). After cooling, 5 mL fractions of starch solution were mixed with 5 mL of 0.05 M NaOH. The Pt solution and the starch solution were heated at 373 K for 20 min before mixing under vigorous stirring. After 20 min, supports, i.e., HT and Mg(OH)₂ (0.5 g) was added to mixed solution under continuously vigorous stirring and refluxed at 373 K for 1 h. Finally, the solution was cooled to room temperature, filtered and washed with deionized water. The solid catalyst was dried overnight at 373 K (see Scheme 2). In addition, time-dependent studies on the generation of Pt NPs were conducted after reduction times of 3, 7, 10, 15 and 20 min. During each of the reduction time intervals, HT (0.5 g) was added to each of the mixed solutions under continuously vigorous stirring and also refluxed at 373 K for 1 h.

2.3 Characterization

The morphology of Pt NPs was analyzed by transmission electron microscopy (TEM; Hitachi H-7100) at 100 kV accelerating voltage. The Pt NPs/HT was dispersed in deionized water and dropped onto a copper grid, then dried overnight in a desiccator. Powder X-ray diffraction patterns were obtained with a Rigaku RINT2000 X-ray diffractometer using Cu K α radiation ($\lambda = 0.154$ nm) and a power of 40 kV and 20 mA. Perkin Elmer spectrum 100 FT-IR spectrometer attached with universal ATR sampling accessory was used for infrared spectral acquisition. Inductively coupled plasma atomic emission spectroscopy (ICP-AES) was operated by Shimadzu ICPS-

7000 ver.2 to estimate the real concentration of Pt on the catalyst. The surface area of HT was analyzed by the Brunauer-Emmett-Teller (BET) method using BELSORP-max (BEL JAPAN, INC.). X-ray absorption near-edge structure (XANES) in the Pt L_3 -edge was recorded at beamline BL01B1 of SPring-8 with the approval of the Japan Synchrotron Radiation Research Institute (JASRI) (Proposal No. 2011A1607). The Pt NPs/HT catalyst was grained and pressed to a pellet ($\phi \sim 10$ mm) for XANES analysis. The oxidation state of Pt was estimated from the Pt L_3 -edge XANES spectra with a linear relationship in the intensities of PtO₂ and Pt foil assigned to be 0 and 100% Pt⁰, respectively. Pattern fitting analysis of XANES spectra using Pt and PtO₂ was also examined. The obtained XANES spectra were analyzed using the Rigaku REX2000 software (ver. 2.5.7).

2.4 Catalytic activity for glycerol oxidation

A catalytic test of supported Pt NPs was evaluated for GLY oxidation in base-free aqueous solution using molecular oxygen. All were allowed to react in a 30 mL Schlenk tube attached to a reflux condenser. The typical reaction parameters were as follows: GLY (0.5 mmol), H₂O (2 mL), supported Pt NPs catalyst (16 mg), temperature (333 K), reaction time (6 h). In addition, the reaction was carried out under a stirring rate of 500 rpm and an oxygen flow of 10 mL·min⁻¹ by forcing oxygen into the Schlenk tube through a stainless-steel needle. After the reaction, the vessel was cooled to room temperature and the catalyst was separated by a Millex filter with 0.20 μ m pore size. The filtrate was analyzed by high performance liquid chromatography (HPLC) equipped with an Aminex HPX-87H column (Bio-Rad

Laboratories) and a refractive index (RI) detector. The analysis conditions were set as follows: eluent (aqueous solution of H₂SO₄ (10 mM)), flow rate (0.5 mL·min⁻¹), column temperature (323 K).

3. Results and Discussion

3.1 Screening of Green synthesis methods and supporting materials

There has been reported that the renewable materials such as polysaccharide can exhibit the functional groups with reducing potential (aldehyde and β-hydroxy ketone) under alkaline treatment.^{[47],[48]} My previous work reports the preparation of colloidal Pt NPs using soluble starch as a reducing and a stabilizing agent. The result indicates that the alkaline degradation of starch molecule is the key factor for the synthesis of Pt NPs. In addition, the generated reducing species related to the alkaline (NaOH) concentration. Under optimized conditions (NaOH (0.05 M), temperature (373 K), time (20 min), Pt ions (5 mM)), soluble starch could be degraded while simultaneously generating reducing species that converted Pt ions into Pt NPs without aggregation.^[42] Therefore, this condition was employed for the preliminary development of Pt NPs/HT heterogeneous catalyst.

The preparation of Pt NPs/HT catalysts by the impregnation and the immobilization method was examined. For the impregnation method, HT was dispersed in an aqueous Pt solution for overnight before reduction using degraded starch as a reducing agent (Scheme 2). After refluxed, washed and dried, the solid catalyst was employed for the oxidation of GLY in base-free aqueous solution at 333

K under atmospheric molecular oxygen. The activity over Pt NPs/HT catalysts was shown in Table 1, entries 1–3.

Table 1 Effect of NaOH concentrations during preparation of HT supported Pt ions ^a

Entry	Catalysts	Conc. of NaOH (M)	Conversion (%)	GA yield (%)
1 ^b	Pt NPs/HT	0.05	9	9
2 ^b	Pt NPs/HT	0.1	16	16
3 ^b	Pt NPs/HT	0.2	18	18
4 ^c	Pt NPs/HT	0.05	49	38

^aReaction conditions: GLY (0.5 mmol), water (5 mL), catalyst (14 mg), HT (Mg/Al = 5), oxygen (10 mL·min⁻¹), temperature (333 K), reaction time (6 h). Prepared by ^bimpregnation method and ^cimmobilization method, catalyst (16 mg).

Generally, the possible products from GLY oxidation at the primary hydroxyl position are glyceraldehyde, glyceric acid (GA), tartronic acid (TA), glycolic acid (HA), mesoxalic acid and oxalic acid (OA) (Scheme 1).^{[17],[18]} The reaction was accomplished by the oxidation of GLY molecule at the primary hydroxyl position to yield glyceraldehyde. Then it was further oxidized to GA, TA, HA and OA.^{[17],[37],[49],[50],[51]} A less activity was observed for the reduction of HT supported-Pt ions using starch treatment with 0.05 M NaOH (Table 1, entry 1). Further increase NaOH concentration, the activities were increased (Table 1, entries 2 and 3). As described, the reducing potential of starch was enhanced as increased NaOH concentration.^[42] Therefore, reduced Pt species are increased as increase NaOH concentration, leading to increase of Pt NPs in metallic state which act as the catalytic

active sites, GLY conversion is increased. However, it was suggested that the reducing potential of degraded starch was not enough for reduction of Pt ions which were expected to bind on the HT surface.

Next, Pt NPs/HT catalyst was prepared by the immobilization method using starch as a reducing and a stabilizing agent under alkaline treatment (see Scheme 2). Firstly, Pt NPs were generated, thereafter, Pt NPs were immobilized on HT surface. Catalytic performance for the aerobic oxidation of GLY was also carried out under same conditions (Table 1). The high catalytic activity (49% conversion and 38% GA yield) was observed (Table 1, entry 4). This implies that the reduction potential of degraded species of starch was enough for the generation of Pt NPs, and preserved the active Pt sites for the aerobic oxidation of GLY even after immobilization on the HT surface. This preliminary observation shows a good sign for the development of green method using a soluble starch, which is renewable and environmentally benign reagent as a reducing and stabilizing agent for the preparation of Pt NPs/HT heterogeneous catalyst in aqueous media. Detailed investigations were further discussed in next section.

To confirm the activity of Pt NPs/HT catalyst for the aerobic oxidation of GLY in base-free aqueous solution under mild conditions, the supported Pt NPs on various materials were also investigated as concluded in Table 2. The TEM images and particle size distribution histograms of Pt NPs supported on various materials were shown in Figure 1, and the average particle size was also summarized in Table 2. Pt NPs/HT showed high activity than other supports for the catalytic oxidation of GLY in base-free aqueous solution (Table 2, entry 3). The activity was much higher

than those of Pt NPs/MgO, Pt/SiO₂, Pt/Al₂O₃ and Pt/AC (Table 2, entries 1 and 3–5). The result showed activity is independent on Pt particles size. For instance, Pt NPs/MgO (Table 2, entries 1 and 5) revealed identical activity to Pt/AC despite the particle size of the former ones smaller than three times, and five times different in activity was found over Pt/SiO₂ and Pt NPs/HT with similar particle size (Table 2, entries 2 and 3). Therefore, it was assumed that different activities of catalysts were due to the basicity of support. It is well known that the catalysis for oxidation reaction of GLY at primary hydroxyl position strongly depend on the basicity of the reaction medium, because the external base can enhances a proton abstraction step of GLY.^[35] The results suggested that the basicity on the HT surface (Mg/Al = 5, base amount 0.16 mmol/g)^[50] which derived from surface OH⁻ and/or HCO₃⁻ species was strong enough for carrying out the reaction in base-free aqueous solution then exhibited the highest activity.

Table 2 Effect of support materials for the catalytic oxidation of GLY^a

Entry	Catalysts	Average Particle size (nm)	Conversion (%)	GA yield (%)
1	Pt NPs/MgO	1.3	10	6
2 ^b	Pt/SiO ₂	1.6	12	12
3 ^c	Pt NPs/HT	1.9	63	43
4 ^b	Pt/Al ₂ O ₃	3.1	6	5
5 ^b	Pt/AC	4.2	13	12

^aReaction conditions: GLY (0.5 mmol), water (2 mL), catalyst (14 mg), oxygen (10 mL·min⁻¹), temperature (323 K), reaction time (6 h). ^bCommercial catalysts. ^cHT (Mg/Al = 5).

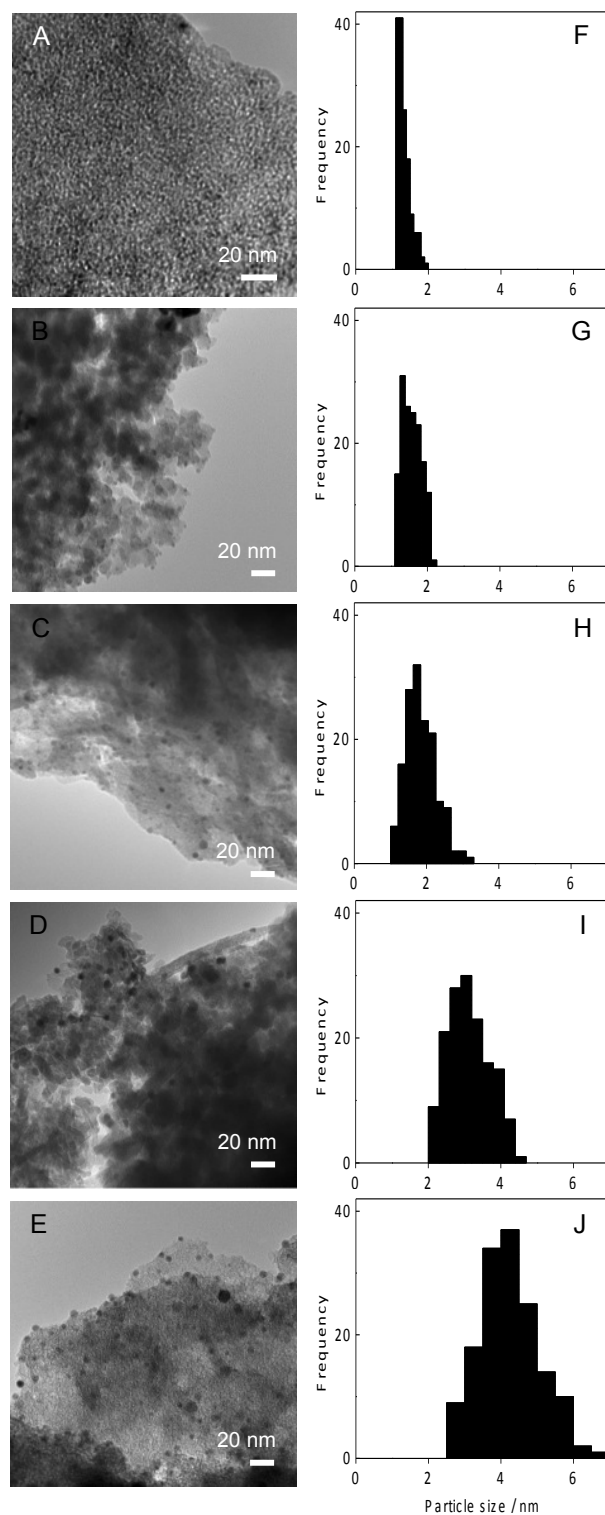


Figure 1 TEM images of Pt NPs supported on various materials: (A) MgOH, (B) SiO₂, (C) HT, (D) Al₂O₃ and (E) activated carbon and (F)–(J) their particle size distribution histograms.

3.2 An investigation of the immobilization time for Pt NPs/HT catalysts

As mentioned, starch-Pt NPs/HT catalyst prepared by the immobilization method possess highest activity. The reduction profile of colloidal Pt NPs using a starch as a reducing and a stabilizing agent indicated a sigmoidal shape with seed nucleation in the first period followed by a rapid particle growth (as suggested by LaMer^{[52],[53]} in colloidal growth mechanism).^[42] Therefore, it would expect that the immobilization of generated Pt NPs in each time interval may play an important role in the catalytic activity. In this section the time-dependence on the generation of Pt NPs before supported on the HT surface was systematically studied.

3.2.1 Characterization of Catalysts

Morphology of Pt NPs/HT catalysts prepared with various reduction times was characterized by TEM. Time-dependent studies on the generation of Pt NPs were conducted after reduction times of 3, 7, 10, 15 and 20 min. During each of the reduction time intervals, HT (0.5 g) was added to each of the mixed solutions under continuously vigorous stirring. The TEM images and particle size distribution histograms of Pt NPs/HT were shown in Figure 2. The size of Pt NPs on HT slightly increased with increasing reduction times, the average size being 0.9, 1.4, 1.9, 1.9 and 2.1 nm for 3, 7, 10, 15 and 20 min, respectively. It was clearly seen that Pt particle size increased as increasing the reduction time, and unchanged after 10 min. The observed phenomena corresponds to the formation mechanism of monodisperse NPs proposed by LaMer model. This model, the particle formation is separated into three stages: generation of atoms, nucleation and growth (see Chapter 1, Figure 8)^{[52],[53]}

Once the concentration of atoms reaches a point of supersaturation, the atoms start to aggregate into small clusters then grow in an accelerated manner and the concentration of metal atoms in solution drops. If metal atoms continuous supply, the nanocrystals will grow and increase in size until an equilibrium state reaching between the atoms on the surface of the nanocrystal and the atoms in the solution.

In addition, the oxidation state of platinum was estimated from the Pt L_3 -edge XANES spectra as shown in Figure 3. It was observed that the intensity of the white-line in the Pt L_3 -edge XANES spectra gradually decreased with increasing reducing time of Pt NPs. It means that the Pt⁰ concentration increased with the increasing reduction time (Table 3). I supposed that the surface of Pt NPs could be easily oxidized when exposed to air, which provided Pt oxides. It was indicated that the Pt particle size and Pt⁰ concentration can be controlled by the reduction time.

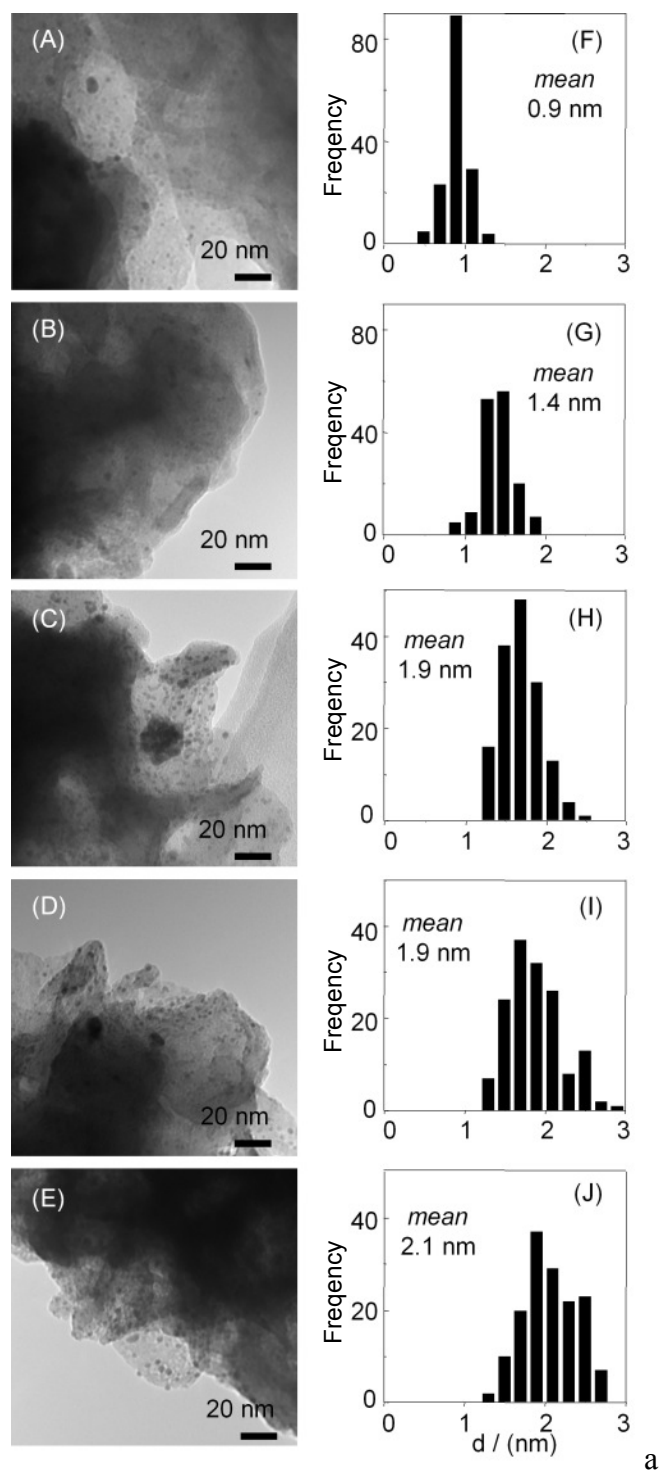


Figure 2 TEM images of HT supported-Pt NPs at various reduction times: (A) 3 min, (B) 7 min, (C) 10 min, (D) 15 min and (E) 20 min and (F)–(J) their particle size distribution histograms.

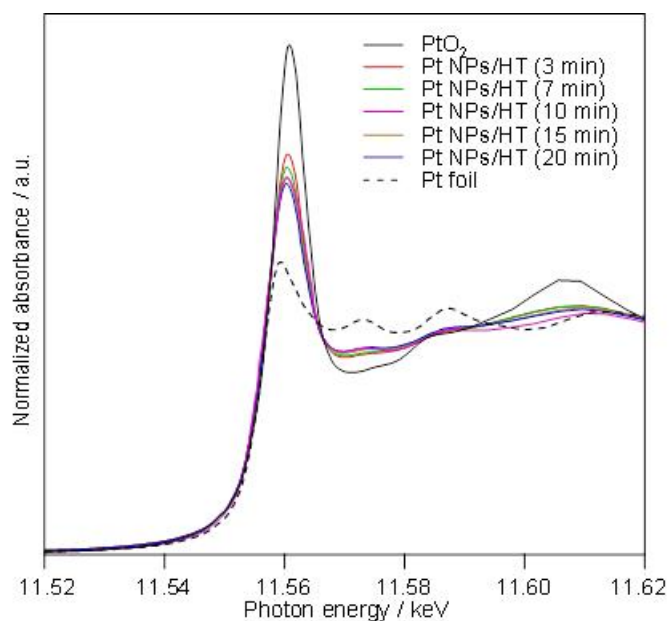


Figure 3 Pt L_3 -edge XANES spectra of Pt NPs/HT catalysts prepared with different reducing times

3.2.2 Oxidation of glycerol over Pt NPs/HT

The catalytic activity of Pt NPs/HT was evaluated for the selective oxidation of GLY in a base-free aqueous solution using molecular oxygen as an oxidant. The reaction was carried out in water at 333 K. The results are shown in Table 3 with the average particle size, Pt loading and Pt^0 concentration estimated by TEM, ICP-AES and XANES analyses, respectively. The GA was the main product in the all Pt NPs/HT catalysts as listed in Table 3. It was consistent with a previous report that the GLY oxidation in base-free aqueous solution catalyzed by supported-Pt heterogeneous catalyst, GA could be obtained as the major product.^{[31],[35]} The highest GLY conversion (80%) was achieved by Pt NPs/HT (3 min) though it exhibited a low selectivity toward GA (40%) (Table 3, entry 1). With increasing reduction time, the

GLY conversion decreased with increasing particle size of Pt NPs whereas the yield of GA slightly increased with increasing Pt⁰ concentration (Table 3, entries 1–5). It was indicated that Pt particle size and Pt⁰ concentration are related to both GLY conversion and yield of GA in the oxidation reaction of GLY. Pt NPs/HT (10 min) (Table 3, entry 3) was found to be the best catalyst when considered in terms of the yield and selectivity for GA with turnover number (TON) of 357.

Table 3 Effect of the reduction time of Pt NPs/HT catalyst for GLY oxidation^a

Entry	Catalysts ^b (Reduction time)	Conv. of GLY / %	Yield of GA / %	Sel. of GA / %	Pt loading / % ^c	TON	Particle size / nm ^d	Pt ⁰ conc. / % ^e
1	Pt NPs/HT (3 min)	80	32	40	0.92	212	0.9	50 (44)
2	Pt NPs/HT (7 min)	72	36	49	0.81	270	1.4	56 (49)
3	Pt NPs/HT (10 min)	55	41	75	0.70	357	1.9	61 (56)
4	Pt NPs/HT (15 min)	57	40	70	0.73	334	1.9	61 (55)
5	Pt NPs/HT (20 min)	49	38	77	0.74	313	2.1	64 (58)
6	blank	1	trace	29	-	-	-	-

^aReaction conditions: GLY (0.5 mmol), H₂O (5 mL), catalyst (16 mg), O₂ flow (10 mL·min⁻¹), 333 K, 6 h. ^b1 wt% Pt NPs supported onto HT (Mg/Al = 5). ^cAnalysis by ICP-AES.

^dDetermined by TEM. ^eEstimated by XANES analysis by intensity (pattern fitting).

3.2.2.1 Influence of initial concentration of glycerol

The influence of the initial concentration of GLY was evaluated using 0.7 wt % Pt NPs/HT catalyst reduced in 10 min. Table 4 shows the GLY conversion with initial GLY concentration in the range from 0.1 to 0.75 M. The conversion was increased to 63% with increasing GLY concentration from 0.1 to 0.25 M; however, that was gradually decreased to 42% with a further increase of the GLY concentration above 0.25 M. It may possibly suggest that there is a mass-transfer limitation in the initial concentration of GLY higher than 0.25 M. At all concentrations, the same products are being formed (i.e., GA, TA, HA and OA) and at GLY concentrations lower than 0.25 M, the sum of product selectivity is nearly 100% in all cases. This suggests that the overoxidation to C₁ products did not occur significantly over starch stabilized Pt NPs/HT catalyst which supposes that the excess oxygen absorption was limited with the starch coverage. However, the overoxidation can occur at GLY concentrations higher than 0.25 M; therefore, the sum of the selectivity for the above compounds is less than 100%. The maximum TON of 852 was obtained at 0.25 M GLY over Pt NP/HT^[49] while maximum TON of 625 was found at 0.3 M GLY over bare Pt/HT catalyst.^[50]

Table 4 Effect of initial concentration for GLY oxidation over Pt NPs/HT^a

Initial concentration GLY / M	Conversion of GLY / %	Selectivity / %			
		GA	TA	HA	OA
0.10 ^b	53	71	8	12	8
0.14 ^c	64	65	9	16	9
0.25 ^d	63	68	8	18	6
0.50 ^e	52	72	6	12	4
0.75 ^f	42	68	4	12	2

^aReaction conditions: GLY (0.5 mmol, GLY/metal = 1000), 0.7 wt% Pt NPs/HT catalyst (14 mg), H₂O (^b5 mL, ^c3.5 mL, ^d2 mL), O₂ flow (10 mL·min⁻¹), 323 K, 6 h. ^eGLY (1 mmol, GLY/metal = 2000), H₂O (2 mL). ^fGLY (1.5 mmol, GLY/metal = 3000), H₂O (2 mL).

3.2.2.2 Influence of glycerol/metal ratio

The influence of GLY/metal ratio was also examined as shown in Figure 4. The ratios of GLY/metal were varied in the range of 571–1424 mol/mol by changing the catalyst amount. At 571 mol/mol, the highest conversion with lowest GA selectivity was achieved, it was supposed due to high initial reaction rate bring about to rapid formation of the main product (i.e., GA) which can further oxidized to by-products (e.g., TA, HA and OA). As increase GLY/metal ratio, higher GA yield (63% selectivity) was observed. Further increase GLY/metal ratio, both GLY conversion and GA yield gradually dropped. It had been reported that the initial reaction rate of the GLY oxidation depends on the catalyst amount.^[24] Then, the result suggested that less amount of catalyst, less metal active sites resulted in low activity. The optimum GLY/metal ratio of 715 (catalyst 14 mg) was achieved in terms of GA yield.

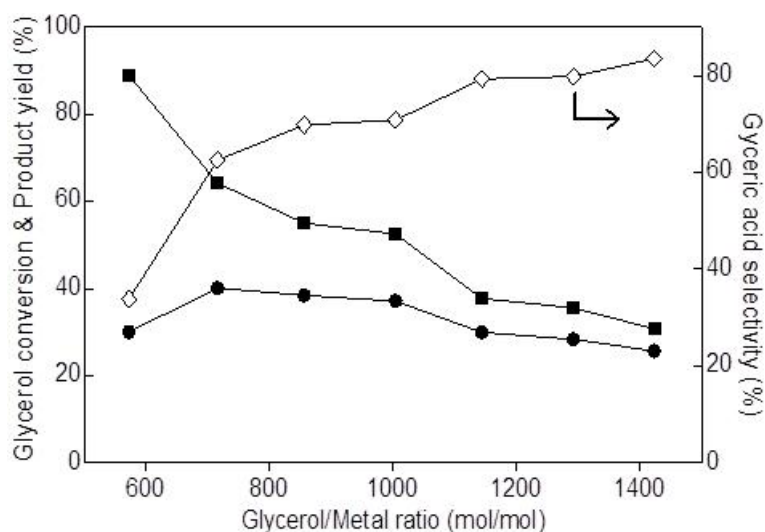


Figure 4 Reaction profile of GLY oxidation catalyzed by 0.7 wt% Pt NPs/HT at various GLY/metal ratios. GLY conversion (■: close square), glyceric acid yield (●: close circle) and glyceric acid selectivity (◇: diamond). Reaction conditions: GLY (0.5 mmol), H₂O (5 ml), temperature (333 K), reaction time (6 h), O₂ flow (10 mL·min⁻¹).

3.2.2.3 Influence of oxygen flow rate

Influence of oxygen flow rate on the aerobic glycerol oxidation was also estimated as shown in Figure 5. The oxygen flow rates were varied from 5 to 30 mL·min⁻¹. Increasing oxygen flow rate from 5 to 10 mL·min⁻¹, GLY conversion much increased significantly from 29% to 63% together with increased GA yield from 23% to 43%. These suggest to the limitation of gas-liquid oxygen diffusion under atmospheric conditions, since the concentration of dissolved oxygen in the aqueous media is known to depend on the oxygen partial pressure.^[53] Further increase oxygen flow rates from 10 to 30 mL·min⁻¹, no significant change in activity was observed.

The result indicated that the oxygen flow rate of $10 \text{ mL}\cdot\text{min}^{-1}$ is adequate to the further experiments for the glycerol oxidation.

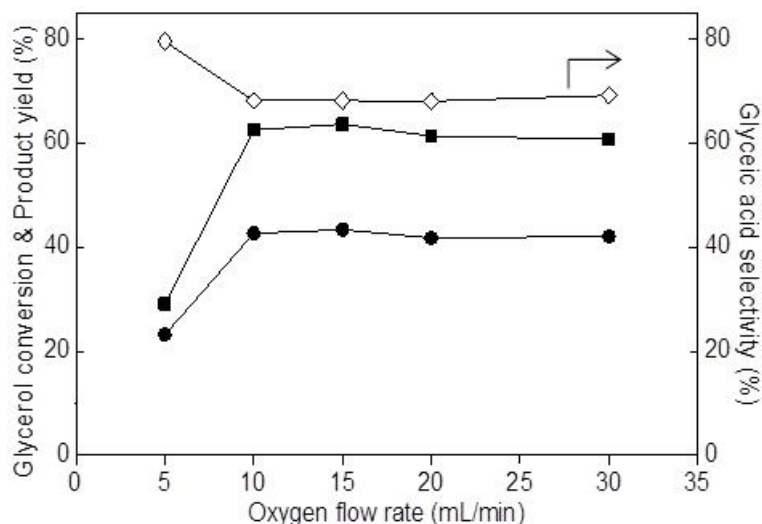


Figure 5 Catalytic activity of Pt NPs/HT at various oxygen flow rate. GLY conversion (■: close square), glyceric acid yield (●: close circle) and glyceric acid selectivity (◇: diamond). Reaction conditions: GLY (0.5 mmol), 0.7 wt% Pt NPs/HT catalyst (14 mg, GLY/metal = 1000), H₂O (2 ml), temperature (333 K), reaction time (6 h).

3.2.2.4 Influence of reaction temperature

Table 5 shows the activity of glycerol oxidation under variation of the reaction temperature (313–353 K). The catalytic activity increased with increase in the temperature from 313 to 323 K, and showed no significant change even the temperature was further increased to 353 K (Table 5). It was implied that the aerobic GLY oxidation under atmospheric conditions was not affected by the moderate reaction temperature (323–353 K).

Table 5 Effect of reaction temperature on GLY oxidation catalyzed by Pt NPs/HT.^a

Entry	Reaction temperature	Conversion of GLY / %	Selectivity of GA / %	Yield of GA / %
1	313	46	78	36
2	323	63	68	43
3	333	64	67	43
4	343	65	67	43
5	353	64	63	40

^aReaction conditions: GLY (0.5 mmol), 0.7 wt% Pt NPs/HT catalyst (14 mg, GLY/metal = 1000), H₂O (2 ml), O₂ flow (10 mL·min⁻¹), reaction time (6 h).

3.2.2.5 Reaction time profile under optimum conditions

The time profile of the GLY oxidation reaction over the Pt NPs/HT reduced in 10 min was plotted in Figure 6. The GLY was converted to GA, TA, HA and OA. The reaction was accomplished by the oxidation of primary alcohol of GLY to glyceraldehyde; thereafter, further oxidation of the formed glyceraldehyde to GA, TA, HA and OA progressed. At the initial stage of the reaction time (1 h), the highest selectivity to GA (78%) was achieved. The selectivity toward GA gradually decreased to 70% with 61% conversion of GLY as the reaction time increased to 9 h. It clearly indicated that the Pt NPs/HT synthesized by the green synthesis method showed high oxidation catalysis for the GLY conversion in base-free aqueous solutions under atmospheric molecular oxygen and moderate reaction conditions, as comparison to the previous reports (see Chapter 1, Tables 2 and 3).^{[30]-[35],[37],[38],[41]}

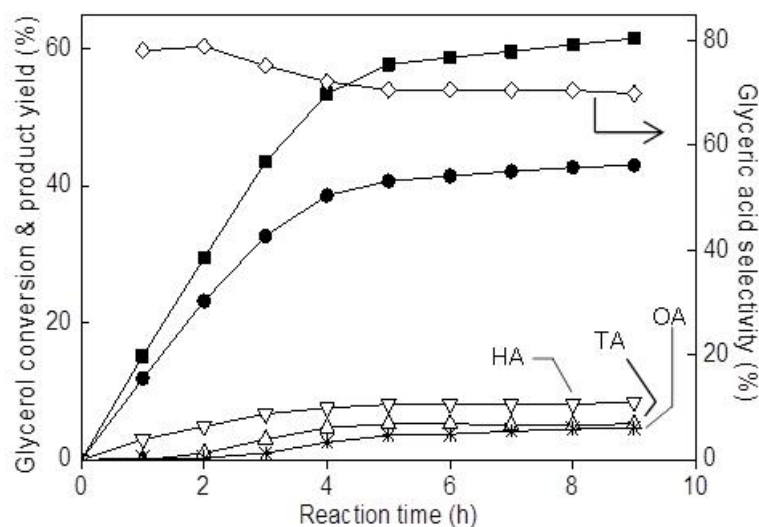


Figure 6 Reaction time profile of GLY oxidation catalyzed by Pt NPs/HT. GLY conversion (■: close square), GA yield (●: close circle), TA yield (△: open up triangle), HA yield (▽: open down triangle), OA yield (*: star) and GA selectivity (◇: diamond). Reaction conditions: GLY (0.5 mmol), H₂O (2.0 mL), 0.7 wt% Pt NPs/HT catalyst (14 mg, GLY/metal = 1000), temperature (323 K), O₂ flow (10 mL·min⁻¹).

3.2.3 Detection of leached Pt NPs in the solution

The leaching of Pt NPs from the support was analyzed by the hot filtration test. Oxidation of GLY by Pt NPs/HT catalyst was performed under the optimal reaction conditions as followed: GLY (0.5 mmol), H₂O (2.0 mL), 0.7 wt% Pt NPs/HT catalyst (14 mg, GLY/metal = 1000), temperature (323 K), O₂ flow (10 mL·min⁻¹). When the reaction achieves 30–40% GLY conversion, the catalyst was filtered off by a Millex filter with 0.20 μm pore size while keeping hot conditions. Then the clear solution was continuously heated for further 7 h. The composition of the filtrate solution was monitored. As shown in Figure 7, the conversion and yield did not

change after removal of the Pt NPs/HT. It means that the active Pt NPs did not leach into the solution under the reaction conditions and the reaction is truly heterogeneous.

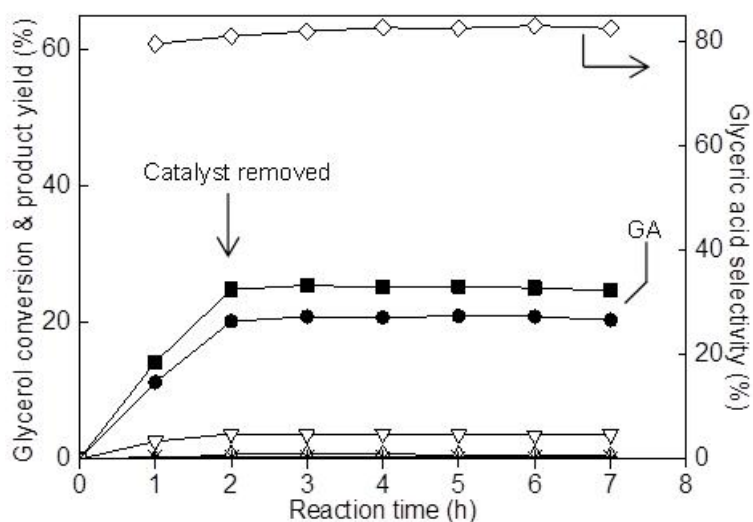


Figure 7 Time course of GLY oxidation catalyzed by Pt NPs/HT. At arrow point, catalyst was removed. GLY conversion (■: close square), GA yield (●: close circle), TA yield (△: open up triangle), HA yield (▽: open down triangle), OA yield (*: star) and GA selectivity (◇: diamond). Reaction conditions: GLY (0.5 mmol), H₂O (2.0 mL), 0.7 wt% Pt NPs/HT catalyst (14 mg, GLY/metal = 1000), temperature (323 K), O₂ flow (10 mL·min⁻¹).

3.2.4 Catalyst recycling

From the viewpoint of pH changes in the reaction mixture (Figure 8), it is supposed that the reaction is interfered by the acidic products after 6 h. To determine the efficiency of the Pt NPs/HT catalyst, the recycling experiments were also carried out. After 6 h of reaction, the catalyst was centrifuged, washed with deionized water and dried under vacuum. Then it was employed again for another GLY oxidation

reaction under the same reaction conditions. On recycling, the catalyst could be reused at least three times.

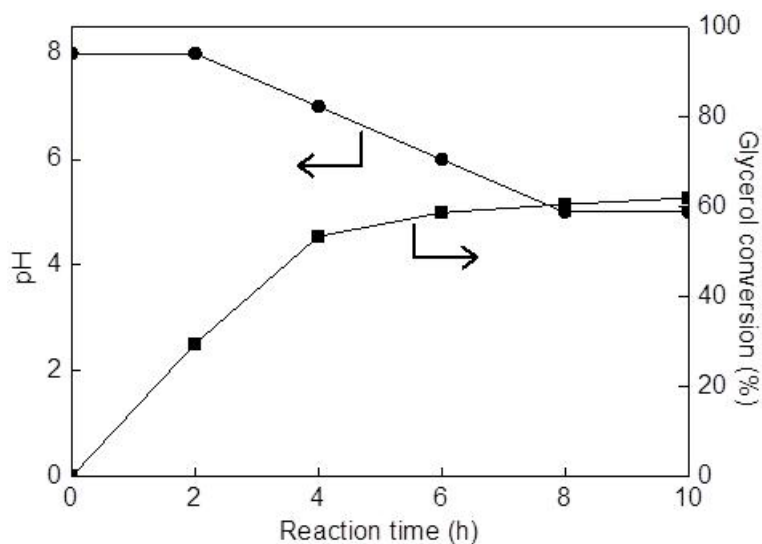


Figure 8 The time-dependence of the pH of the solution during the GLY oxidation reaction. Reaction conditions: GLY (0.5 mmol), 0.7 wt% Pt NPs/HT catalyst (14 mg, GLY/metal = 1000), H₂O (2 ml), temperature (323 K), O₂ flow (10 mL·min⁻¹).

Figure 9 indicates only a slightly decrease in GLY conversion (i.e., 63, 59 and 56% for first, second and third recycled, respectively) with no considerable change in the selectivity (e.g., 68 and 71% selectivity for first and third recycled, respectively). The morphology of recycled catalysts was investigated by XRD and TEM. The XRD patterns of recycled catalyst were identical to that of the initial catalyst (Figure 10). TEM images showed no change in recycled catalyst in terms of particle size and particle size distribution (Figure 11).

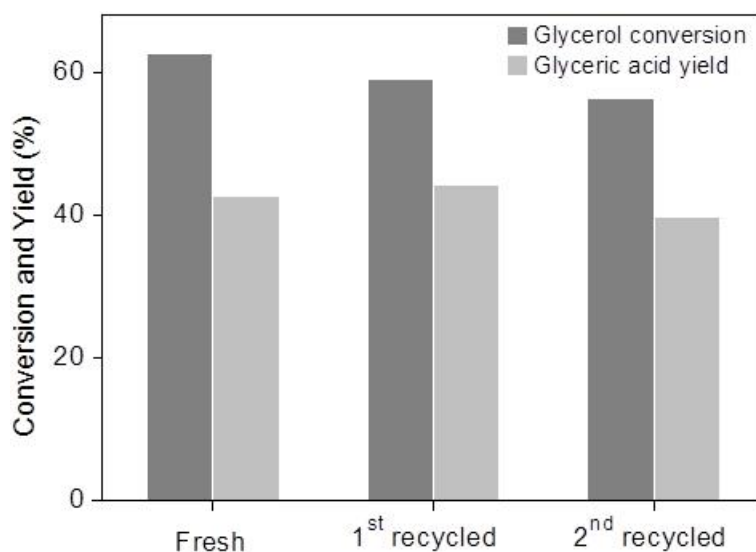


Figure 9 Recycling of Pt NPs/HT catalyst. Reaction conditions: GLY (0.5 mmol), H₂O (2.0 mL), 0.7 wt% Pt NPs/HT catalyst (14 mg, GLY/metal = 1000), temperature (323 K), reaction time (6 h), O₂ flow (10 mL·min⁻¹).

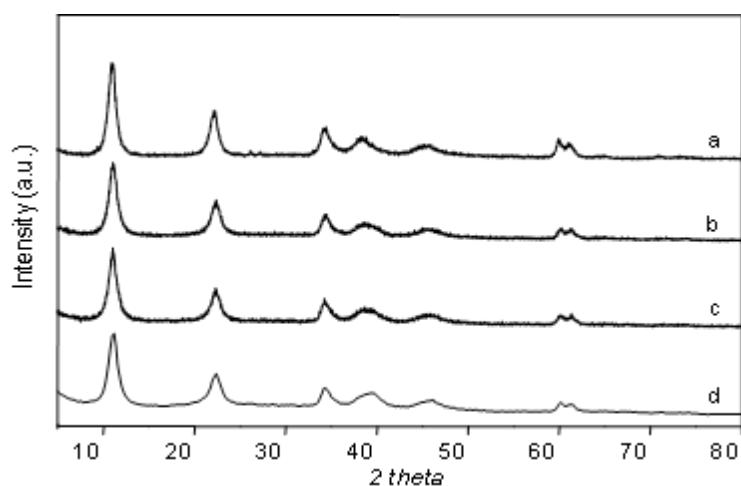


Figure 10 XRD patterns of Pt NPs/HT before and after recycled: (a) pure Pt NPs/HT, (b) Pt NPs/HT 1st recycled, (c) Pt NPs/HT 2nd recycled and (d) Pt NPs/HT 3rd recycled.

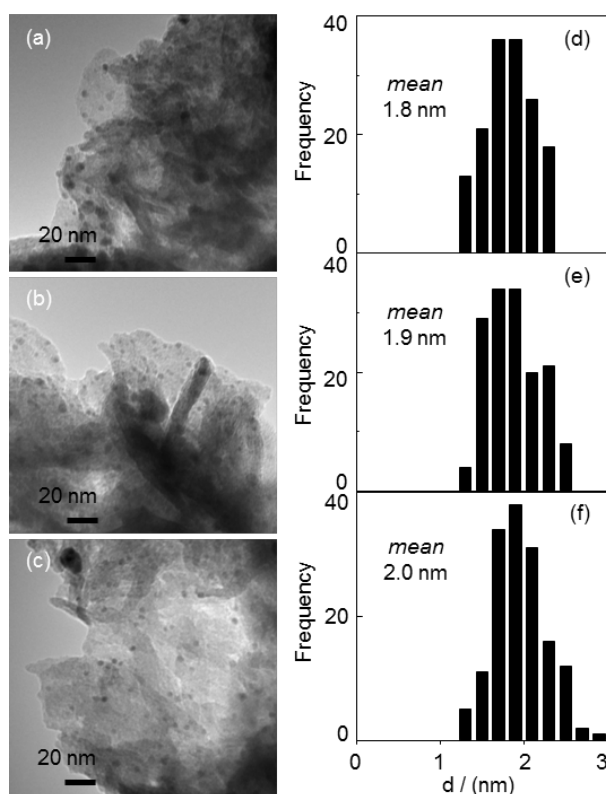


Figure 11 TEM images of recycled Pt NPs/HTs catalyst: (a) Pt NPs/HTs 1st recycled, (b) Pt NPs/HTs 2nd recycled and (c) Pt NPs/HTs 3rd recycled and (d-f) their particle size distribution histograms.

Furthermore, the FT-IR spectra indicated the existence of the characteristic peaks at around 1200–900 cm^{-1} contributed from the glycosidic linkage of the starch bridge even after 3 uses (Figure 12). These results suggested that the Pt NPs/HT was stable and reusable as a catalyst for the GLY oxidation reaction.

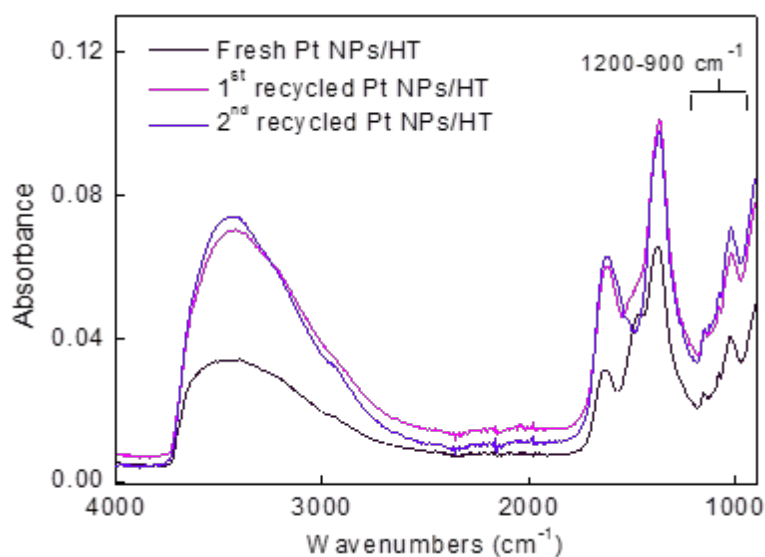


Figure 12 FT-IR spectra of the Pt NPs/HT catalysts before and after recycling reactions.

4. Conclusion

The research in this chapter has successfully synthesized hydrotalcite supported Pt nanoparticle (Pt NPs/HT) catalyst using starch as a “green” reducing and a stabilizing agent. It was found that Pt NPs/HT prepared by the immobilization method showed higher catalytic activity for the aerobic oxidation of GLY than that of catalyst prepared by the impregnation method. Pt particle size and the Pt⁰ concentration increased with the increasing reduction time. Pt NPs were partially oxidized when exposed to air and provided the Pt oxides on their surface. Furthermore, the preparation time was influence the catalytic activity under base-free aqueous solution and moderate reaction conditions. The highest GLY conversion (80%) was achieved by immobilization of Pt NPs on HT support after reduction time of 3 min (Pt NPs/HT (3 min)). Pt NPs/HT (10 min) was found to be the best catalyst

when considered in terms of the yield and selectivity for GA with turnover number (TON) of 357. It was indicated that Pt particle size and Pt⁰ concentration are related to both GLY conversion and yield of GA in the oxidation reaction of GLY. In addition, at GLY concentrations lower than 0.25 M, the sum of product selectivity is nearly 100% in all cases. After the reaction, the catalyst was easily removed by hot filtration and no Pt leaching was detected in the solution. The catalyst retained high activity in recycling experiments. In addition, Pt NPs/HT showed high activity than Pt on other supports (i.e., Pt NPs/MgO, Pt/C, Pt/SiO₂ and Pt/Al₂O₃) for the catalytic oxidation of GLY in base-free aqueous solution.

5. References

- [1] P. Raveendran, J. Fu and S. L. Wallen, Completely “green” synthesis and stabilization of metal nanoparticles, *J. Am. Chem. Soc.*, 2003, **125**, 13940–13941.
- [2] J. Clark and D. Macquarrie, Handbook of green chemistry and technology, Blackwell Science Ltd, Oxford, **2002**.
- [3] J. A. Dahl, B. L. S. Maddux and J. E. Hutchison, Toward greener nanosynthesis, *Chem. Rev.*, 2009, **107**, 2228–2269.
- [4] M. N. Nadagouda and R. S. Varma, Green and controlled synthesis of gold and platinum nanomaterials using vitamin B₂: density-assisted self-assembly of nanospheres, wires and rods, *Green Chem.*, 2006, **8**, 516–518.
- [5] K. Kaneda, K. Ebitani, T. Mizugaki and K. Mori, Design of high-performance heterogeneous metal catalysts for green and sustainable chemistry, *Bull. Chem. Soc. Jpn.*, 2006, **79**, 981–1016.
- [6] M. Adlim, M. A. Baker, K. Y. Liew and J. Ismail, Synthesis of chitosan-stabilized platinum and palladium nanoparticles and their hydrogenation activity, *J. Mol. Catal. A-Chem.*, 2004, **212**, 141–149.
- [7] W. Yang, Y. Ma, J. Tang and X. Yang, “Green synthesis” of monodisperse Pt nanoparticles and their catalytic properties, *Colloids Surf. A.*, 2007, **302**, 628–633.
- [8] W. Yang, C. Yang, M. Sun, F. Yang, Y. Ma, Z. Zhang and X. Yang, Green synthesis of nanowire-like Pt nanostructures and their catalytic properties, *Talanta*, 2009, **78**, 557–564.

- [9] L. Johnson, W. Thielemans and D. A. Walsh, Synthesis of carbon-supported Pt nanoparticle electrocatalysts using nanocrystalline cellulose as reducing agent, *Green Chem.*, 2011, **13**, 1686–1693.
- [10] L. Bournay, D. Casanave, B. Delfort, G. Hilliona and J. A. Chodorge, New heterogeneous process for biodiesel production: a way to improve the quality and the value of the crude glycerin produced by biodiesel plants, *Catal. Today*, 2005, **106**, 190–192.
- [11] C.-H. (Clayton) Zhou, J. N. Beltramini, Y.-X. Fan and G. Q. (Max) Lu, Chemoselective catalytic conversion of glycerol as a biorenewable source to valuable commodity chemicals, *Chem. Soc. Rev.*, 2008, **37**, 527–549.
- [12] A. Brandner, K. Lehnert, A. Bienholz, M. Lucas and P. Claus, Production of biomass-derived chemicals and energy: chemocatalytic conversions of glycerol, *Top. Catal.*, 2009, **52**, 278–287.
- [13] E. P. Maris and R. J. Davis, Hydrogenolysis of glycerol over carbon-supported Ru and Pt catalysts, *J. Catal.*, 2007, **249**, 328–337.
- [14] Z. Yuan, P. Wu, J. Gao, X. Lu, Z. Hou and X. Zheng, Pt/solid-base: a predominant catalyst for glycerol hydrogenolysis in a base-free aqueous solution, *Catal. Lett.*, 2009, **130**, 261–265.
- [15] Y. Nakagawa and K. Tomishige, Heterogeneous catalysis of the glycerol hydrogenolysis, *Catal. Sci. Technol.*, 2011, **1**, 179–190.
- [16] K. Biswas, S. Datta, S. Chaudhuri, K. Kargupta, S. Datta and S. K. Sanyal, Dehydration of glycerol-water mixtures using pervaporation: influence of process parameters, *Sep. Sci. Technol.*, 2000, **35**, 1391–1408.

- [17] S. Carretin, P. McMorn, P. Johnston, K. Griffin, C. J. Kiely and G. J. Hutchings, Oxidation of glycerol using supported Pt, Pd and Au catalysts, *Chem. Chem. Phys.*, 2003, **5**, 1329–1336.
- [18] N. Dimitratos, C. Messi, F. Porta, L. Prati and A. Villa, Investigation on the behaviour of Pt(0)/carbon and Pt(0),Au(0)/carbon catalysts employed in the oxidation of glycerol with molecular oxygen in water, *J. Mol. Catal. A: Chem.*, 2006, **256**, 21–28.
- [19] R. F. Stockel, Method of treating dermatological conditions, U.S. Patent 2007/086 977 A1, April 19, 2007.
- [20] S. K. Gupta, Novel hydroxyl acid complexes for antiaging and skin renovation, U.S. Patent 2007/092 461 A1, April 26, 2007.
- [21] A. Rau, H. Renker, N. Quinn, Packaging materials and structures for compositions including an exothermic agent and a volatile agent, U.S. Patent 2007/0003675 A1, January 4, 2007.
- [22] A. Behr, J. Eilting, K. Irawadi, J. Leschinski and F. Lindner, Improved utilisation of renewable resources: new important derivatives of glycerol, *Green Chem.*, 2008, **10**, 13–30.
- [23] N. Dimitratos, F. Porta and L. Prati, Au, Pd (mono and bimetallic) catalysts supported on graphite using the immobilisation method: synthesis and catalytic testing for liquid phase oxidation of glycerol, *Appl. Catal. A-Gen.*, 2005, **291**, 210–214.
- [24] S. Demirel-Gülen, M. Lucas and P. Claus, Liquid phase oxidation of glycerol over carbon supported gold catalysts, *Catal. Today*, 2005, **102–103**, 166–172.

- [25] D. Wang, A. Villa, F. Porta, D. Sua and L. Prati, Single-phase bimetallic system for the selective oxidation of glycerol to glycerate, *Chem. Commun.*, 2006, 1956–1958.
- [26] N. Dimitratos, J. A. Lopez-Sanchez, D. Lennon, F. Porta, L. Prati and A. Villa, Effect of particle size on monometallic and bimetallic (Au,Pd)/C on the liquid phase oxidation of glycerol, *Catal. Lett.*, 2006, **108**, 147–153.
- [27] S. Demirel, K. Lehnert, M. Lucas and P. Claus, Use of renewables for the production of chemicals: glycerol oxidation over carbon supported gold catalysts, *Appl. Catal. B-Environ.*, 2007, **70**, 637–643.
- [28] S. Demirel, P. Kern, M. Lucas and P. Claus, Oxidation of mono- and polyalcohols with gold: comparison of carbon and ceria supported catalysts, *Catal. Today*, 2007, **122**, 292–300.
- [29] W. C. Ketchie, Y.-L. Fang, M. S. Wong, M. Murayama and R. J. Davis, Influence of gold particle size on the aqueous-phase oxidation of carbon monoxide and glycerol, *J. Catal.*, 2007, **250**, 94–101.
- [30] L. Prati, A. Villa, C. Campione and P. Spontoni, Effect of gold addition on Pt and Pd catalysts in liquid phase oxidations, *Top. Catal.*, 2007, **44**, 319–324.
- [31] J. Gao, D. Liang, P. Chen, Z. Hou and X. Zheng, Oxidation of glycerol with oxygen in a base-free aqueous solution over Pt/AC and Pt/MWNTs catalysts, *Catal. Lett.*, 2009, **130**, 185–191.
- [32] L. Prati, P. Spontoni and A. Gaiassi, From renewable to fine chemicals through selective oxidation: the case of glycerol, *Top. Catal.*, 2009, **52**, 288–296.

- [33] N. Dimitratos, A. Villa and L. Prati, Liquid phase oxidation of glycerol using a single phase (Au–Pd) alloy supported on activated carbon: effect of reaction conditions, *Catal. Lett.*, 2009, **133**, 334–340.
- [34] N. Dimitratos, J. A. Lopez-Sanchez, J. M. Anthonykutty, G. Brett, A. F. Carley, R. C. Tiruvalam, A. A. Herzing, C. J. Kiely, D. W. Knight and G. J. Hutchings, Oxidation of glycerol using gold–palladium alloy-supported nanocrystals, *Phys. Chem. Chem. Phys.*, 2009, **11**, 4952–4961.
- [35] D. Liang, J. Gao, J. Wang, P. Chen, Z. Hou and X. Zheng, Selective oxidation of glycerol in a base-free aqueous solution over different sized Pt catalysts, *Catal. Commun.*, 2009, **10**, 1586–1590.
- [36] A. Villa, A. Gaiassi, I. Rossetti, C. L. Bianchi, K. van Benthem, G. M. Veith and L. Prati, Au on MgAl₂O₄ spinels: the effect of support surface properties in glycerol oxidation, *J. Catal.*, 2010, **275**, 108–116.
- [37] I. Sobczak, K. Jagodzinska and M. Ziolek, Glycerol oxidation on gold catalysts supported on group five metal oxides—A comparative study with other metal oxides and carbon based catalysts, *Catal. Today*, 2010, **158**, 121–129.
- [38] G. L. Brett, Q. He, C. Hammond, P. J. Miedziak, N. Dimitratos, M. Sankar, A. A. Herzing, M. Conte, J. A. Lopez-Sanchez, C. J. Kiely, D. W. Knight, S. H. Taylor and G. J. Hutchings, Selective oxidation of glycerol by highly active bimetallic catalysts at ambient temperature under base-free conditions, *Angew. Chem. Int. Ed.*, 2011, **50**, 10136–10139.

- [39] Z. Huang, F. Li, B. Chen, F. Xue, Y. Yuan, G. Chena and G. Yuan, Efficient and recyclable catalysts for selective oxidation of polyols in H₂O with molecular oxygen, *Green Chem.*, 2011, **13**, 3414–3422.
- [40] D. Liang, J. Gao, H. Sun, P. Chen, Z. Hou and X. Zheng, Selective oxidation of glycerol with oxygen in a base-free aqueous solution over MWNTs supported Pt catalysts, *Appl. Catal. B-Environ.*, 2011, **106**, 423–432.
- [41] A. Villa, G. M. Veith and L. Prati, Selective oxidation of glycerol under acidic conditions using gold catalysts, *Angew. Chem. Int. Ed.*, 2010, **49**, 4499–4502.
- [42] D. Tongsakul, K. Wongravee, C. Thammacharoen and S. Ekgasit, Enhancement of the reduction efficiency of soluble starch for platinum nanoparticles synthesis, *Carbohydr. Res.*, 2012, **357**, 90–97.
- [43] K. Kaneda, K. Yamaguchi, K. Mori, T. Mizugaki and K. Ebitani, Catalyst design of hydrotalcite compounds for efficient oxidations, *Catal. Surv. Jpn.*, 2000, **4**, 31–38.
- [44] K. Motokura, D. Nishimura, K. Mori, T. Mizugaki, K. Ebitani and K. Kaneda, A ruthenium-grafted hydrotalcite as a multifunctional catalyst for direct α -alkylation of nitriles with primary alcohols, *J. Am. Chem. Soc.*, 2004, **126**, 5662–5663.
- [45] K. Ebitani, K. Motokura, T. Mizugaki and K. Kaneda, Heterotrimetallic RuMnMn species on a hydrotalcite surface as highly efficient heterogeneous catalysts for liquid-phase oxidation of alcohols with molecular oxygen, *Angew. Chem. Int. Ed.*, 2005, **44**, 3423–3426.

- [46] K. Kaneda, T. Mitsudome, T. Mizugaki and K. Jitsukawa, Development of heterogeneous olympic medal metal nanoparticle catalysts for environmentally benign molecular transformations based on the surface properties of hydrotalcite, *Molecules*, 2010, **15**, 8988–9007.
- [47] C. J. Knill and J. F. Kennedy, Degradation of cellulose under alkaline conditions, *Carbohydr. Polym.*, 2003, **51**, 281–300.
- [48] M. A. Clarke, L. A. Edey and G. Eggleston, In *Advances in Carbohydrate Chemistry and Biochemistry*, Academic Press, **1997**.
- [49] D. Tongsakul, S. Nishimura, C. Thammacharoen, S. Ekgasit and K. Ebitani, Hydrotalcite-supported platinum nanoparticles prepared by a green synthesis method for selective oxidation of glycerol in water using molecular oxygen, *Ind. Eng. Chem. Res.*, 2012, **51**, 16182–16187.
- [50] A. Tsuji, K. T. V. Rao, S. Nishimura, A. Takagaki and K. Ebitani, Selective oxidation of glycerol by using a hydrotalcite-supported platinum catalyst under atmospheric oxygen pressure in water, *ChemSusChem*, 2011, **4**, 542–548.
- [51] S. Hirasawa, Y. Nakagawa and K. Tomishige, Selective oxidation of glycerol to dihydroxyacetone over a Pd–Ag catalyst, *Catal. Sci. Technol.*, 2012, **2**, 1150–1152.
- [52] C.-H. Yu, K. Tam, E. S. C. Tsang, *Handbook of Metal Physics*; Elsevier, **2009**.
- [53] Y. Xia, Y. Xiong, B. Lim and S. E. Skrabalak, Shape-controlled synthesis of metal nanocrystals: simple chemistry meets complex physics?, *Angew. Chem. Int. Ed.*, 2009, **48**, 60–103.

Chapter 3

PROBING THE EFFECT OF POLYMER STABILIZED-PLATINUM NANOPARTICLES

1. Introduction

In these decades, metal nanoparticles (NPs) stabilized by polymer have been used as a catalyst, since polymer produces the uniform shape and prevents aggregation of NPs for more efficient catalysis. Various kinds of stabilizers had been used to produce metal NPs with well-defined size and shape; for instance, sodium citrate,¹ poly(vinyl alcohol) (PVA),^{[1]-[3]} and poly(vinyl pyrrolidone) (PVP)^{[4]-[6]} have been widely attempted to prepare the fine metal NPs. Beside, the particle size and their stability, particle shape, composition, electronic state and surrounding material also affect the catalytic activity of metal particles.^[7] In many cases, the stabilizing/capping agent might influence not only particle size but also the electronic state of NPs as summarized in Chapter 1, Table 5, and contribute their novel catalytic performances.^{[1],[8]-[14]} Villa *et al.* revealed that the particle size of Au sols depends on kind of stabilizer. Smallest particle size was found for tetrakis(hydroxypropyl)phosphonium chloride stabilized-Au sols follows by PVA and citrate, which brings the highest catalytic activity for glycerol oxidation.^[1] Lee *et al.* demonstrated that Platinum (Pt) NPs regulated with tetradecyltrimethylammonium

bromide exhibited much higher activity than Pt NPs prepared with PVP for the ethylene hydrogenation.^{[15],[16]} Au/Pt/Ag trimetallic NPs were found to show higher activity than that of Au NPs with nearly same particle size for aerobic glucose oxidation, because the negative charge on the Au surface atoms by electron donation from neighboring Ag atoms and PVP ligand.^[17] Borodko *et al.* probed the interaction between PVP and Pt nanocrystals by using UV-Raman and FT-IR techniques, and concluded that PVP adheres to the NPs *via* a charge-transfer interaction between the pyrrolidone rings and surface Pt atoms.^[18]

Pt metal has been exclusively employed as the catalyst for many applications such as the oxidation reactions of alcohol and polyols^{[7],[19],[20]} and the electrocatalytic oxygen reduction reaction.^{[21],[22]} The uniform particle size distribution and their stability are essential for the preparation of Pt catalyst.^[7] The immobilization method has been widely used for the preparation of supported Pt catalyst, because the method possesses the reproducible synthesis of particle size with controlled size distribution.^[23] Pt NPs are generated by reduction of metal precursor with a reducing agent, and in this step stabilizing/capping agent is required to prevent Pt NPs aggregation.

Very recently, I developed green synthetic method using soluble starch as a reducing and a stabilizing agent,^[24] and reported for preparation of the hydrotalcite (HT) supported starch stabilized–Pt NPs (Pt–starch/HT), which exhibited the good catalysis for aerobic glycerol oxidation under mild reaction conditions.^[25] The soluble starch is a linear polysaccharide with α –(1→4) linkages between *D*-glucose units

adopt a left-handed helical conformation in aqueous solution where hydroxyl groups in starch might complex with metal ion into molecular matrix and prevent NPs aggregation.^{[24],[26]} HT is known as double-layered metal hydroxide which possesses basicity derived from HCO_3^- species on the surface,^{[27]-[30]} which could abstract proton of hydroxyl groups of alcohols. Furthermore, we developed starch-stabilized PtAu bimetallic NPs supported on HT surface (PtAu–starch/HT), which acted as active and reusable solid catalysts for base-free aerobic oxidation of polyols in aqueous solution at room temperature (RT).^[31] It was proposed that the PtAu NPs gained charge from the starch ligand, which leads to improvement of the catalysis of active Pt sites for polyol oxidation. However, roles of the starch ligand are still unclear because the PtAu particles with different Pt/Au ratios have different particle sizes; geometric and electronic modifications by starch ligand cannot be discussed separately in that case.

In our previous comparisons on simple monometallic catalysts between bare Pt/HT and Pt–starch/HT, Pt–starch/HT exhibited a higher selectivity toward GA than bare Pt/HT in aerobic glycerol oxidation. It was suggested that the some part of starch polymer structure covered the surface of Pt NPs and limited the oxygen diffusion leading to decrease the over-oxidation to C_1 products, leading the high selectivity for GA on Pt–starch/HT.^{[25]-[32]} For simplification to understand the roles of polymer agents on Pt NPs/HT catalyst in aerobic oxidation in water, further investigation over monometallic catalyst supposedly helps essential and efficient discussion. Herein, in order to elucidate the role of starch ligand, supported Pt NPs with the same size (2.2 nm) were prepared using starch and conventional stabilizing polymers (PVP and PVA), as shown in Figure 1, on the HT surface (Pt–polymer/HT). I investigated effect

of the above three polymers on catalysis for the base-free aerobic oxidation of 1,2-propanediol (PG), a simpler substrate than glycerol, in an aqueous solution at RT on basis of electronic state and hydrophilic property of Pt-polymer/HT. The Pt-starch/HT was found to be the most effective catalyst for the aerobic PG oxidation among three types of Pt-polymer/HT. Pt 4f XPS and Pt L_3 -edge XANES analyses suggested that Pt atoms in the Pt NPs stabilized by starch and PVA were more negative than that stabilized by PVP. Furthermore, the measurement of water contact angle suggested that Pt-starch/HT and Pt-PVA/HT had less hydrophilic natures than that of Pt-PVP/HT. Based on the above results, we proposed the role of starch as a stabilizing ligand of HT-supported Pt NPs in the PG oxidation in the aqueous solution.

2. Experimental

2.1 Chemicals

Hexachloroplatinic acid ($\text{H}_2\text{PtCl}_6 \cdot 6\text{H}_2\text{O}$, 99.9%; Cat. No: 089-05311), 1,2-propanediol (99%; Cat. No: 164-04996), soluble starch (Cat. No: 195-03961), poly(vinyl alcohol) (PVA; partially hydrolyzed, 90 mol% saponification; Cat. No: 163-16355), sodium borohydride (90%; Cat. No: 0194-01471), and magnesium nitrate hexahydrate ($\text{Mg}(\text{NO}_3)_2 \cdot 6\text{H}_2\text{O}$; Cat. No: 134-00255) were purchased from Wako Pure Chemicals. Poly(vinyl pyrrolidone) (PVP; K12; Cat. No: 276142500) was provided from Acros Organics. Hydrotalcite (HT, Mg/Al = 5; Cat. No: TOMITA-AD-550PF) was purchased from Tomita Pharmaceutical.

2.2 Preparation of hydrotalcite supported-Pt NPs catalysts

Pt-polymer/HT catalysts were prepared by a chemical reduction method using NaBH_4 and polymer of soluble starch, PVP or PVA as a stabilizing agent. Thereafter, the generated Pt particles were immobilized on the HT surface as follows: $\text{H}_2\text{PtCl}_6 \cdot 6\text{H}_2\text{O}$ (0.1 mmol) was dissolved in 5 mL of aqueous solutions containing stabilizer (0.025–0.200 g) and stirring for 90 min. Then 10 mL of aqueous NaBH_4 solution (50 mM NaBH_4) was dropwisely added ($1.5 \text{ mL} \cdot \text{min}^{-1}$) into the mixed solution with continuous stirring. After 20 min, 0.5 g of HT was added to the solution under vigorous stirring for 1 h at RT. Finally, the resultant solid was filtered and washed with deionized water, and then the obtained solid catalyst was dried overnight at 373 K (Scheme 1).

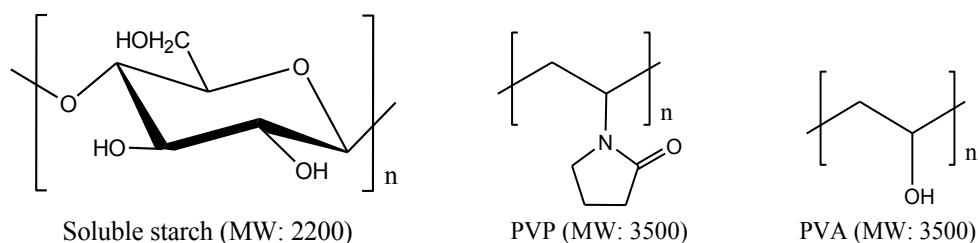
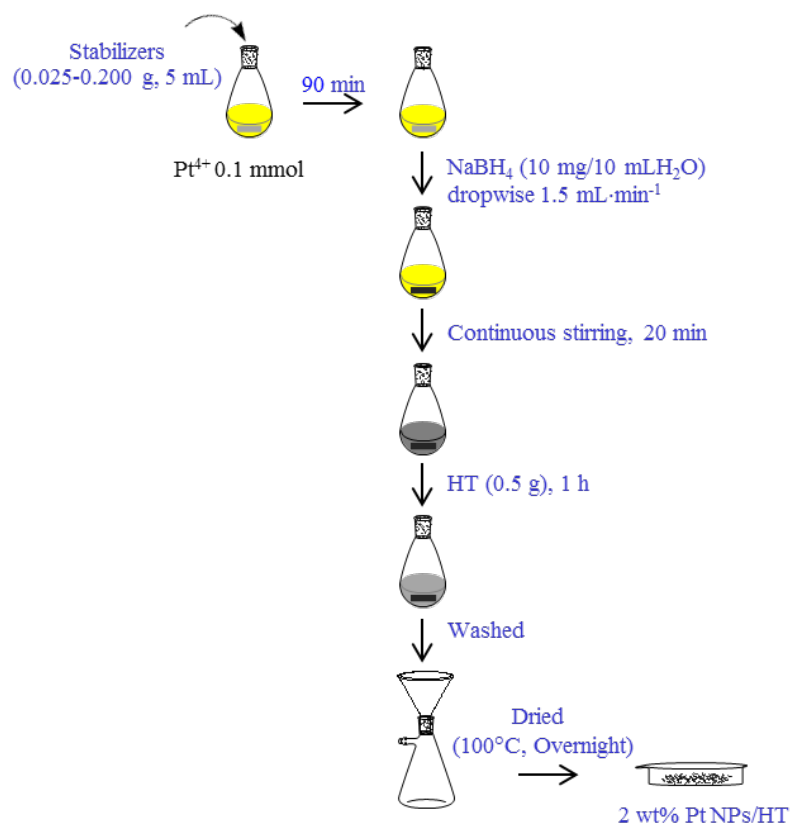


Figure 1 Structure of polymers used for stabilization of Pt NPs.



Scheme 1 Synthesis of polymer stabilized-Pt NPs/HT by a chemical reduction method using NaBH_4 as a reducing agent in water.

2.3 Characterization

The morphology of Pt-polymer/HT was analyzed by transmission electron microscopy (TEM; Hitachi H-7100) at 100 kV accelerating voltage. The Pt-polymer/HT was dispersed in deionized water and dropped onto a copper grid, then dried overnight in a desiccator. Inductively coupled plasma atomic emission spectroscopy (ICP-AES) was operated by Shimadzu ICPS-7000 ver. 2 to determine real concentrations of Pt on the catalyst. X-ray photoelectron spectroscopy (XPS) was measured on Shimadzu-Kuratos AXIS-ULTRA DLD spectrometer using an Al target

at 15 kV and 10 mA. The binding energies were calibrated with the O 1s peak (531.0 eV) as the internal standard reference. X-ray absorption near edge structure (XANES) in X-ray absorption spectra of Pt L_3 -edge were recorded at beamline BL-9C of KEK-PF under the approval of the Photon Factory Program Advisory Committee (Proposal No. 2013G586). The Pt-polymer/HT catalyst was grained and pressed to a pellet ($\phi \sim 10$ mm) for XANES analysis. The obtained XANES features were analyzed using Athena software (version. 0.8.056).

The water wettability of Pt-polymer/HT catalysts was studied by measuring the contact angle of a water droplet using Drop-Master DM 300 of Kyowa Interface Science Co. Catalyst was grained and pressed to a pellet ($\phi \sim 10$ mm) for the contact angle measurement. A water droplet with a volume of 2 μL was dropped onto each catalyst. Measurements were taken in three times for each catalyst to calculate average values.

2.4 Catalytic activity for 1,2-propanediol oxidation

Catalysis of Pt-polymer/HT was evaluated in the PG oxidation in base-free aqueous solution under atmospheric conditions. All reactions were performed in a 30 mL Schlenk tube attached to a reflux condenser. The general reaction conditions were as follows: PG (0.5 mmol), H_2O (2 mL), catalyst (32 mg), temperature (298 K), oxygen flow (10 mL min^{-1}), stirring rate (500 rpm). After the reaction, the catalyst was separated by filtration. The filtrate was analyzed by a high performance liquid chromatography (HPLC) equipped with an Aminex HPX-87H column (Bio-Rad Laboratories) and a refractive index detector. The analysis conditions were set as

follows: eluent (aqueous solution of H₂SO₄ (10 mM)), flow rate (0.5 mL min⁻¹), column temperature (323 K). Turnover number (TON) was calculated by the LA yield per mol of actual metal loading on the Pt–polymer/HT catalyst in the reaction mixtures.

3. Results and discussion

3.1 Preparation of HT supported–Pt NPs with same diameter using three polymers

In order to compare the influence of stabilizer onto the catalytic activity of Pt NPs, the size of Pt NPs would be the same using the proper amount of the polymer stabilizer. The Pt–polymer/HTs were prepared by a chemical reduction method using NaBH₄ as a reducing agent, and then immobilization on the HT surface. TEM images and particle size distribution histograms of starch, PVP and PVA stabilized–Pt/HTs at various polymer amounts (0.025–0.200 g) were shown in Figures 2–4. All showed the uniform and narrow size distribution, and the mean particle size gradually became smaller with increase of the polymer amount. Same mean particle size of Pt NPs with 2.2 nm was obtained when polymers of starch, PVP and PVA were used with 0.200 g, 0.200 g and 0.025 g for preparation, respectively (Figures 2-B4, 3-B4, and 4-B1). It is notable that the amount of PVA to produce 2.2 nm Pt particles is one-eighth of those of starch and PVP.

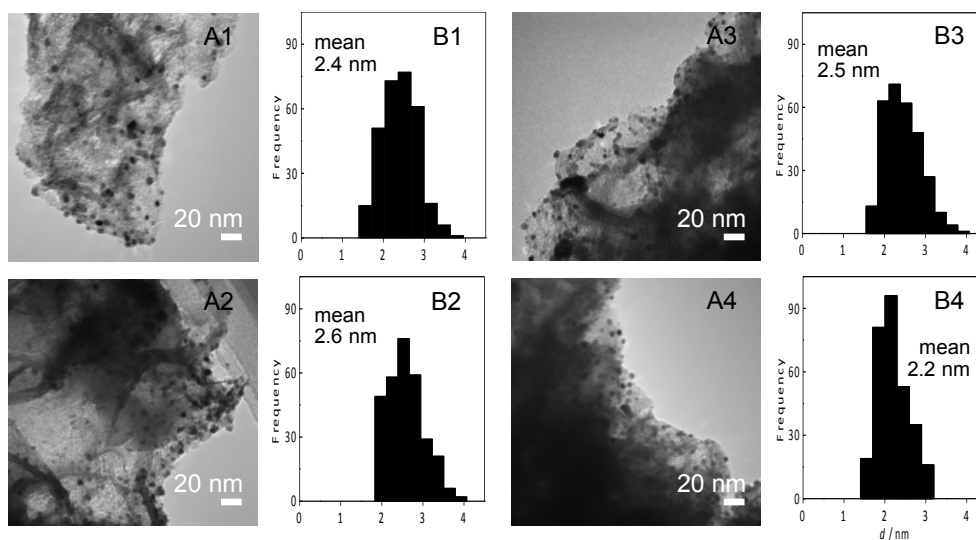


Figure 2 TEM images of starch–Pt NPs/HT at various amount of starch: (A1) 0.025 g, (A2) 0.050 g, (A3) 0.100 g and (A3) 0.200 g and (B1–B4) their particle size distribution histograms, respectively.

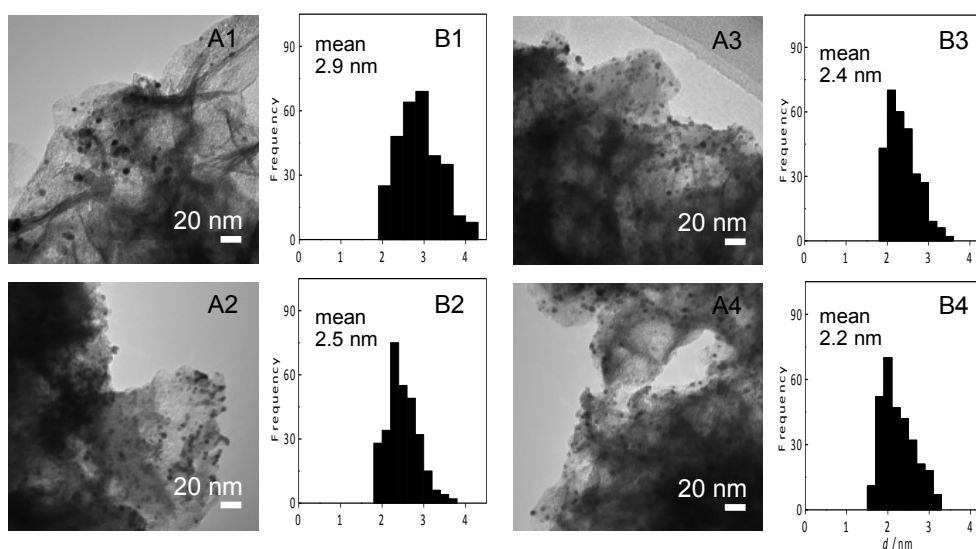


Figure 3 TEM images of PVP–Pt NPs/HT at various amount of PVP: (A1) 0.025 g, (A2) 0.050 g, (A3) 0.100 g and (A3) 0.200 g and (B1–B4) their particle size distribution histograms, respectively.

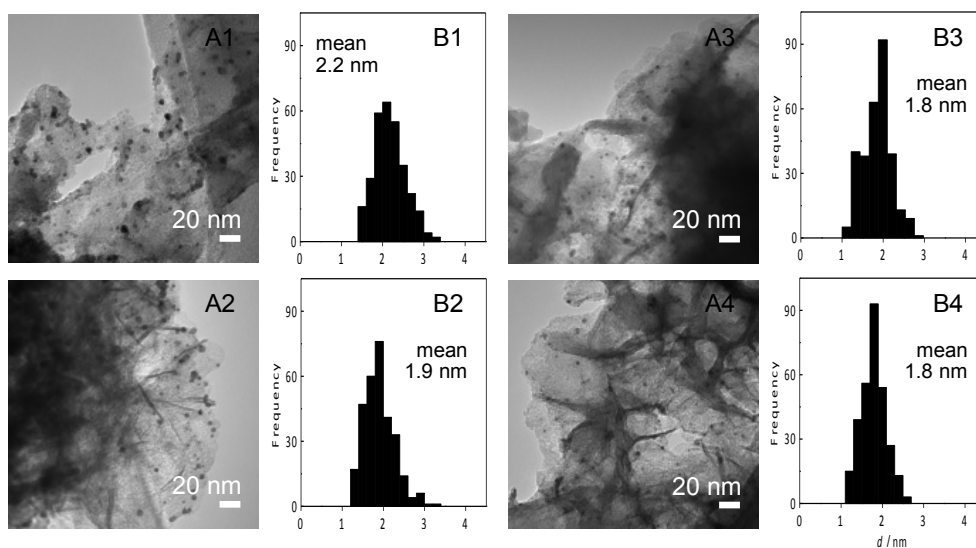


Figure 4 TEM images of PVA–Pt NPs/HT at various amount of PVA: (A1) 0.025 g, (A2) 0.050 g, (A3) 0.100 g and (A3) 0.200 g and (B1–B4) their particle size distribution histograms, respectively.

3.2 Oxidation of 1,2-propanediol

PG is a glycerol-derived product that is renewable and eco-friendly chemical from the industrial waste, and can be serving as a substrate for the manufacture of high-end chemicals such as LA.^{[27],[33]} LA has been applied to various industrial fields of food and pharmaceutical products.^{[34]-[36]} Supported metal particles on metal oxide or carbon could catalyze the PG oxidation, however, it needs pressurized O₂, NaOH and high temperatures (Chapter 1, Table 5).^{[2],[37]-[41]}

I found that the Pt–polymer/HTs with a mean diameter of 2.2 nm could catalyze the aerobic oxidation of PG in base-free aqueous solution using 1 atm of O₂ at RT, as shown in Table 1. Generally, the reaction was accomplished by the oxidation of primary hydroxyl group of PG to LA which could be further oxidized to

pyruvic acid (PA). The C-C bond cleavage affords acetic acid (AA) and C₁ product (ex. CO₂). In this case, the Pt-polymer/HTs showed the selective catalysis at primary hydroxyl group to form LA. Among them, the Pt-starch/HT exhibited the highest activity (57% conversion, 43% LA yield) with TON of 71, followed by the Pt-PVP/HT (42% conversion, 25% LA yield) and the Pt-PVA/HT (22% conversion, 12% LA yield) with TON of 40 and 17, respectively. It was indicated that the kind of stabilizer had a strong influence on the catalytic activity, and starch was better polymer than conventional polymers (PVP and PVA) for the PG oxidation reaction in water at RT.

Table 1 Oxidation of 1,2-propanediol (PG) in water over the Pt-polymer/HT

catalysts^a

Entry	Catalyst ^b	Metal loading ^c / mmol g ⁻¹	PG Conv. / %	Yield /%			TON
				LA	PA	AA	
1	Pt-starch/HT	0.095	57	43	9	5	71
2	Pt-PVP/HT	0.099	42	25	7	5	40
3	Pt-PVA/HT	0.118	22	12	6	3	17

^aReaction conditions: PG (0.5 mmol), H₂O (2 mL), catalyst (32 mg), oxygen (10 mL min⁻¹), 298 K, 6 h. ^bMean diameters of Pt NPs were 2.2 nm. ^cDetermined by ICP-AES.

3.3 Electronic structure of Pt–polymer NPs

XPS spectra of the Pt–polymer NPs were shown in Figure 5.^[42] The binding energy (BE) of Pt foil for Pt 4f_{7/2} and Pt 4f_{5/2} are 71.2 eV and 74.4 eV, respectively. All spectra showed the asymmetric peak and the large negative shift to lower BE as comparable to the position of Pt foil (71.2 eV for 4f_{7/2} and 74.4 eV for 4f_{5/2}). The differences of BE between sample and Pt foil (Δ BE) were shown in Table 2. The Pt–PVA NPs exhibited the Δ BE of 2.1 eV which is identical to the Pt–starch NPs (2.0 eV) and higher than the Pt–PVP NPs (0.9 eV). Since three Pt NPs have same mean particle size, the large negative BE shifts of Pt 4f were supposedly due to the interaction between Pt NPs and surrounding ligand. There were shoulder peaks at higher side in binding energy that will be attributed to the formation of PtO_x species on the surface of Pt–polymer NPs (discussed in the next paragraph).

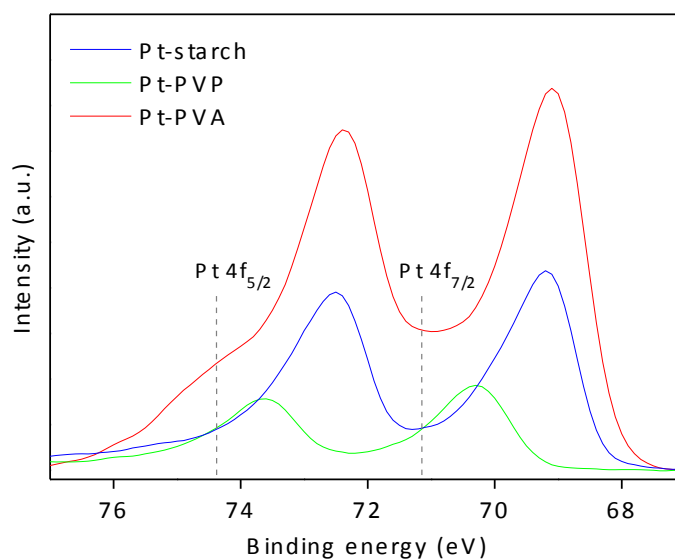


Figure 5 XPS spectra of the Pt–polymer NPs.

Table 2 Binding energy and its shift of the Pt–polymer NPs

Entry	Sample	BE (Δ BE ^a)	
		Pt 4f _{7/2} / eV	Pt 4f _{5/2} / eV
1	Pt–starch NPs	69.2 (2.0)	72.5 (1.9)
2	Pt–PVP NPs	70.3 (0.9)	73.6 (0.8)
3	Pt–PVA NPs	69.1 (2.1)	72.4 (2.0)

^a Δ BE = BE (Pt foil) – BE (sample).

In order to further investigate the electronic state of Pt–polymer/HT, the catalysts were analyzed by XANES features. Normalized Pt L_3 -edge XANES features of the Pt–polymer/HT were shown in Figure 6. The white-lines (WLs) were observed on Pt L_3 -edge XANES features (Figure 6A). As a typical feature, WL is very strong for most transition metals with partially filled d band and intensity is related to the unoccupied densities of d states, more number of electrons in 5d states make lower intensity in the WL area.^{[9],[43]} All Pt L_3 -edge of Pt–polymer/HT exhibit the WL intensity between the Pt foil (electron configuration of Pt: [Xe] 6s¹ 4f¹⁴ 5d⁹) and PtO₂ (Figures 6B and 7). These little higher intensities in the WL than Pt foil advocated the presence of PtO_x species which presumable due to the adsorption of some oxygens from polymer agents on the surface of Pt–polymer NPs stabilized on HT. Though those effects were also appeared in the WL feature, the observed differences among three Pt–polymer/HTs could be compared because the WL intensity of Pt–starch/HT or Pt–PVA/HT was lower than Pt–PVP/HT as shown in Figure 6B; if the expected PtO_x were dominant species, the former was higher than the latter considering with

the possible structures of these Pt–polymer/HTs (as described in Figure 8 (*vide infra*)). The WL intensity and the BE shift for each Pt–polymer NPs were plotted in Figure 7. The Pt–starch/HT and the Pt–PVA/HT displayed the similarity of the WL intensity which is lower than that of the Pt–PVP/HT together with large negative BE shift. These results indicated that Pt atoms in the Pt NPs stabilized by starch and PVA were more negative than that stabilized by PVP. Additionally, it seemed that the interference of HT support scarcely influenced on the differences on electronic structure of Pt–NPs/HT estimated from XPS and XANES analysis.

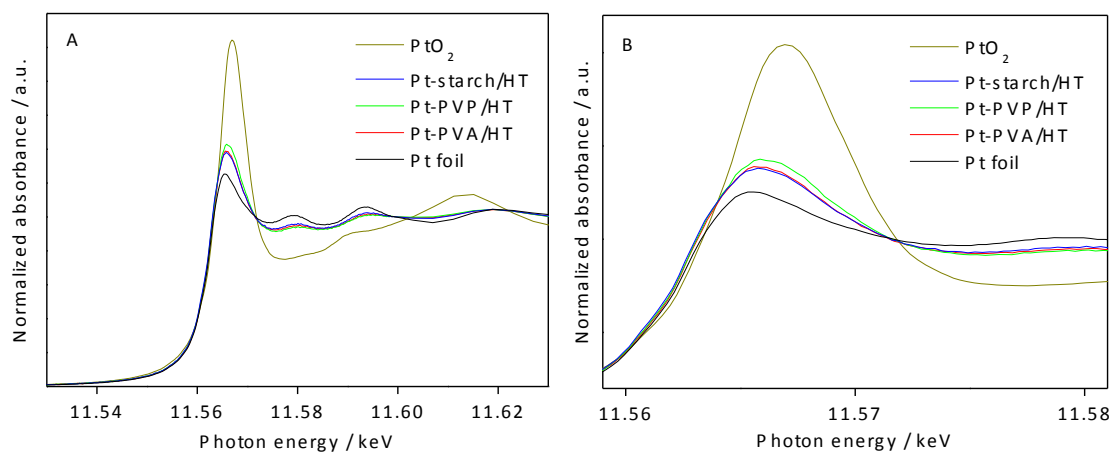


Figure 6 (A) Pt L_3 -edge XANES features of the Pt–polymer/HT and (B) emphasize detail near the WL region.

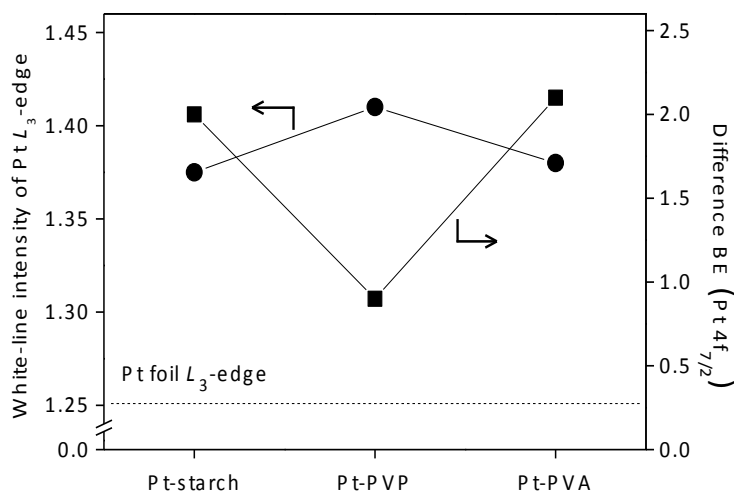


Figure 7 WL intensity of Pt L_3 -edge XANES features and difference BE shift of Pt-polymer/HT. Dash line represents WL intensity of Pt foil L_3 -edge.

3.4 Water wettability of the Pt-polymer/HT

Since the present PG oxidation was performed in water, we considered the surface hydrophilicity/hydrophobicity played important roles in the oxidation reaction. To get information on water wettability of the catalyst, the water contact angles on the surface were measured. The images of a water droplet on the Pt-polymer/HT were shown in Figure 8 and the average water contact angles were summarized in Table 3. The water contact angles were found as following orders: Pt-PVP/HT < Pt-starch/HT < Pt-PVA/HT. It indicated the Pt-PVP/HT showed higher water wettability (hydrophilicity) than the Pt-starch/HT and the Pt-PVA/HT.

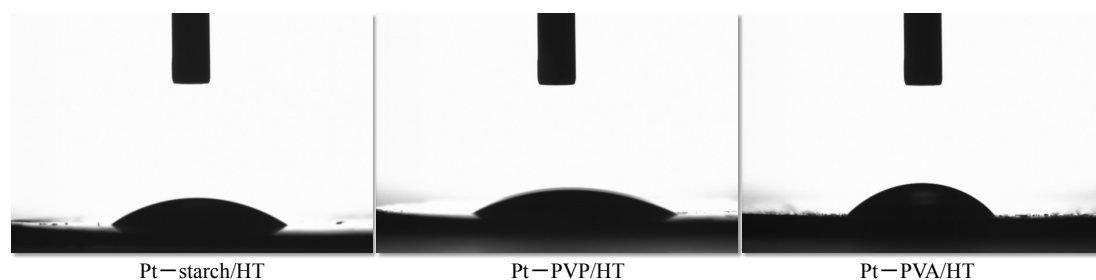


Figure 8 Images of water droplet on the Pt-polymer/HT.

Table 3 Average water contact angle on the Pt-polymer/HT

Entry	Catalyst	Contact angle, θ ($^{\circ}$)
1	Pt-starch/HT	36
2	Pt-PVP/HT	31
3	Pt-PVA/HT	46

4. Discussion

4.1 Effect of polymer on the Pt-polymer/HT and their catalytic activity

TEM images and their histograms revealed that the Pt particle with the same mean diameter (2.2 nm) could be prepared by controlling the polymer amount during the particle preparation, in which only 0.025 g of PVA was adequate to stabilized NPs while PVP and starch loading were required up to 0.200 g. It is suggested that PVA shows strong stabilization power to prevent metal aggregation than starch and PVP. In general, the nonionic polymers can control particle size and prevent NPs aggregation by anchored on their surfaces which refers to steric stabilization (van der Waals attraction).^[44] As polymer contains the electron donating functional atoms such as

oxygen and nitrogen, the polymer molecules can adsorb on the surface of NPs through the coordination (e.g., ion-dipole, dipole-dipole, and other bonds).^[45] Soluble starch is a linear polymer formed by the α -(1 \rightarrow 4) linkages between *D*-glucose units and adopts a left-handed helical conformation in aqueous solution,^[26] whereas PVP and PVA are long chain polymers with a random coil structure.^[11] The possible electron donations from polymers to the Pt NPs surface were proposed in Figure 9, where starch may stabilize the Pt NPs *via* Pt-O interactions as a helical coordination (Figure 9A), nitrogen and oxygen atoms of PVP could surround Pt NPs surface (Figure 9B), and PVA would adhere Pt NPs surface *via* oxygen atoms of OH groups of alkyl chain (Figure 9C).

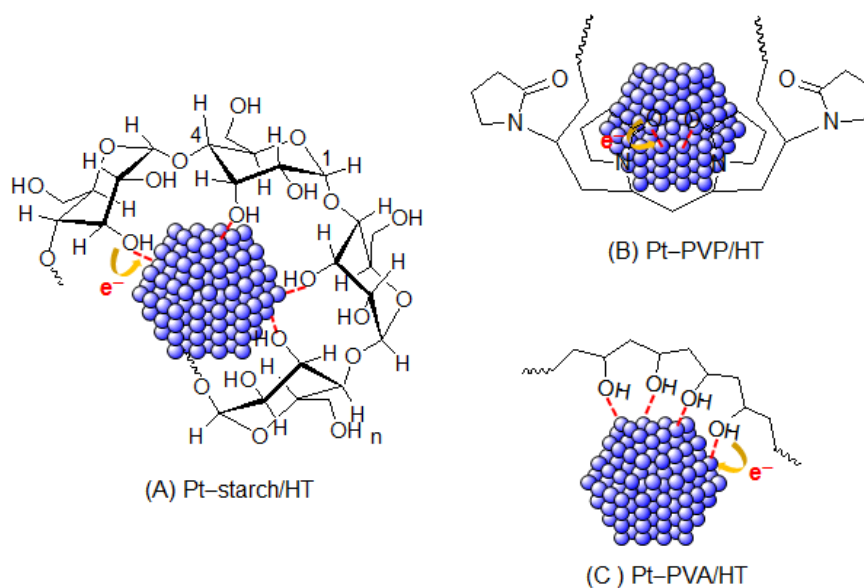


Figure 9 Possible electron donations from polymers to Pt NPs surface.

Three polymers could donate electrons into surface Pt atoms of NPs by coordination to form negatively charged surface Pt atoms. There has been reported that stabilizer such as PVP donates electron *via* carbonyl group to metal NPs such as

Pt, Au, and Ag NPs, which causes negative shifts of BE.^{[14],[18],[37]} From the results by XPS and XANES analyses, the donation ability of starch is compatible to that of PVA, and is stronger than that of PVP (as shown Figure 7). In case of Pt–starch/HT, the high activity of 57% conversion with 43% LA yield (TON = 71) well-explained by the abundance of electronically charged on the Pt surface atoms; these were also assisted by our previously worked indicating that starch ligand donated electron to the Pt surface and facilitated the surface Pt sites to being catalytically active.^[31] However, the electronic charge phenomena are not enough for explanation of their differences in catalytic activity for aerobic oxidation of PG in aqueous solution; *i.e.* the negatively charged on Pt surface atoms estimated by XPS and XANES analyses were following order: Pt–starch/HT \cong Pt–PVA/HT > Pt–PVP/HT, but these hardly elucidated the order for catalytic activity: Pt–starch/HT > Pt–PVP/HT > Pt–PVA/HT. Therefore, we postulated that the other factors such as the affinity of the ligand capped–Pt NPs for the solvent had also affected on the catalytic oxidation.

Considering the water wettability of catalysts, Pt–PVA/HT showed the highest contact angle value (46°, Figure 8 and Table 3) which implied to the lowest water wettability of three. Recently, some research groups have reported the importance of hydrophilicity-hydrophobicity of the catalyst in which directly affect the adsorption and desorption of the reactant and product in the elementary step for catalysis.^{[46]-[49]} This well-related to the proposal of the structural arrangement of polymer as illustrated in Figure 9C, in which PVA using oxygens of polymer stabilized NPs and rotated the non-polar side chain out then limited the wettability of catalyst in aqueous media under RT. Besides, as shown in Figure 4, even eight times less of PVA use

than starch and PVP was adequate to stabilize Pt particle in size of 2.2 nm, suggested the strong ability for stabilization of PVA which related to the much electron donation to Pt NPs. Following to these results, it was indicated that Pt-PVA/HT was negatively charged by the electron donation but showed low activity because of its low wettability for water solvent, both phenomena were attributed to the effect of PVA capping agent.

On the other hand, the contact angle of Pt-PVP/HT (31° , Figure 8 and Table 3) is proximately 0.7 times value of Pt-PVA/HT, it suggests that PVP facilitates the water wettability of catalyst: Pt-PVP/HT possessed more hydrophilic surface than Pt-PVA/HT. Whereas, the Pt-starch/HT showed 36° in the contact angle against water (Figure 8 and Table 3), which was between Pt-PVP/HT and Pt-PVA/HT. These results related to the contact angle value suggested that the affinity for water sorption of catalyst could be varied by polymer capping agent. In addition, this result may possible to essential evidence for the explanation of moderate catalytic activity of Pt-PVP/HT even less negatively charged presents on the Pt surface atoms. Accordingly, we confirmed that the high activity of Pt-starch/HT for aerobic oxidation of PG in aqueous solution at RT was due to not only the high electron negativity but also the suitable wettability for water solvent (hydrophilicity).

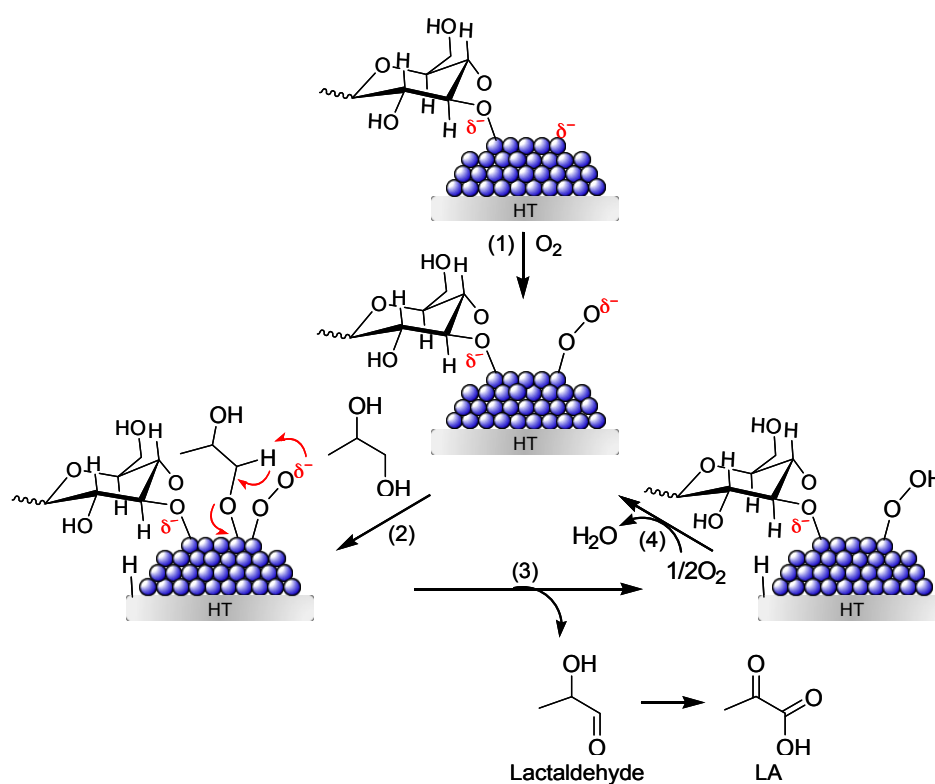
Overall, the preparation of supported metal catalyst using polymer as a stabilizing agent, it should show strong power to stabilize particle in small size together with exposes of the catalytic surface and facilitate the sorption-desorption of reactant, product and solvent. Furthermore, the active atoms in the molecule of

polymer may promote the highly active surface leading to high efficacy for the catalysis under mild conditions.

4.2 Proposal mechanism for aerobic oxidation of PG over Pt–polymer/HT in aqueous solution

As the above result, starch is a suitable ligand for preparation of catalyst, since starch acts as a good stabilizer which produces small Pt NPs and liberates the hydrophilic surface for catalysis in aqueous solution. The electronic charge-transfer from starch to Pt surface atoms induces the highly active surface for catalysis at RT. Therefore, the reaction mechanism of PG oxidation over Pt–starch/HT was proposed in Scheme 2. First, O₂ is adsorbed onto the surface of negatively charged Pt atoms (1). This step is proposed to be a crucial in the aerobic oxidation of PG in aqueous media at RT because the previous works reported that anionic metal (e.g., Au and Pt) can activate molecular oxygen by donating an excess electron charge to adsorbed oxygen generation of anionic O₂ like superoxo or peroxy oxygen.^{[5],[11],[50]-[59]} The charge on an adsorbate like oxygen is indication of the amount of charge transfer from the metal.^[60] These phenomenon has also been reported for oxidation of polyols,^[31] aerobic oxidation of *p*-hydroxybenzyl alcohol^{[11],[52]} and CO oxidation.^[53] Then, the basic support abstracts proton from PG to form the alkoxide (2). The proton in adsorbed alkoxide carbon is transformed to the adsorbed oxygen; releasing lactaldehyde (3) which is further oxidized to LA, and H₂O to generate back anionic O₂⁻ species (4). LA can be further over-oxidized to pyruvic acid (PA) followed by C-C bond cleavage to acetic acid (AA). The wettability for water (hydrophilicity) may

play the crucial role in accessibility of substrate and intermediates to the catalyst surface and/or dispensability of catalyst in water. Pt–starch/HT catalyst was hardly dispersed in nonpolar solvent such as toluene though bare Pt/HT could be dispersed. It suggested that affinity for the solvent strongly related to the dispersibility of the catalyst, and these were influenced by capping agents.



Scheme 2 A proposed reaction pathway for PG oxidation catalyzed by the Pt–starch/HT.

5. Conclusion

The research in this chapter discovered that polymers have a strong influence on the properties of Pt–polymer catalyst by difference stabilizing power to metal NPs and may determine the preserving or limiting the catalytically active site of NPs. PVA shows strong electron donation to Pt surface atoms, however, it limits the wettability of active Pt surface atoms for water solvent. PVP facilitates the affinity for water sorption though exploits weak electron donation. Starch is found to be a suitable ligand for creating negative charge on Pt surface atoms with better wettability for water than PVA. Overall, the major effects on the catalytic activity of Pt NPs stabilized by polymer are the electronic charge on the Pt atoms to facilitate O₂ activation for PG oxidation in aqueous solution and wettability for water solvent. Accordingly, the polymer stabilizing agent effects on the charge in active metal and/or affinity for solvent, and played an important role for the catalysis.

6. References

- [1] A. Villa, D. Wang, D. S. Su, L. Prati, Gold sols as catalysts for glycerol oxidation: the role of stabilizer, *ChemCatChem* **2009**, *1*, 510–514.
- [2] N. Dimitratos, J. A. Lopez-Sanchez, S. Meenakshisundaram, J. M. Anthonykutti, G. Brett, A. F. Carley, S. H. Taylor, D. W. Knight, G. J. Hutchings, Selective formation of lactate by oxidation of 1,2-propanediol using gold palladium alloy supported nanocrystals, *Green Chem.* **2009**, *11*, 1209–1216.
- [3] G. L. Brett, P. J. Miedziak, N. Dimitratos, J. A. Lopez-Sanchez, N. F. Dummer, R. Tiruvalam, C. J. Kiely, D. W. Knight, S. H. Taylor, D. J. Morgan, A. F. Carley, G. J. Hutchings, Oxidative esterification of 1,2-propanediol using gold and gold-palladium supported nanoparticles, *Catal. Sci. Technol.* **2012**, *2*, 97–104.
- [4] H. Tsunoyama, H. Sakurai, Y. Negishi, T. Tsukuda, Size-Specific catalytic activity of polymer-stabilized gold nanoclusters for aerobic alcohol oxidation in water, *J. Am. Chem. Soc.* **2005**, *127*, 9374–9375.
- [5] J. N. Kuhn, W. Huang, C.-K. Tsung, Y. Zhang, Somorjai, G. A. Structure sensitivity of carbon-nitrogen ring opening: impact of platinum particle size from below 1 to 5 nm upon pyrrole hydrogenation product selectivity over monodisperse platinum nanoparticles loaded onto mesoporous silica, *J. Am. Chem. Soc.* **2008**, *130*, 14026–14027.
- [6] S. Nishimura, Y. Yakita, M. Katayama, K. Higashimine, K. Ebitani, The role of negatively charged Au states in aerobic oxidation of alcohols over hydrotalcite

- supported AuPd nanoclusters, *Catal. Sci. Technol.* **2013**, 3, 351–359.
- [7] Y. Xia, Y. Xiong, B. Lim, S. E. Skrabalak, Shape-controlled synthesis of metal nanocrystals: simple chemistry meets complex physics, *Angew. Chem., Int. Ed.* **2009**, 48, 60–103.
- [8] J. N. Kuhn, C.-K. Tsung, W. Huang, G. A. Somorjai, Effect of organic capping layers over monodisperse platinum nanoparticles upon activity for ethylene hydrogenation and carbon monoxide oxidation, *J. Catal.* **2009**, 265, 209–215.
- [9] P. Zhang, T. K. Sham, Tuning the electronic behavior of Au nanoparticles with capping molecules. *Appl. Phys. Lett.* **2002**, 81, 736–738.
- [10] L. Qiu, F. Liu, L. Z. Zhao, W. Yang, J. Yao, Evidence of a unique electron donor–acceptor property for platinum nano-particles as studied by XPS, *Langmuir* **2006**, 22, 4480–4482.
- [11] M. Okumura, Y. Kitagawa, T. Kawakami, M. Haruta, Theoretical investigation of the hetero-junction effect in PVP-stabilized Au₁₃ cluster. The role of PVP in their catalytic activities, *Chem. Phys. Lett.* **2008**, 459, 133–136.
- [12] H. Tsunoyama, N. Ichikuni, H. Sakurai, T. Tsukuda, Effect of electronic structures of Au clusters stabilized by poly(N-vinyl-2-pyrrolidone) on aerobic oxidation catalysis, *J. Am. Chem. Soc.* **2009**, 131, 7086–7093.
- [13] G.-R. Zhang, B.-Q. Xu, Surprisingly strong effect of stabilizer on the properties of au nanoparticles and PtAu nanostructures in electrocatalysis, *Nanoscale* **2010**, 2, 2798–2804.
- [14] Y. Li, M. A. El-Sayed, The effect of stabilizers on the catalytic activity and stability of Pd colloidal nanoparticles in the Suzuki reactions in aqueous

- solution, *J. Phys. Chem. B* **2001**, *105*, 8938–8943.
- [15] H. Lee, S. E. Habas, S. KweSkin, D. Butcher, G. A. Somorjai, P. Yang, Morphological control of catalytically active platinum nanocrystals, *Angew. Chem.* **2006**, *118*, 7988–7992.
- [16] H. Lee, S. E. Habas, S. KweSkin, D. Butcher, G. A. Somorjai, P. Yang, Morphological control of catalytically active platinum nanocrystals, *Angew. Chem., Int. Ed.* **2006**, *45*, 7824–7828.
- [17] H. Zhang, M. Okumura, N. Toshima, Stable dispersions of PVP-protected Au/Pt/Ag trimetallic nanoparticles as highly active colloidal catalysts for aerobic glucose oxidation, *J. Phys. Chem. C* **2011**, *115*, 14883–14891.
- [18] Y. Borodko, S. E. Habas, M. Koebel, P. Yang, H. Frei, G. A. Somorjai, Probing the interaction of poly(vinylpyrrolidone) with platinum nanocrystals by UV-Raman and FTIR, *J. Phys. Chem. B* **2006**, *110*, 23052–23059.
- [19] C.-H. (Clayton) Zhou, J. N. Beltramini, Y.-X. Fan, G. Q. (Max). Lu, Chemoselective catalytic conversion of glycerol as a biorenewable source to valuable commodity chemicals, *Chem. Soc. Rev.* **2008**, *37*, 527–549.
- [20] B. Katryniok, H. Kimura, E. Skrzyńska, J.-S. Girardon, P. Fongarland, M. Capron, R. Ducoulombier, N. Mimura, S. Paul, F. Dumeignil, Selective catalytic oxidation of glycerol: perspectives for high value chemicals, *Green Chem.* **2011**, *13*, 1960–1979.
- [21] Z. Peng, H. Yang, Designer platinum nanoparticles: control of shape, composition in alloy, nanostructure and electrocatalytic property, *Nano Today* **2009**, *4*, 143–164.

- [22] J. Chen, B. Lim, E. P. Lee, Y. Xia, Shape-controlled synthesis of platinum nanocrystals for catalytic and electrocatalytic applications, *Nano Today* **2009**, *4*, 81–95.
- [23] N. Dimitratos, C. Messi, F. Porta, L. Prati, A. Villa, Investigation on the behaviour of Pt(0)/carbon and Pt(0),Au(0)/carbon catalysts employed in the oxidation of glycerol with molecular oxygen in water, *J. Mol. Catal. A: Chem.* **2006**, *256*, 21–28.
- [24] D. Tongsakul, K. Wongravee, C. Thammacharoen, S. Ekgasit, Enhancement of the reduction efficiency of soluble starch for platinum nanoparticles synthesis, *Carbohydr. Res.* **2012**, *357*, 90–97.
- [25] D. Tongsakul, S. Nishimura, C. Thammacharoen, S. Ekgasit, K. Ebitani, Hydrotalcite-supported platinum nanoparticles prepared by a green synthesis method for selective oxidation of glycerol in water using molecular oxygen, *Ind. Eng. Chem. Res.* **2012**, *51*, 16182–16186.
- [26] N. Vigneshwaran, R. P. Nachane, R. H. Balasubramanya, P. V. Varadarajan, A novel one-pot ‘green’ synthesis of stable silver nanoparticles using soluble starch, *Carbohydr. Res.* **2006**, *341*, 2012–2018.
- [27] K. Kaneda, K. Yamaguchi, K. Mori, T. Mizugaki, K. Ebitani, Catalyst design of hydrotalcite compounds for efficient oxidations, *Catal. Surv. Jpn.* **2000**, *4*, 31–38.
- [28] K. Motokura, D. Nishimura, K. Mori, T. Mizugaki, K. Ebitani, K. Kaneda, A ruthenium-grafted hydrotalcite as a multifunctional catalyst for direct α -alkylation of nitriles with primary alcohols, *J. Am. Chem. Soc.* **2004**, *126*,

5662–5663.

- [29] K. Ebitani, K. Motokura, T. Mizugaki, K. Kaneda, Heterotrimetallic RuMnMn species on a hydrotalcite surface as highly efficient heterogeneous catalysts for liquid-phase oxidation of alcohols with molecular oxygen, *Angew. Chem., Int. Ed.* **2005**, *44*, 3423–3426.
- [30] K. Kaneda, T. Mitsudome, T. Mizugaki, K. Jitsukawa, Development of heterogeneous olympic medal metal nanoparticle catalysts for environmentally benign molecular transformations based on the surface properties of hydrotalcite, *Molecules* **2010**, *15*, 8988–9007.
- [31] D. Tongsakul, S. Nishimura, K. Ebitani, Platinum/gold alloy nanoparticles-supported hydrotalcite catalyst for selective aerobic oxidation of polyols in base-free aqueous solution at room temperature, *ACS Catal.* **2013**, *3*, 2199–2207.
- [32] A. Tsuji, K. T. V. Rao, S. Nishimura, A. Takagaki, K. Ebitani, Selective oxidation of glycerol by using a hydrotalcite-supported platinum catalyst under atmospheric oxygen pressure in water, *ChemSusChem* **2011**, *4*, 542–548.
- [33] M. Pagliaro, R. Ciriminna, H. Kimura, M. Rossi, C. D. Pina, From glycerol to value-added products, *Angew. Chem., Int. Ed.* **2007**, *46*, 4434–4440.
- [34] R. Datta, M. Henry, Lactic acid: recent advances in products, processes and technologies—A review, *J. Chem. Technol. Biotechnol.* **2006**, *81*, 1119–1129.
- [35] S. Lux, P. Stehring, M. Siebenhofer, Lactic acid production as a new approach for exploitation of glycerol, *Sep. Sci. Technol.* **2010**, *45*, 1921–1927.
- [36] E. P. Maris, R. J. Davis, Hydrogenolysis of glycerol over carbon-supported Ru

- and Pt catalysts, *J. Catal.* **2007**, *249*, 328–337.
- [37] C.-W. Chen, M. Akashi, Synthesis, characterization, and catalytic properties of colloidal platinum nanoparticles protected by poly(N-isopropylacrylamide), *Langmuir* **1997**, *13*, 6465–6472.
- [38] Z. Huang, F. Li, B. Chen, F. Xue, Y. Yuan, G. Chen, G. Yuan, Efficient and recyclable catalysts for selective oxidation of polyols in H₂O with molecular oxygen, *Green Chem.* **2011**, *13*, 3414–3422.
- [39] C. Bianchi, F. Porta, L. Prati, M. Rossi, Selective liquid phase oxidation using gold catalysts, *Top. Catal.* **2000**, *13*, 231–236.
- [40] S. Demirel, P. Kern, M. Lucas, P. Claus, Oxidation of mono- and polyalcohols with gold: comparison of carbon and ceria supported catalysts, *Catal. Today* **2007**, *122*, 292–300.
- [41] E. Taarning, A. T. Madsen, J. M. Marchetti, K. Egeblad, C. H. Christensen, Oxidation of glycerol and propanediols in methanol over heterogeneous gold catalysts, *Green Chem.* **2008**, *10*, 408–414.
- [42] XPS peaks of Pt–polymer/HT in Pt 4f regions were hardly elucidated because of energy overlapping around at 74.4 eV corresponding to Al 2p region in Mg-Al HT support.
- [43] I. E. Beck, V. V. Kriventsov, D. P. Ivanov, V. I. Zaikovsky, V. I. Bukhtiyarov, XAFS study of Pt/Al₂O₃ nanosystem with metal-oxide active component, *Nucl. Instrum. Methods, Sect. A* **2009**, *603*, 108–110.
- [44] C.-W. Chen, D. Tano, M. Akashi, Colloidal platinum nanoparticles stabilized by vinyl polymers with amide side chains: dispersion stability and catalytic activity

- in aqueous electrolyte solutions, *J. Colloid Interface Sci.* **2000**, *225*, 349–358.
- [45] S. Chen, K. Kimura, Synthesis of thiolate-stabilized platinum nanoparticles in protolytic solvents as isolable colloids, *J. Phys. Chem. B* **2001**, *105*, 5397–5403.
- [46] M. Wang, F. Wang, J. Ma, C. Chen, S. Shi, J. Xu, Insights into support wettability in tuning catalytic performance in the oxidation of aliphatic alcohol to acids, *Chem. Commun.* **2013**, *49*, 6623–6625.
- [47] Z. Zhong, Y. Zhong, C. Liu, S. Yin, W. Zhang, D. Shi, Study on the surface wetting properties of treated indium-tin-oxide anodes for polymer electroluminescent devices, *Phys. Status Solidi A* **2003**, *198*, 197–203.
- [48] H. M. Yu, C. Ziegler, M. Oszcipok, M. Zobel, C. Hebling, Hydrophilicity and hydrophobicity study of catalyst layers in proton exchange membrane fuel cells, *Electrochim. Acta* **2006**, *51*, 1199–1207.
- [49] S. Aguado, J. Canivet, Y. Schuurman, D. Farrusseng, Tuning the activity by controlling the wettability of MOF eggshell catalysts: a quantitative structure–activity study, *J. Catal.* **2011**, *284*, 207–214.
- [50] M. Okumura, Y. Kitagawa, M. Haruta, K. Yamaguchi, DFT studies of interaction between O₂ and Au clusters. The role of anionic surface Au atoms on Au clusters for catalyzed oxygenation, *Chem. Phys. Lett.* **2001**, *346*, 163–168.
- [51] M. Okumura, Y. Kitagawa, M. Haruta, K. Yamaguchi, The interaction of neutral and charged Au clusters with O₂, CO and H₂, *Appl. Catal., A* **2005**, *291*, 37–44.
- [52] N. K. Chaki, H. Tsunoyama, Y. Negishi, H. Sakurai, T. Tsukuda, Effect of Ag-doping on the catalytic activity of polymer-stabilized Au clusters in aerobic

- oxidation of alcohol, *J. Phys. Chem. C* **2007**, *111*, 4885–4888.
- [53] Y. D. Kim, M. Fischer, G. Ganteför, Origin of unusual catalytic activities of Au-based catalysts, *Chem. Phys. Lett.* **2003**, *377*, 170–176.
- [54] T. M. Bernhardt, Gas-phase kinetics and catalytic reactions of small silver and gold clusters, *Int. J. Mass Spectrom.* **2005**, *243*, 1–29.
- [55] B. Yoon, H. Hakkinen, U. Landman, Interaction of O₂ with gold clusters: molecular and dissociative adsorption, *J. Phys. Chem. A* **2003**, *107*, 4066–4071.
- [56] I. Panas, P. A. Siegbahn, Theoretical study of the peroxy and superoxy forms of molecular oxygen on metal surfaces, *Chem. Phys. Lett.* **1988**, *153*, 458–464.
- [57] K. Gustafsson, S. Andersson, Infrared spectroscopy of physisorbed and chemisorbed O₂ on Pt(111), *J. Chem. Phys.* **2004**, *120*, 7750–7754.
- [58] Y. S. Kim, A. Bostwick, E. Rotenberg, P. N. Ross, S. C. Hong, B. S. Mun, The study of oxygen molecules on Pt (111) surface with high resolution X-ray photoemission spectroscopy, *J. Chem. Phys.* **2010**, *133*, 034501–1–035404–2.
- [59] The bonding of atomic oxygen to Pt(111) was formed through interaction of the 2p_{xy} orbitals of oxygen with the 6 sp states of the Pt metal and the oxygen 2p_z orbital with the 5d Pt orbitals.⁶⁰
- [60] M. Chen, S. P. Bates, R. A. van Santen, C. M. Friend, The chemical nature of atomic oxygen adsorbed on Rh(111) and Pt(111): a density functional study, *J. Phys. Chem. B* **1997**, *101*, 10051–10057.

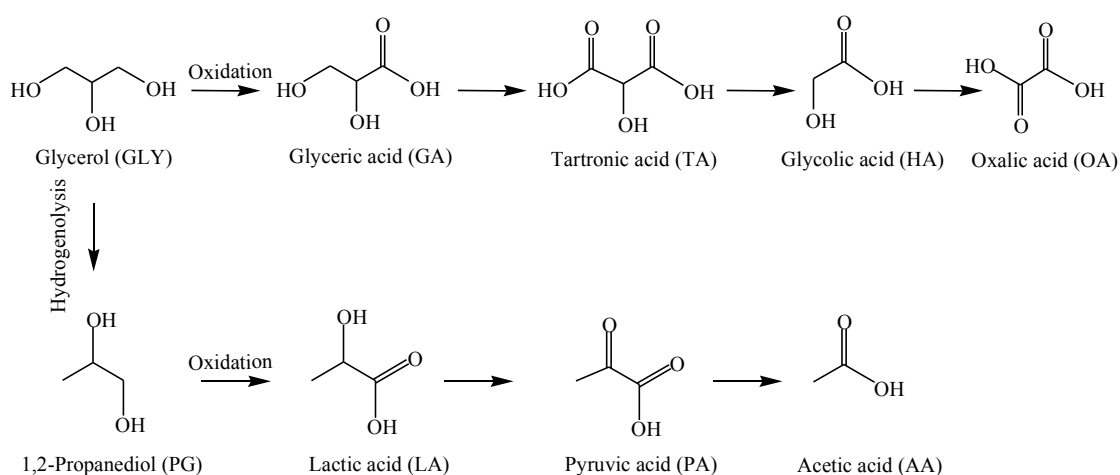
Chapter 4

EVOLUTION OF STARCH STABILIZED SUPPORTED PLATINUM-BASED BIMETALLIC CATALYSTS FOR SELECTIVE AND AQUEOUS POLYOLS OXIDATION USING MOLECULAR OXYGEN

1. Introduction

Biomass is biological material derived from plants, and the transformation of biomass-derived compounds into energy sources and valuable chemicals will serve as an alternative resource instead of fossil fuel.^{[1]-[3]} Biodiesel fuel (BDF) is the one of biomass-derived energy produced by transesterification of biomass (triglycerides) with alcohols, and a huge amount of glycerol (GLY) is obtained as a byproduct during the production of BDF.^{[4]-[6]} GLY-derived products can serve various substrates for the manufacture of high-end chemicals. For instance, from the controlled partial oxidation of GLY, various value-added chemicals, such as glyceric acid (GA), dihydroxyacetone, and tartronic acid (TA), can be provided.^{[4],[5],[7]} Particularly, GA is a very important one, affording medicine and skin care treatment.^{[1],[7-9]} In addition, 1,2-propanediol (PG), the product of GLY hydrogenolysis,^[10] is a crucial starting material for the chemical synthesis of lactic acid (LA) by a partial oxidation.^{[5],[6],[11]}

LA is used in the industrial fields of food and pharmaceutical products.^{[12],[13]} General reaction pathways for the oxidation of GLY and PG are shown in Scheme 1. Research on supported monometallic nanoparticle (NP) catalysts, especially Pt, Au, and Pd catalysts, for the oxidation of polyols in the presence of base have been reported during the past decade.^{[14]–[19]} Many publications have detailed that the supported bimetallic NPs also possessed a catalytic activity superior to the monometallic ones for oxidation of polyols in the presence of base (see Chapter 1, Tables 2–4).^{[11],[14],[20–24]} For example, Dimitratose et al. found that alloyed AuPd/TiO₂ improved activity and selectivity for PG oxidation to LA in the presence of NaOH under pressurized oxygen (10 atm) at 333 K.^[14] Brett et al. observed that the addition of Pd to Au atoms significantly enhanced the activity and retained high selectivity to methyl lactate in the presence of sodium methoxide (NaOMe) at 373 K under pressurized oxygen (3 atm).^[11]



Scheme 1 General reaction pathways for the oxidation of GLY and PG.

It is well-known that the catalysis for the oxidation reaction of polyols (e.g., GLY) strongly depends on the basicity of the reaction medium because the external base can enhance a proton abstraction step from the hydroxyl group of GLY. However, the salt of the products, such as glycerate, was formed when a homogeneous base was used, and then the obtained products required an additional neutralization or acidification. In advanced research, the oxidation reaction has been performed with metal species supported on basic materials, which permitted a base-free oxidation, producing the free carboxylic acid rather than the salt form. The modern oxidation process prefers an atmospheric pressure of molecular oxygen (O_2) as a green oxidant because the classical oxidant, such as CrO_3 and $KMnO_4$, had large harmful impacts for the environment.^{[15],[25],[26]} Recently, the catalytic oxidation of GLY over a bimetallic catalyst in base-free aqueous solution under oxygen flow has been reported. Hou and co-workers showed that PtCu/C and PtSb/multiwall carbon nanotubes (MWCNTs) were more active and selective toward GA than Pt/C and Pt/MWCNT, respectively.^[27-29] Tomishige et al. also found that PdAg/C showed higher activity and selectivity to dihydroxyacetone than Pd/C for GLY oxidation with molecular oxygen (3 atm) under neutral conditions at 373 K.^[30]

Very recently, I succeeded in the synthesis of a novel hydrotalcite-supported Pt–starch NPs (Pt–starch/HT) catalyst using soluble starch as a green reducing and a stabilizing agent.^[31] The Pt–starch/HT became an environmentally friendly and a highly efficient catalyst which suppressed the overoxidation of GLY to C_1 products in comparison with the bare Pt/HT catalyst^[32] for selective oxidation of GLY in base-free aqueous solution with molecular oxygen under atmospheric pressure. This

achievement inspired me to further challenge for the preparation of an efficient bimetallic NP catalyst in selective oxidation of polyols. Herein, I explore the efficient catalytic oxidation of polyols (GLY and PG) in base-free aqueous solution under ambient conditions over HT-supported Pt_xAu_y -starch NPs (Pt_xAu_y -starch/HT) catalysts. The Pt_xAu_y -starch/HTs were prepared by a sol immobilization method with various Pt/Au molar ratios (x/y) using soluble starch as a green reducing and stabilizing agent.^{[31],[33]} HT is well-known as a reusable basic layered double hydroxide that is frequently used as a support for Pd, Ru, and Au species.^{[34],[35]} Following the results shown below, we found that the Pt_xAu_y -starch/HT catalysts exhibited high selectivities for GA and LA formation in aerobic and aqueous base-free oxidations of GLY and PG under ambient conditions (i.e., room temperature and an atmospheric pressure of molecular oxygen). The negative charge on Pt atoms induced by the electron transfer from both neighbor Au atoms and starch ligand were detected by XPS and XANES analyses. I suggested that both geometric and electronic change of the catalytically active Pt sites by adjacent Au atoms and starch ligands contributed to improvement of the activity and selectivity toward the target products.

2. Experiment

2.1 Chemicals

Hexachloroplatinic acid ($\text{H}_2\text{PtCl}_6 \cdot 6\text{H}_2\text{O}$, 99.9%; Cat. No: 089-05311), tetrachloroauric acid ($\text{HAuCl}_4 \cdot 4\text{H}_2\text{O}$, 99.9%; Cat. No: 073-00933), palladium chloride (PdCl_2 , 99%; Cat. No: 168-24713), ruthenium chloride n-hydrate ($\text{RuCl}_3 \cdot n\text{H}_2\text{O}$,

99.9%; Cat. No: 187-00821), 1,2-propanediol (99%; Cat. No: 164-04996) and soluble starch (Cat. No: 195-03961) were purchased from Wako Pure Chemicals. Glycerol (99.9%; Cat. No: 17018-25) was provided from Nacalai Tesque. Silver nitrate (AgNO_3 , 99.9%; Cat. No: 204390-10G) was received from Sigma-Aldrich. Sodium hydroxide (NaOH , 97%; Cat. No: 37184-00 JIS K 8576) was obtained from Kanto Chemicals. Hydrotalcite (HT, $\text{Mg}/\text{Al} = 5$; Cat. No: TOMITA-AD-550PF) was provided from Tomita Pharmaceutical. Chemical. 2,6-Di-*tert*-butyl-*p*-cresol (BHT); Cat. No: D0228) was received from Tokyo Chemical Industry.

2.2 Preparation of hydrotalcite supported Pt-based bimetallic catalysts

2.2.1 Fast co-reduction method (FCR)

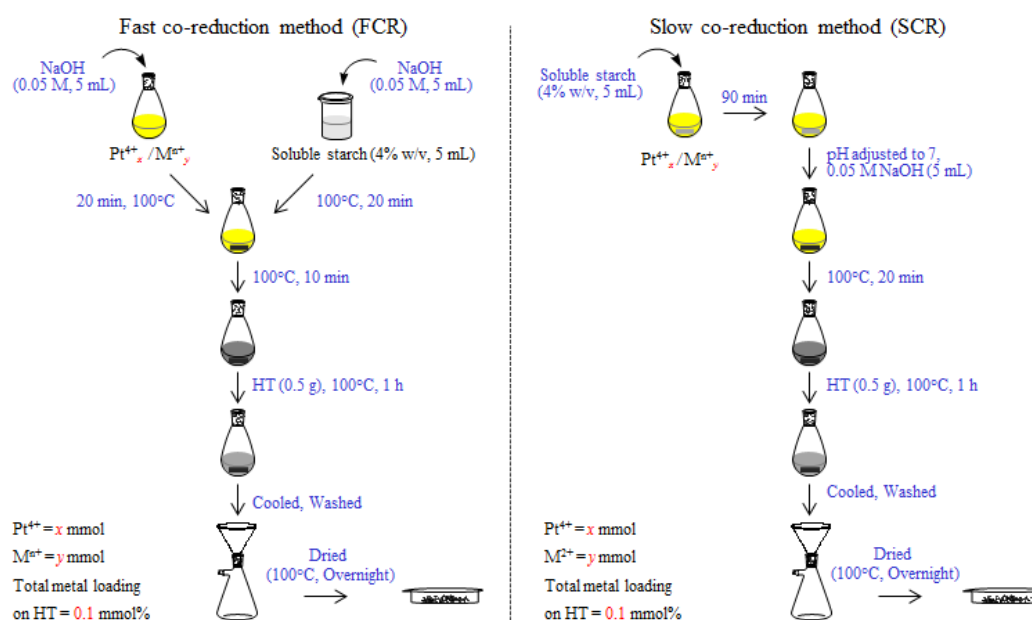
HT supported bimetallic Pt-based NPs catalysts (Pt-M NPs/HT, M = Pd, Ru, Ag and Au) were synthesized by the fast co-reduced reduction method using soluble starch as a reducing and a stabilizing agent (Scheme 1). Thereafter, they were immobilized onto the HT surface. Various ratios of metal mixed solution (Pt_x/M_y) were kept at 0.1 mmol%. Different mixed metal solutions were prepared as follows:

Preparation of PtRu solution. A variety ratios of Pt_xRu_y solution were prepared by the dispersion of $\text{H}_2\text{PtCl}_6 \cdot 6\text{H}_2\text{O}$ (x mmol) and $\text{RuCl}_3 \cdot 3\text{H}_2\text{O}$ (y mmol). The pH of the solutions was adjusted to neutral with 1 M NaOH . Thereafter, the solutions were individually pH adjusted with 5 mL of 0.05 M NaOH .

Preparation of PtAg NPs solution. All ratios of Pt_xAg_y solution were manipulated by the dispersion of $H_2PtCl_6 \cdot 6H_2O$ (x mmol) and $AgNO_3$ (y mmol) in water. The pH of the solutions was adjusted to neutral with 1 M NaOH.

Preparation of PtPd NPs solution. Various ratios of Pt_xPd_y solution were prepared by the dispersion of $H_2PtCl_6 \cdot 6H_2O$ (x mmol) and $PdCl_2$ (y mmol) with 0.033 g KCl in water. The pH of the solutions was adjusted to pH 6 with 1 M NaOH.

Preparation of PtAu NPs solution. The different ratios of Pt_xAu_y solution were provided by the dispersion of $H_2PtCl_6 \cdot 6H_2O$ (x mmol) and $HAuCl_4 \cdot 4H_2O$ (y mmol) in water. The pH of the solutions was adjusted to neutral with 1 M NaOH. Each ratio of the solution was individually pH adjusted with 5 mL of 0.05 M NaOH.



Scheme 2 Synthesis of Pt_xM_y NPs/HT heterogeneous catalysts by immobilization.

A 4% w/v soluble starch solution was prepared by dissolving 4 g of soluble starch in hot water (100 mL). After cooling, 5 mL fractions of starch solution were mixed with 5 mL of 0.05 M NaOH. The Pt_xM_y ions solution and the starch solution were heated at 373 K for 20 min before mixing under vigorous stirring. After 10 min, Pt_xM_y NPs were immobilized onto the HT surface by addition of 0.5 g HT to the mixed solutions under continuously stirring and refluxed at 373 K for 1 h. Finally, the solution was cooled, filtered and washed with water. The solid catalyst was dried overnight at 373 K (Scheme 2).

2.2.2 Slow co-reduction method (SCR)

Pt_xAu_y NPs/HT catalysts were prepared by the immobilization method. Along with the method, Pt_xAu_y NPs were pre-generated by the slow co-reduction using soluble starch as a reducing and a stabilizing agent. Thereafter, they were immobilized onto the HT surface. The reduction procedure was investigated as follows; firstly, different ratios of $H_2PtCl_6 \cdot 6H_2O$ (x mmol) and $HAuCl_4 \cdot 4H_2O$ (y mmol) were mixed with 5 mL starch solution (0.2 g starch contents) and stirring for 90 min. Then, pH of the metal solution was adjusted to neutral with 1 M NaOH. Thereafter, further 5 mL NaOH (0.05 M) was added before heating up to 373 K. After refluxing for 20 min, 0.5 g HT was added to the solution with vigorous stirring, then the mixture was continuously refluxed for 1 h. Finally, the solution was cooled, filtered and washed with water. The solid catalyst was dried overnight at 373 K (see also Scheme 2).

2.3 Catalytic activity for polyols oxidation

Catalytic activity of Pt_xM_y NPs/HT was evaluated for polyols (GLY and PG) oxidation in base-free aqueous solution under atmospheric conditions. All reactions were performed in a 30 mL Schlenk tube attached to a reflux condenser. The general reaction procedures were as follows: polyol (0.5 mmol), H₂O (2 mL), Pt_xM_y NPs/HT catalyst, stirring speed (500 rpm). After the reaction, the catalyst was separated by filtration. The filtrate was analyzed by a high performance liquid chromatography (HPLC) equipped with an Aminex HPX-87H column (Bio-Rad Laboratories) and a refractive index (RI) detector. The analysis conditions were set as follows: eluent (aqueous solution of H₂SO₄ (10 mM)), flow rate (0.5 mL·min⁻¹), column temperature (323 K).

2.4 Characterization

The morphology of Pt_xAu_y NPs/HT was analyzed by transmission electron microscopy (TEM; Hitachi H-7100) at 100 kV accelerating voltage. The Pt_xAu_y NPs/HT was dispersed in deionized water and dropped onto a copper grid, then dried overnight in a desiccator. Powder X-ray diffraction (XRD) patterns were obtained with a Rigaku Smartlab X-ray diffractometer using Cu K α radiation ($\lambda = 0.154$ nm) at 40 kV and 20 mA. Inductively coupled plasma atomic emission spectroscopy (ICP-AES) was operated by Shimadzu ICPS-7000 ver.2 to estimate the real concentration of Pt on the catalyst. Ultraviolet and visible (UV/vis) spectra were measured by Perkin-Elmer Lambda35 spectrometer at room temperature with light path length of 1

cm. X-ray photoelectron spectroscopy (XPS) was measured on Shimadzu-Kratos AXIS-ULTRA DLD spectrometer using Al target at 15 kV and 10 mA. The binding energies were calibrated with the C 1s level (284.5 eV) as the internal standard reference. X-ray absorption near-edge structure (XANES) in the Pt L_3 -edge and Au L_3 -edge were recorded at beamline BL01B1 of SPring-8 with the approval of the Japan Synchrotron Radiation Research Institute (JASRI) (Proposal No. 2011A1607). The Pt_xAu_y NPs/HT catalysts were grained and pressed to a pellet ($\phi \sim 10$ mm) for XANES analysis. The obtained XANES spectra were analyzed using the Athena software (ver. 0.8.056).

3. Results and Discussion

As mentioned in Chapter 2, a green method was successfully developed using soluble starch as a reducing and a stabilizing agent for preparation of efficient and reusable HT supported-Pt NPs heterogeneous catalyst. In this section, the developed method was employed for preparation of HT supported-Pt-based bimetallic heterogeneous catalyst. The catalysis was examined for the selective polyols (GLY and PG) oxidation in base-free aqueous solution under atmospheric pressure of molecular oxygen at moderate reaction temperature.

3.1 Preparation of Pt-based bimetallic heterogeneous catalysts

TEM images and particle size distribution histograms of HT supported-Pt-based bimetallic catalysts (Pt_xM_y NPs/HT) were shown in Figure 1. The average particles size of Pt-based bimetallic NPs on HT being 2.4, 2.5, 5.2 and 5.5 for Pt₈₀Pd₂₀

NPs/HT, Pt₈₀Ru₂₀ NPs/HT, Pt₈₀Ag₂₀ NPs/HT and Pt₈₀Au₂₀ NPs/HT, respectively, were summarized (Table 1). The average particle size of monometallic NPs of Pt, Pd, Ru, Ag and Au have been given for comparison, which being 1.9, 2.6, 2.4, 15 and 18 nm for Pt₁₀₀ NPs/HT, Pd₁₀₀ NPs/HT, Ru₁₀₀ NPs/HT, Ag₁₀₀ NPs/HT and Au₁₀₀ NPs/HT, respectively (Table 1). All bimetallic catalysts reveal larger size than Pt₁₀₀ NPs/HT.

The catalytic aerobic oxidation of PG over various HT supported-monometallic catalysts were shown in Table 1, entries 1–5. Pt₁₀₀ NPs/HT was the best active catalyst which exhibited selective oxidation towards LA while Pd₁₀₀ NPs/HT, Ru₁₀₀ NPs/HT, Ag₁₀₀ NPs/HT and Au₁₀₀ NPs/HT were inactive under present condition. The PG oxidation results over bimetallic Pt_xM_y NPs/HT catalysts (M = Ru, Ag, Pd, Au) were also shown in Table 1, entries 6–9. All catalysts exhibited the selective oxidation toward LA, especially Pt₈₀Au₂₀ NPs/HT (Table 1, entry 9) showed the best selective (45% LA yield). Pt₈₀Pd₂₀ NPs/HT and Pt₈₀Ru₂₀ NPs/HT presented the identical activity to pure Pt₁₀₀ NPs/NPs, however, lower activity than pure Pt₁₀₀ NPs/NPs was found over Pt₈₀Ag₂₀ NPs/HT. It means that no improvement or depression in catalytic activities is obtained over Pt modified with Pd, Ru and Ag. Base on the above results, it can be said that Pt modified with Au significantly enhanced the selectivity toward LA formation even though particle size is 3 times larger than pure Pt₁₀₀ NPs/HT. Therefore, I expect that Pt₈₀Au₂₀ NPs/HT with small particle size should show an effective improvement in catalytic activity.

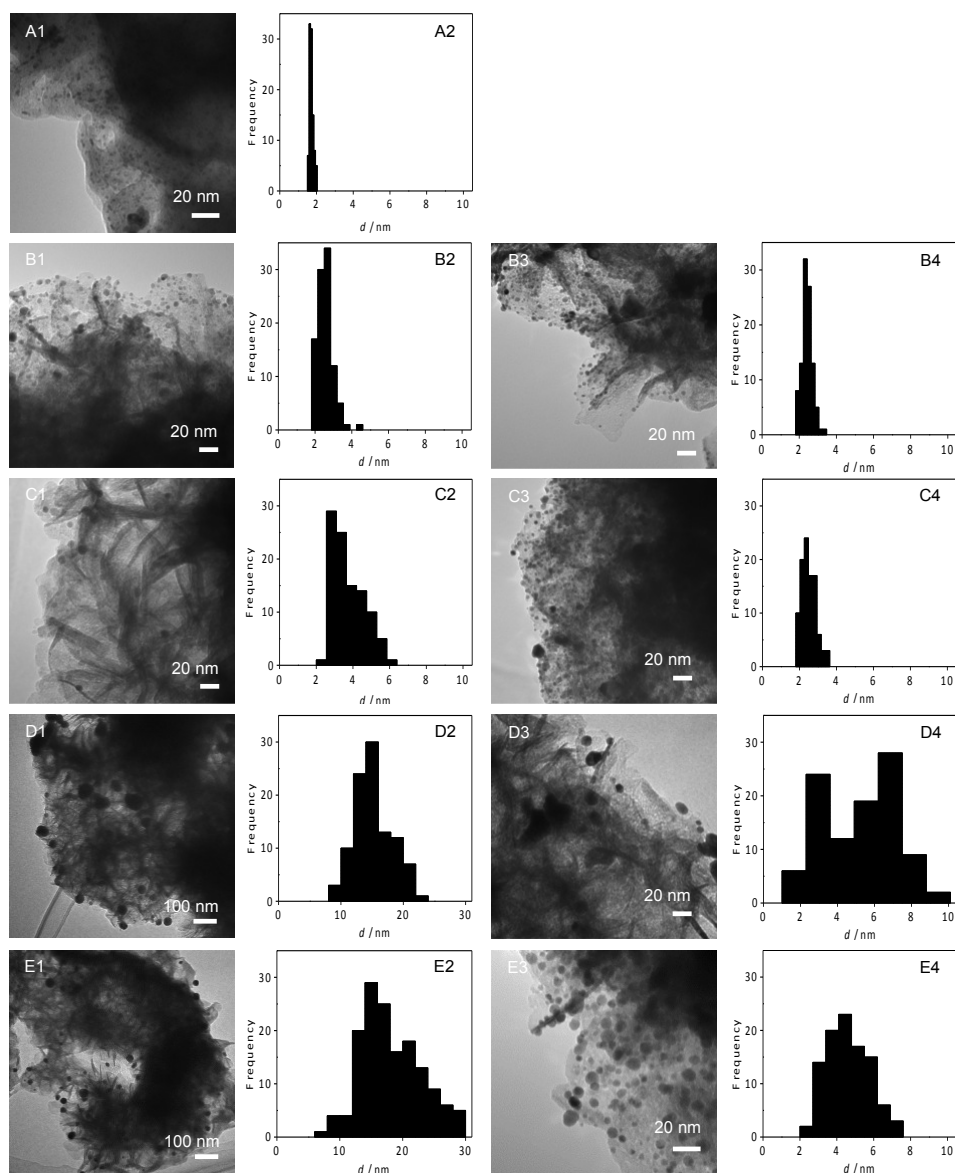


Figure 1 TEM images of (A1) Pt₁₀₀ NPs/HT, (B1) Pd₁₀₀ NPs/HT, (C1) Ru₁₀₀ NPs/HT, (D1) Ag₁₀₀ NPs/HT, (E1) Au₁₀₀ NPs/HT, (B3) Pt₈₀Pd₂₀ NPs/HT, (C3) Pt₈₀Ru₂₀ NPs/HT, (D3) Pt₈₀Ag₂₀ NPs/HT and (E3) Pt₈₀Au₂₀ NPs/HT, and (A2–E2) and (B4–E4) their particle size distribution histograms.

Table 1 Oxidation of PG over various mono- and bimetallic Pt-based heterogeneous catalysts^a

Entry	Catalysts	Particle size (nm)	Conversion (%)	LA yield (%)
1	Pt ₁₀₀ NPs/HT	1.9	69	39
2	Pd ₁₀₀ NPs/HT	2.6	6	4
3	Ru ₁₀₀ NPs/HT	2.4	trace	trace
4	Ag ₁₀₀ NPs/HT	15	trace	trace
5	Au ₁₀₀ NPs/HT	18	trace	trace
6 ^b	Pt ₈₀ Pd ₂₀ NPs/HT	2.4	65	36
7 ^b	Pt ₈₀ Ru ₂₀ NPs/HT	2.5	61	37
8 ^b	Pt ₈₀ Ag ₂₀ NPs/HT	5.2	37	25
9 ^b	Pt ₈₀ Au ₂₀ NPs/HT	5.5	65	45

^aReaction conditions: PG (0.5 mmol), water (2 mL), catalyst (20 mg), oxygen (10 mL·min⁻¹), temperature (353 K), reaction time (3 h). ^bPt + M (Ru, Ag, Pd, Au) = 0.1 mmol.

3.2 Improvement of the synthetic method for preparation of Pt_xAu_y NPs/HT

The aim of this section is to control the generation of small PtAu NPs size, therefore, further development of the preparation method (slow co-reduction method, SCR) was investigated (Scheme 2, right side). The catalysis was examined for the aerobic oxidation of polyols (GLY and PG) and the activity was compared with previous developed method (fast co-reduction method, FCR) (Scheme 2, left side).

3.2.1 Glycerol and 1,2-propanediol oxidation

Results of selective oxidation of PG over Pt_xAu_y NPs/HT catalysts prepared by the FCR and SCR were shown in Table 2. The moderate selectivity improvement

toward LA was observed over Pt₈₀Au₂₀ NPs/HT prepared by FCR (Table 2, entry 2) as compare to Pt₁₀₀ NPs/HT (Table 2, entry 1) at 353 K, whereas Au₁₀₀ NPs/HT was inactive (Table 2, entry 3). The aerobic oxidation over Pt₆₀Au₄₀ NPs/HT prepared by the SCR was found to show significant catalytic improvement for the PG and GLY oxidation in base-free aqueous solution under atmospheric pressure of molecular oxygen at room temperature (298 K). 74% (TON of 162, Table 3) and 39% (TON of 82, Table 3) of GLY and PG conversion were obtained over Pt₆₀Au₄₀ NPs/HT (SCR) (Table 2, entry 5) while lower conversion of 21% and 8% were achieved over Pt₆₀Au₄₀ NPs/HT (FCR) (Table 2, entry 4). These result indicated that the catalyst prepared by the SCR were more effective than that prepared by the FCR method.

Table 2 Effect of preparation method on the catalytic oxidation of polyols (GLY and PG)^a

Entry	Methods	Catalysts	Temperature (K)	GLY Conv. (%)	GA Yield (%)	PG Conv. (%)	LA Yield (%)
1 ^b	FCR ^c	Pt ₁₀₀ NPs/HT	353	-	-	69	39
2 ^b	FCR	Pt ₈₀ Au ₂₀ NPs/HT	353	-	-	65	45
3 ^b	FCR	Au ₁₀₀ NPs/HT	353	-	-	trace	trace
4	FCR	Pt ₆₀ Au ₄₀ NPs/HT	298	21	19	8	trace
5	SCR ^d	Pt ₆₀ Au ₄₀ NPs/HT	298	74	57	39	29

^aReaction conditions: GLY (0.5 mmol), water (2 mL), catalyst (20 mg), oxygen flow (10 mL·min⁻¹), reaction time (6 h). ^bPG (0.5 mmol), oxygen flow (10 mL·min⁻¹), reaction (3 h).

^cFast co-reduction method. ^dSlow co-reduction method.

3.2.2 Characterization of catalysts

Figure 2 shows UV/vis spectra of Pt_xAu_y NPs prepared by FCR and SCR. The characteristic peak of Au NPs by 520 nm was not observed in spectra of $Pt_{60}Au_{40}$ NPs. It was indicated the $Pt_{60}Au_{40}$ NPs prepared by the FCR and SCR formed as alloy rather than phase-segregation bimetallic NPs. TEM images of $Pt_{60}Au_{40}$ NPs/HT prepared by the FCR and SCR were displayed in Figure 3. The mean particle size of catalysts together with the total metal loading were listed in Table 3. $Pt_{60}Au_{40}$ NPs/HT (FCR) had larger particle size (9.8 nm) (Table 3, entry 1) than that of prepared by the SCR (2.2 nm) (Table 3, entry 2) together with lower metal loading. Therefore, it can be said that the SCR is an effective method for the preparation of alloy PtAu NPs/HT in small particle size, leading to enhancement of catalytic activity for the aerobic polyols oxidation under atmospheric conditions.

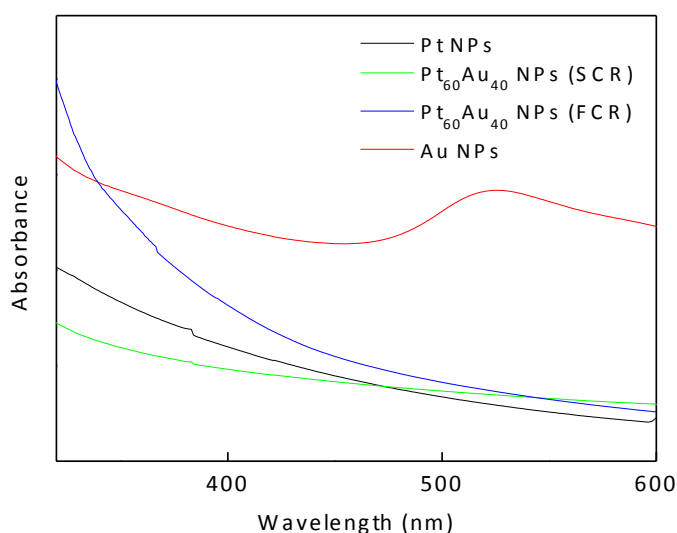


Figure 2 UV/vis spectra of Pt_xAu_y NPs prepared by the SCR and FCR methods.

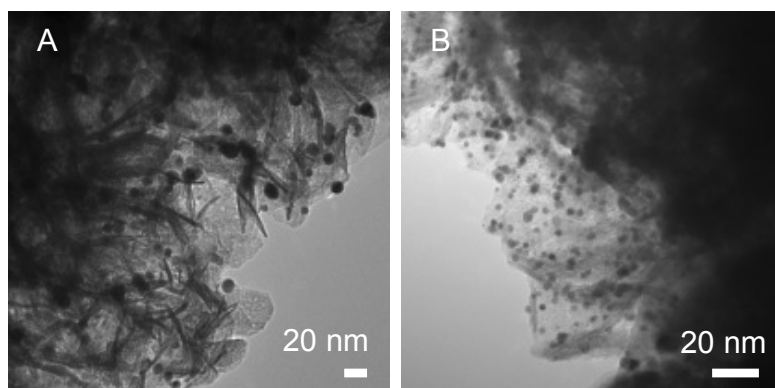


Figure 3 TEM images of Pt₆₀Au₄₀ NPs/HT prepared by the (A) FCR and (B) SCR methods.

Table 3 Characterization of Pt₆₀Au₄₀ NPs/HT prepared by FCR and SCR^a

Entry	Methods	Catalysts	Metal loading (mmol·g ⁻¹) ^d	Particle size (nm) ^e	TON ^f	
					GA	LA
1	FCR ^b	Pt ₆₀ Au ₄₀ NPs/HT	0.064	9.8	74	trace
2	SCR ^c	Pt ₆₀ Au ₄₀ NPs/HT	0.087	2.2	162	82

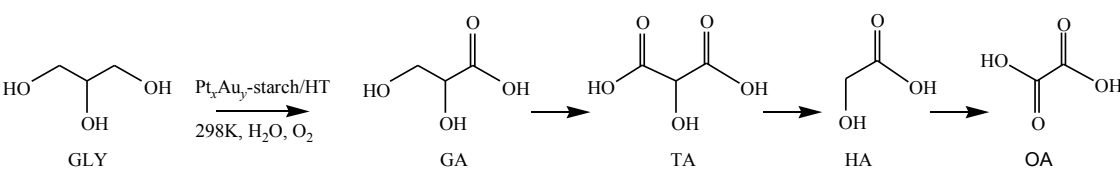
^aReaction conditions: GLY (0.5 mmol), water (2 mL), catalyst (20 mg), oxygen flow (10 mL·min⁻¹), reaction time (6 h). ^bFast co-reduction method. ^cSlow co-reduction method. ^dAnalysis by ICP-AES. ^eDetermined by TEM. ^fTON: normalized GA or LA yield to total metal amount in oxidation of GLY and PG, respectively.

3.3 An investigation of the immobilization Pt/Au ratio for the PtAu NPs/HT catalysts

3.3.1 Glycerol oxidation

Results of activity over Pt_xAu_y-starch/HT catalysts for the aerobic GLY oxidation under atmospheric conditions are summarized in Table 4, together with total

metal loading and mean particle size. All catalysts except for Au₁₀₀-starch/HT promoted the selective oxidation toward GA, and minor amounts of tartronic acid (TA), glycolic acid (HA), and oxalic acid (OA) were also observed. The formation of dihydroxyacetone, oxidation at the secondary hydroxyl group, was not detected in all cases. It was consistent with previous reports that GA was obtained as the major product, and it could be further oxidized to TA, HA, and OA in the aerobic oxidation of GLY catalyzed by the Pt-based heterogeneous catalyst.^{[31],[32],[37-39]} The highest GLY conversion (88%) was achieved by Pt₁₀₀-starch/HT, although it exhibited a low selectivity toward GA (48%) (Table 4, entry 1). Because the sum of GA, TA, HA, and OA was ~78% yield (89% selectivity), another overoxidation product toward C₁ product (ex. CO₂) seemed to be expected in Pt₁₀₀-starch/HT. As the Au amounts increased from $y = 20$ to 80, the GLY conversion gradually decreased with increasing selectivity for GA and suppressed overoxidation to the formation of byproduct (Table 4, entries 2-5), when the sum of product selectivity is nearly 100%. Au₁₀₀-starch/HT was inactive at room temperature (RT), whereas it showed a small activity at 333 K (Table 4, entry 6), even though its exhibited particle size of 5.5 nm was similar to that of Pt₂₀Au₈₀-starch/HT (5.4 nm). The aerobic oxidation over bare Au/HT with 3.2 nm was also inactive at RT (Table 4, entry 7). Thus, the aerobic oxidation over a supported Au catalyst cannot proceed at RT. These results suggest that the replacement of active Pt atoms with inactive Au atoms likely has some roles for prohibition of overoxidation, and it supports increasing the mass balance close to 100%. The Pt₆₀Au₄₀-starch/HT showed the most effective catalyst with a TOF of 84.7 h⁻¹ at RT (Table 4, entry 3).

Table 4 Results of GLY oxidation over Pt_xAu_y-starch NPs/HT catalysts^a


Entry	Catalysts	Conv. of GLY / %	Sel. of GA / %	Yield / %				Total metal loading / mmol·g ⁻¹ ^c	Particle size / nm	TOF (h ⁻¹)
				GA	TA	HA	OA			
1	Pt ₁₀₀ -starch/HT	88	48	42	13	11	12	0.087	2.0	70.4
2	Pt ₈₀ Au ₂₀ -starch/HT	80	64	51	10	8	7	0.086	2.2	81.1
3	Pt ₆₀ Au ₄₀ -starch/HT	73	78	57	9	6	6	0.087	2.2	84.7
4	Pt ₄₀ Au ₆₀ -starch/HT	74	73	54	10	4	5	0.086	3.8	69.2
5	Pt ₂₀ Au ₈₀ -starch/HT	50	84	42	4	2	1	0.089	5.4	34.8
6	Au ₁₀₀ -starch/HT	trace, 11 ^b	-, 37 ^b	trace, 4 ^b	0, 3 ^b	0, 3 ^b	0, 1 ^b	0.087	5.5	-
7	Au/HT	trace	-	trace	0	0	0	0.096	3.2	-

^aReaction conditions: GLY (0.5 mmol), H₂O (2 mL), catalyst (20 mg, GLY/metal = 287), oxygen flow (10 mL·min⁻¹), room temperature (298 K), reaction time (6 h). ^b333 K. ^cAnalysis by ICP-AES.

The time profile of the GLY oxidation over Pt₆₀Au₄₀-starch/ HT is plotted in Figure 4. The reaction was accomplished by the oxidation of the primary hydroxyl group of GLY to GA, together with the formation of side products (i.e., TA, HA and OA) via the overoxidation. At the initial stage of the reaction within 1 h, the highest selectivity to GA (87%) was achieved. Nevertheless, the glyceraldehyde, which was expected to be an intermediate, was not observed. The GLY conversion and yield of GA are 68% and 52%, respectively, as the reaction time reaches 5 h. When the reaction time was increased to 10 h, nearly 80% conversion of GLY was obtained. There was no significant increase in the GA yield after a reaction time of 5 h. A small amount of the overoxidation of GA to TA and further C–C bond cleavage to

HA and OA scarcely occurred during the reaction. Although the pH values were gradually decreased with the progressive reaction that we reported on previously,^[31] the basicity of the HT support seems to be enough for further reaction because the PtAu/HT catalyst was recyclable for 3 runs (*vide infra*). Previous reports on GLY oxidation at near room temperature are summarized in Chapter 1, Tables 2 and 3.^{[21],[22],[40–42]} Most reactions were carried out in the presence of NaOH under pressurized oxygen (3–10 atm). The oxidation of GLY under pressurized oxygen (3 atm) with GLY conversions of 30% and 43% over AuPd (1:3)/MgO and AuPt(1:3)/MgO has also been reported.^[37]

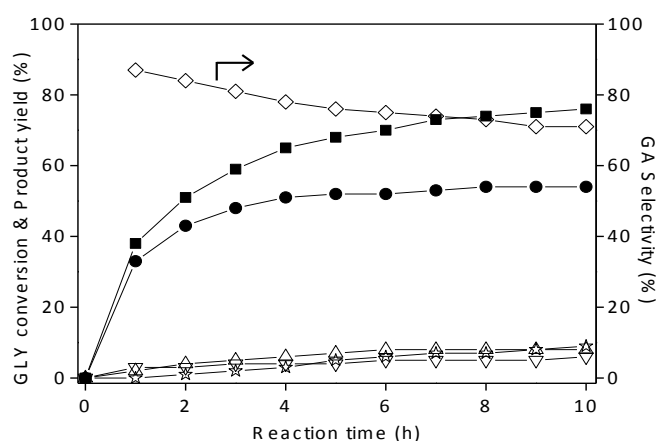


Figure 4 Time course of GLY oxidation catalyzed by Pt₆₀Au₄₀-starch/HT. GLY conversion (■: close square), GA yield (●: close circle), TA yield (△: open up triangle), HA yield (▽: open down triangle), OA yield (☆: star) and GA selectivity (◇: diamond). Reaction conditions: GLY (0.5 mmol), H₂O (2 mL), catalyst (20 mg), oxygen flow (10 mL·min⁻¹), room temperature (298 K).

3.3.2 1,2-Propanediol (PG) oxidation

To confirm the highly selective catalysis at the primary hydroxyl group of C₃ polyol under ambient conditions, Pt_xAu_y-starch/HT catalysts were further applied for

the aerobic oxidation of PG. The selective oxidation at the primary hydroxyl group of PG to LA as a main product was observed over Pt_xAu_y -starch/HT except for Au_{100} -starch/HT (Table 5). LA was also previously obtained as the main product in the PG oxidation reaction.^{[14],[15]} PG conversion of 23% was found over Pt_{100} -starch/HT (Table 5, entry 1), and it was further enhanced as the Au content was increased, $y = 20-60$ (Table 5, entries 2-4). Thereafter, the conversion dropped to 27% and trace amounts at $y = 80$ and 100, respectively (Table 5, entries 5 and 6). The $Pt_{60}Au_{40}$ -starch/HT also showed the most effective catalysis for PG oxidation with TOF of 62.3 h^{-1} at RT (Table 5, entry 3).

Table 5 Results of PG oxidation over Pt_xAu_y -starch/HT catalysts^a

Entry	Catalysts	Conv. of PG / %	Sel. of LA / %	Yield / %			Total metal loading / $\text{mmol}\cdot\text{g}^{-1c}$	Particle size / nm	TOF (h^{-1})
				LA	PA	AA			
1	Pt_{100} -starch/HT	23	82	19	2	2	0.087	2.0	45.1
2	$Pt_{80}Au_{20}$ -starch/HT	38	75	28	6	3	0.086	2.2	61.8
3	$Pt_{60}Au_{40}$ -starch/HT	39, 63 ^b	74, 75 ^b	29, 47 ^b	6, 12 ^b	1, 3 ^b	0.087	2.2	62.3, 77.2 ^b
4	$Pt_{40}Au_{60}$ -starch/HT	38	74	28	7	1	0.086	3.8	43.6
5	$Pt_{20}Au_{80}$ -starch/HT	27	75	20	4	1	0.089	5.4	21.6
6	Au_{100} -starch/HT	trace	-	trace	0	0	0.087	5.5	-

^aReaction conditions: PG (0.5 mmol), H_2O (2 mL), catalyst (20 mg, PG/metal = 287, ^b32 mg; PG/metal = 179), oxygen flow ($10\text{ mL}\cdot\text{min}^{-1}$), room temperature (298 K), reaction time (6 h, ^b16 h). ^cAnalysis by ICP-AES.

Figure 5 shows the time profile of PG oxidation over the Pt₆₀Au₄₀-starch/HT. Lactaldehyde, which was expected to be an intermediate, was not observed. After the reaction was prolonged to 16 h, the high conversion of 63% was achieved with selectivity to LA of 75%. In addition, the overoxidation of LA to pyruvic acid (PA) followed by C–C bond cleavage to acetic acid (AA) did not occur until reaction past 4 h. Previous reports on PG oxidation are summarized in the Chapter 1, Table 4.^{[14]–[19]} Most of them required basic conditions and pressurized oxygen.

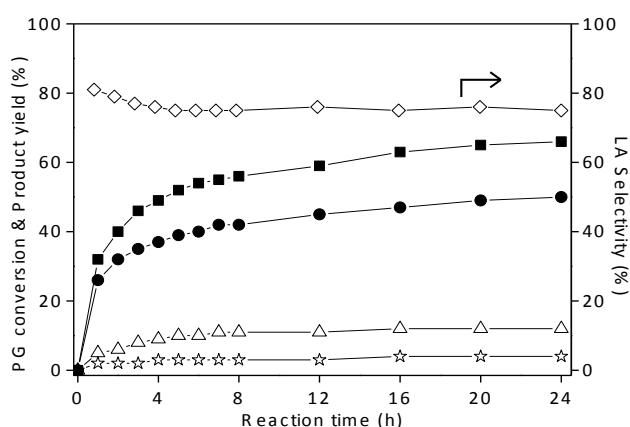


Figure 5 Time course of PG oxidation catalyzed by Pt₆₀Au₄₀-starch/HT. PG conversion (■: close square), LA yield (●: close circle), PA yield (△: open triangle), AA yield (☆: star) and LA selectivity (◇: diamond). Reaction conditions: PG (0.5 mmol), H₂O (2 mL), catalyst amount (32 mg), oxygen flow (10 mL·min⁻¹), room temperature (298 K).

3.3.3 Polyols oxidation in the presence of a radical scavenger

To evaluate the reaction pathway of aerobic oxidation of polyols over Pt₆₀Au₄₀-starch/HT, the reaction was operated in the presence of a radical scavenger (BHT), as shown in Figure 6. BHT slightly influenced the initial oxidation rate of the oxidation of the polyols; however, after prolonged reaction time, the yields of GA and

LA in the presence and absence of BHT were the same. This result suggests that the aerobic oxidation over Pt₆₀Au₄₀-starch/HT did not proceed through the free-radical mechanism.

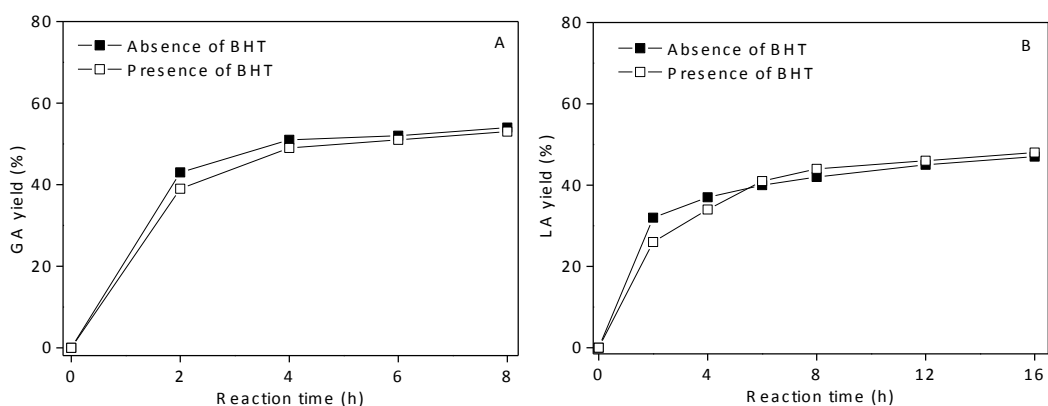


Figure 6 Time course of aerobic oxidation of (A) GLY and (B) PG over Pt₆₀Au₄₀-starch/HT catalyst in the absence (close square) or presence (open square) of BHT. Reaction conditions: H₂O (2 mL), oxygen flow (10 mL·min⁻¹), room temperature (298 K). (A): GLY (0.5 mmol), catalyst (20 mg). (B): PG (0.5 mmol), catalyst (32 mg). BHT/polyol = 1/10 (11 mg).

3.3.4 Catalyst recycling

To examine the stability of the Pt₆₀Au₄₀-starch/HT catalyst, the recycling experiments were carried out. After 6 and 16 h of reaction for GLY and PG oxidation, the catalyst was centrifuged, washed with deionized water, and dried under vacuum, then it was employed for further oxidation reaction under the same reaction conditions. Figure 7 indicates that the catalyst slightly decreased in activity but retained high selectivity during the recycling experiment in the oxidations of GLY and PG. The morphology of the recycled catalysts from glycerol oxidation was

investigated by TEM. Although the particle size was slightly increased after the reaction (Figure 8), it scarcely influenced its activity for glycerol oxidation.

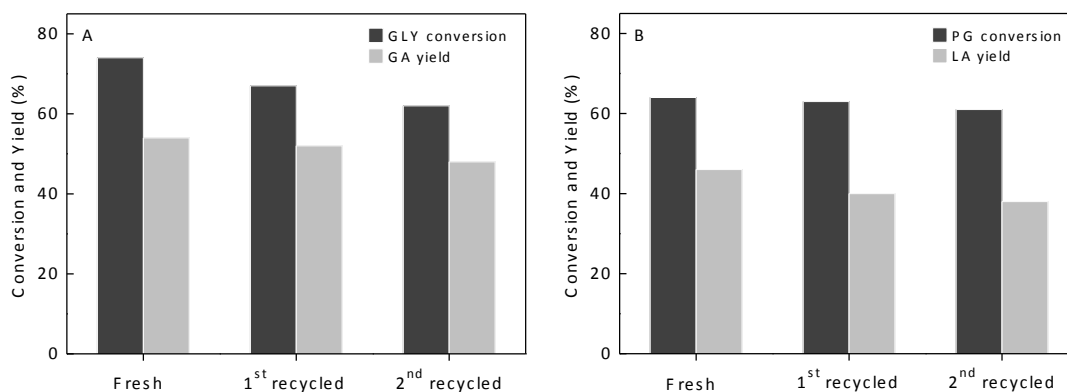


Figure 7 Recycling of Pt₆₀Au₄₀-starch/HT catalyst. Reaction conditions: H₂O (2 mL), oxygen flow (10 mL·min⁻¹), room temperature (298 K). (A): GLY (0.5 mmol), catalyst (20 mg), reaction time (6 h). (B): PG (0.5 mmol), catalyst (32 mg), reaction time (16 h).

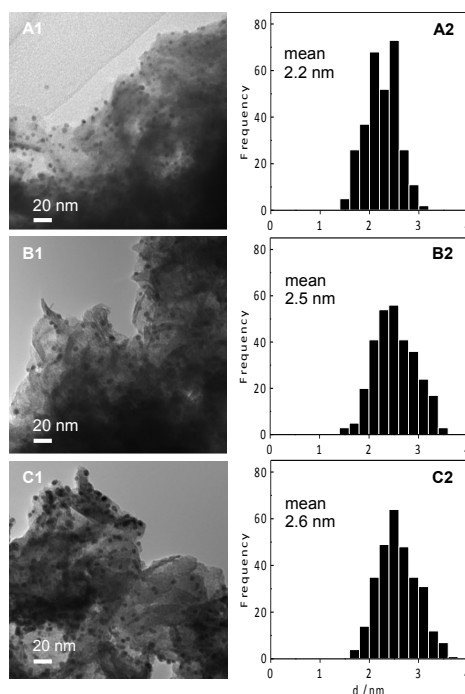


Figure 8 TEM images of recycled Pt₆₀Au₄₀-starch/HT catalysts from glycerol oxidation: (A1) fresh catalyst, (B1) 1st recycled catalyst, and (C1) 2nd recycled catalyst and (A2–C2) their particle size distribution histograms.

3.3.5 Characterization of Pt_xAu_y NPs/HT catalysts

The absorption band (localized surface plasmon resonance) of Au–starch NPs appears around 500–600 nm by UV-vis characterization.^{[43],[44]} This characteristic peak of Au–starch NPs was not observed in all Pt_xAu_y–starch NPs spectra, indicating PtAu alloy formation rather than phase-segregated bimetallic NPs. Figure 11A exhibits the XRD patterns of Pt_xAu_y–starch NPs. All XRD patterns of Pt_xAu_y–starch NPs describe the characteristic of the face-centered cubic (fcc) structure of metallic Pt or Au, the reflection corresponding to the planes (111), (200), (220), (311), and (222).^[45] Furthermore, these five diffraction peaks shifted to higher angle with a decrease in the Au amount in each position. For example, the (111) reflection of Pt_xAu_y–starch NPs gradually shifted from $2\theta = 38.3, 38.5, 38.8, 39.1, 39.4,$ and 39.7 with changes in $y = 100$ to 0 . According to the previous literature,^[46] $2\theta = 38.3$ and 39.7 correspond to the (111) reflection of metallic Au and Pt, respectively. Lattice parameters of Pt_xAu_y–starch NPs estimated from the XRD diffraction pattern of (111)^[47] as a function of the Au amount are plotted in Figure 11B.

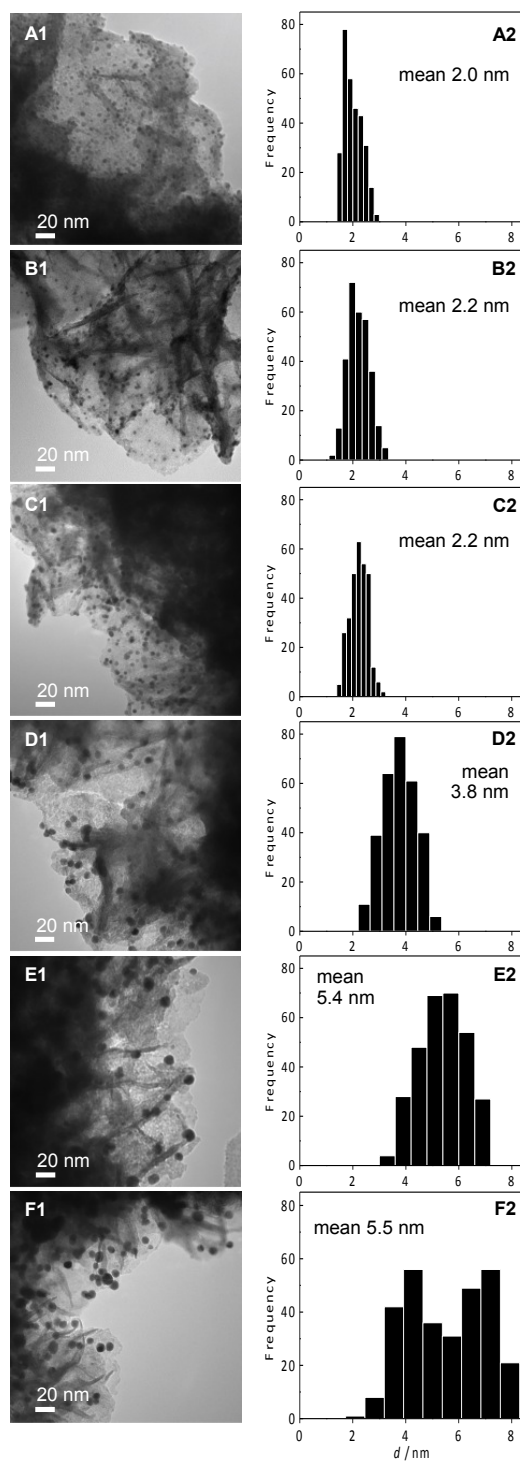


Figure 9 TEM images of Pt_xAu_y-starch/HT: (A1) Pt₁₀₀-starch/HT, (B1) Pt₈₀Au₂₀-starch/HT, (C1) Pt₆₀Au₄₀-starch/HT, (D1) Pt₄₀Au₆₀-starch/HT, (E1) Pt₂₀Au₈₀-starch/HT and (F1) Au₁₀₀-starch/HT and (A2)–(F2) their particle size distribution histograms.

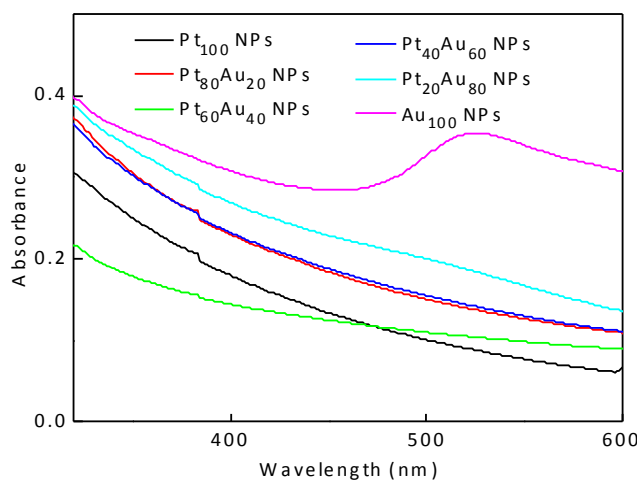


Figure 10 UV-vis spectra of Pt_xAu_y -starch NPs.

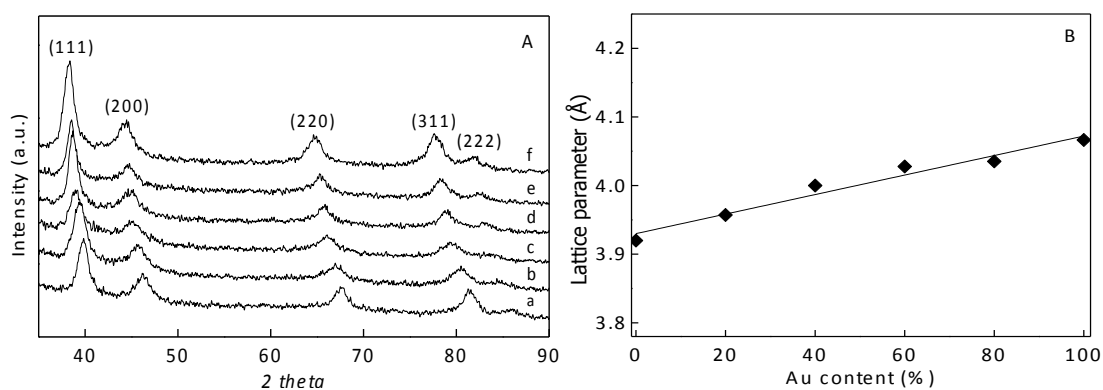


Figure 11 (A) XRD patterns of (a) Au_{100} -starch NPs, (b) $Pt_{20}Au_{80}$ -starch NPs, (c) $Pt_{40}Au_{60}$ -starch NPs, (d) $Pt_{60}Au_{40}$ -starch NPs, (e) $Pt_{80}Au_{20}$ -starch NPs, and (f) Pt_{100} -starch NPs. (B) Dependence of the lattice parameters for Pt_xAu_y -starch NPs on the relative composition of Au amount.

The lattice parameters of metallic Pt and Au were 3.92 and 4.07, respectively. Increasing the concentration of Au (y) in Pt_xAu_y -starch NPs leads to an increase in the lattice distance from 3.92 to 3.96, 4.0, 4.03, 4.04, and 4.07 Å, and a linear relationship between the lattice parameter and their composition was obtained. These results indicate that the nanostructures of Pt_xAu_y -starch NPs are homogeneous PtAu alloys.^[45] XPS spectra of Pt_xAu_y -starch NPs are shown in Figure 12. Peaks at 85.6

and 82 eV in Figure 12A were assigned to Au 4f_{5/2} and Au 4f_{7/2}, respectively. All spectra showed the large negative shift to lower binding energy (BE), as compared with Au foil (Au 4f_{5/2}:88 eV and Au 4f_{7/2}:84 eV).

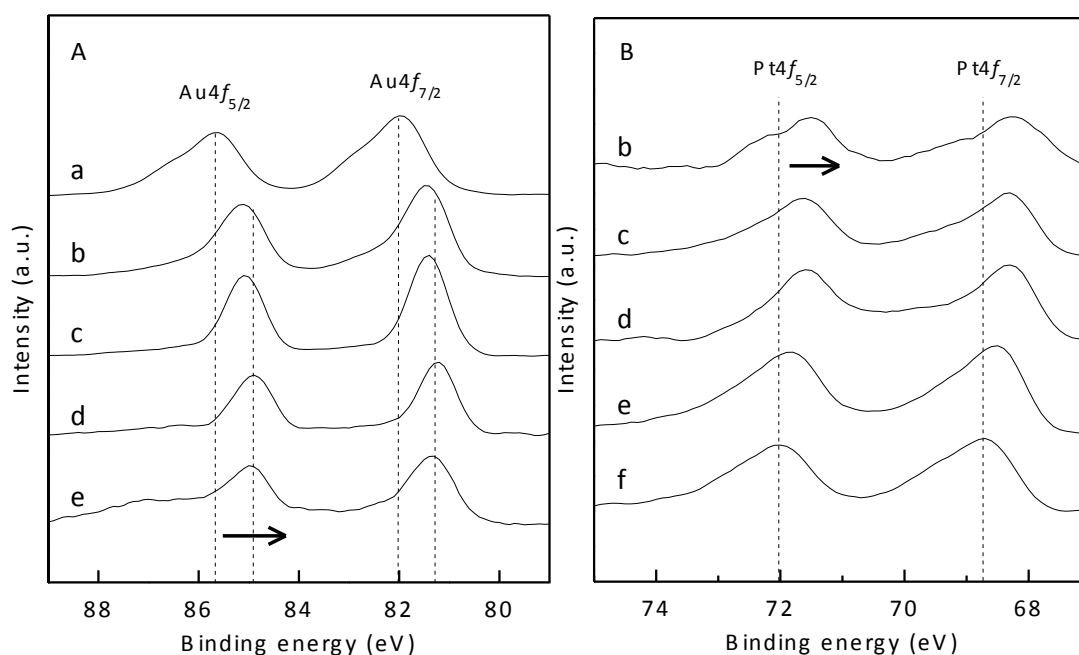


Figure 12 XPS spectra of (A) Au4f and (B) Pt4f of Pt_xAu_y-starch NPs; (a) Au₁₀₀-starch NPs (5.5 nm), (b) Pt₂₀Au₈₀-starch NPs (5.4 nm), (c) Pt₄₀Au₆₀-starch NPs (3.8 nm), (d) Pt₆₀Au₄₀-starch NPs (2.2 nm), (e) Pt₈₀Au₂₀-starch NPs (2.2 nm), and (f) Pt₁₀₀-starch NPs (2.0 nm).

The same negative shifts also appeared in all peaks around 72 and 68.7 eV attributed to Pt 4f_{5/2} and Pt 4f_{7/2}, respectively, as compared with Pt foil (Pt 4f_{5/2}:74.4 eV and Pt 4f_{7/2}:71.2 eV) in Figure 7B. These large negative shifts in both Au 4f and Pt 4f in alloy Pt_xAu_y-starch NPs suggests that a negative charge is loaded on PtAu-starch NPs,^[48] which is supposed by the interaction between PtAu-starch NPs and starch ligand. It has been reported that the electron donated from the stabilizer (for example, poly(vinyl pyrrolidone) (PVP)) to a metal such as Pt, Au, and Ag NPs,

results in a negative shift of the BE in XPS spectra.^{[43],[49],[50]} In addition, hydroxyl groups in soluble starch can facilitate the complexation of metal ions to a molecular matrix.^{[51],[52]} Therefore, it is supposed that the large negative shift in both Pt 4f and Au 4f are due to electron donation from the starch ligand to both Pt and Au atoms.^[53] Considering the peak of Au 4f the decrease in the Au content from $y = 100$ to 20 leads to a more negative shift in Figure 12A, it was supposedly attributed to decreasing the particle size because the number of ligand capped surface sites will become larger with the reduced particle size. Although the same phenomenon is also expected to be encountered for Pt 4f, the enhancement of a negative shift of Pt 4f was not observed; even their particle sizes were diminished with a decreasing Au content (Figure 12B).

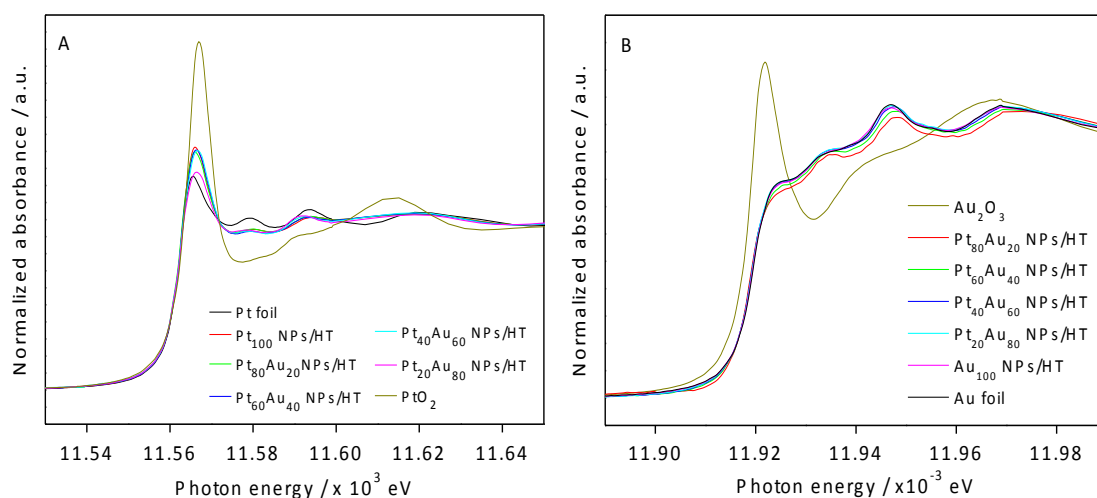


Figure 13 Normalized (A) Pt L_3 -edge and (B) Au L_3 -edge XANES spectra of Pt_xAu_y-starch/HT.

On the contrary, reductions in the negative shift in Pt 4f were found as the Au content was reduced from $y = 80$ to 0. In other words, the Pt 4f peaks gradually shifted to the lower side of the binding energy. It is postulated that the excess electrons on Au atoms transferred to the adjacent Pt atoms. Figure 13 shows

normalized Pt L_3 -edge and Au L_3 -edge XANES spectra of Pt_xAu_y -starch/HT. The white-line (WL) feature in the L_3 -edge XANES was related to the electron transfer phenomena induced by an X-ray absorption from the p to d states in the element; thus, it indicated the unoccupied densities of the d states.^{[54],[55]} Au L_3 -edge XANES spectra have no WL feature, since the 5d orbitals full in theory; however, the s-p-d hybridization leads to electron transformation from 5d to the s-p state, leading the small WL intensity in the Au L_3 -edge XANES.^[55-57] Lower WL intensities than Au foil were observed for all Au L_3 -edges, implicating a Au gained electron (Figure 13B).

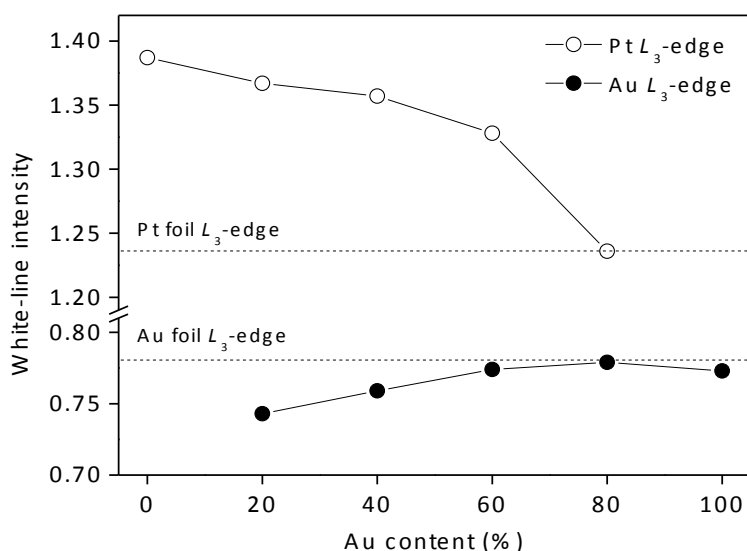
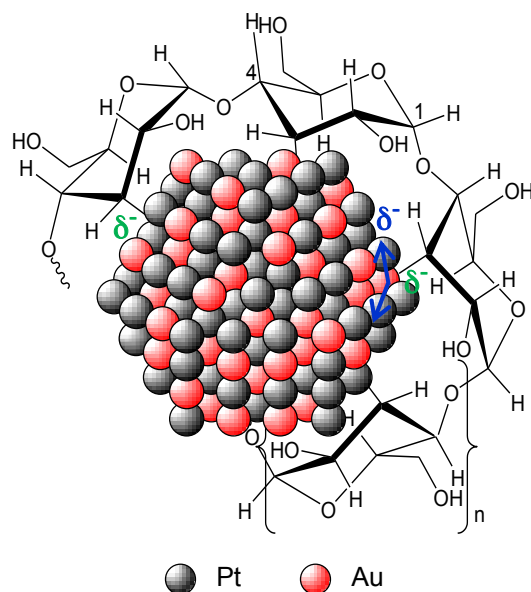


Figure 14 White-line intensity of Pt L_3 -edge (at 11.565 keV) and Au L_3 -edge (at 11.924 keV) XANES spectra of Pt_xAu_y -starch/HT. Dash lines represent white-line intensity of Pt and Au foils.

Figure 14 shows plots of WL intensities in Pt and Au L_3 -edges XANES as a function of Au content. The heights of the WL in the L_3 -edges gradually became lower, whereas that in Au L_3 -edges were higher with an increase of in the Au content. The decreasing tendency of the Pt L_3 -edge WL intensity is related to the increase in

that of the Au L_3 -edge as the Au content increases from $y = 20$ to 80. Previous works have reported that the NPs' size affected the WL intensity of the XANES spectra.

Small NPs reduced the number of metal–metal bonds by the s–p–d hybridization change, resulting in a decrease in the number of d-holes density, leading to a decrease in the WL intensity.^[58] As the above result, an increase in the Au content, the size of the Pt_xAu_y –starch NPs increased while the WL intensity of the Pt L_3 -edge decreased. Therefore, XPS together with XANES confirmed that a negative charge was present on both the Au and Pt atoms, in which the starch ligand donates electrons, and the excess electrons on the Au atoms can also transfer to the Pt atoms. There have been reports of the electron transfer from Au (EN = 2.54) to Pt (EN = 2.28) in the core–shell structure of NPs, leading to an increase in the active oxygen species on the surface.^{[59],[60]} In addition, it has also been reported that a stabilizing/capping agent can play a direct role in regulating the electronic structures.^{[49],[57],[61],[62]} Soluble starch is a linear polymer formed by the α -(1 \rightarrow 4) linkages between D-glucose units and adopts a left-handed helical conformation in aqueous solution,^[52] therefore, it is supposedly possible that the electrons can be transfer via complexation of the starch ligand onto Pt and Au atoms, as illustrated in Scheme 3.

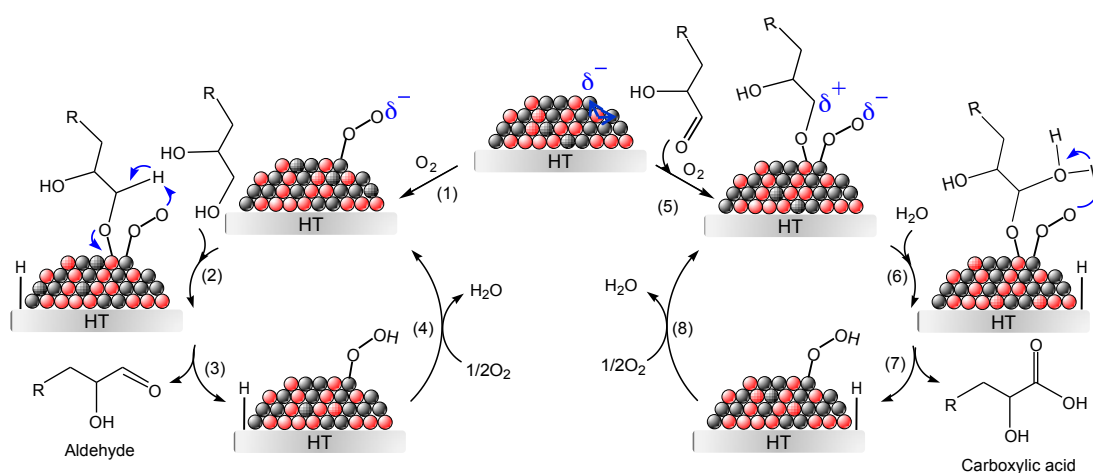


Scheme 3 The possible electron transfer from starch ligand to alloy PtAu–starch NPs and from Au atoms to adjacent Pt atoms.

3.3.6 Oxidation Mechanism

As mentioned, the geometric (d-spacing) and electronic changes of the catalytically active Pt sites by adjacent Au atoms and the starch ligand can lead to improvement of the activity and selectivity to target products. The replacing of active atoms (Pt site) with inactive atoms (Au site) changed the geometry of the Pt surface or modified the strength of the surface adsorption then controlling oxygen coverage.^[63–66] Pt₆₀Au₄₀–starch/HT showed the highest yield, with a high selectivity for catalytic oxidation of GLY and PG toward GA and LA, respectively, under an atmospheric pressure of molecular oxygen because of both geometric and electronic changes. The reaction mechanism of oxidation of polyols is proposed in Scheme 4. First, O₂ is adsorbed onto the surface of negatively charged Pt atoms (1). It has been reported that anionic metal can activate molecular oxygen by donating an excess

electron charge to the antibonding orbital, resulting in the generation of anionic O_2 such as superoxo or peroxy oxygen.^[67-70] Then the basic support abstracts a proton from the polyol to form the alkoxide, which enhances the polyol's binding to the metal atom (2). The proton in the adsorbed alkoxide carbon is transferred to the adsorbed oxygen; releasing aldehyde (3) and H_2O to generate back the peroxy form (4). Aldehyde, thus formed, is attracted by the adjacent metal atom with adsorbed oxygen (Au atoms) (5). This creates a partial positive charge on the carbonyl carbon. The nucleophilic oxygen atom of water attacks the electron-deficient carbonyl carbon (6). The adsorbed oxygen abstracts the proton to yield carboxylic acid (7) and is changed back to the peroxy form (8) to complete the catalytic cycle.



Scheme 4 A proposed reaction mechanism for polyols oxidation catalyzed by PtAu-starch/HT.

4. Conclusion

I explored the efficient and recyclable heterogeneous Pt_xAu_y -starch/HT catalyst for the oxidation of polyols without additional bases under an atmospheric pressure of molecular oxygen. Bimetallic Pt_xAu_y -starch/HT showed higher selectivity for the oxidation at the primary hydroxyl groups of GLY and PG toward GA and LA, respectively, than those of each monometallic ones. $\text{Pt}_{60}\text{Au}_{40}$ -starch/HT is found to be the most selective catalyst for oxidation of polyols. UV-vis and XRD revealed that Pt_xAu_y -starch formed as an alloy, and their d-spacing was changed from individual metals. XPS and XANES showed the negative charge on both Au and Pt atoms. It was supposed that the PtAu-starch NPs gained charge from the starch ligand. Au L_3 -edge XANES spectra revealed an increase in the white-line intensity as the amount of Au was increased, indicating the excess electrons on the Au atoms also transfer to the Pt atoms. The negatively charged Pt atoms may enhance the oxygen absorption and generate anionic O_2 such as superoxo or peroxy oxygen to oxidize polyols. I conclude that the geometric and electronic changes of the catalytically active Pt sites by adjacent Au atoms and the starch ligand lead to improvement of the activity and selectivity to target products.

5. References

- [1] A. Corma, S. Iborra and A. Velty, Chemical routes for the transformation of biomass into chemicals, *Chem. Rev.*, 2007, **107**, 2411–2502.
- [2] J. N. Chheda, G. W. Huber and J. A. Dumesic, Liquid-phase catalytic processing of biomass-derived oxygenated hydrocarbons to fuels and chemicals, *Angew. Chem. Int. Ed.*, 2007, **46**, 7164–7183.
- [3] A. Takagaki, S. Nishimura and K. Ebitani, Catalytic transformations of biomass-derived materials into value-added chemicals, *Catal. Surv. Asia*, 2012, **16**, 164–182.
- [4] B. Katryniok, H. Kimura, E. Skrzyńska, J.-S. Girardon, P. Fongarland, M. Capron, R. Ducoulombier, N. Mimura, S. Paul and F. Dumeignil, Selective catalytic oxidation of glycerol: perspectives for high value chemicals, *Green Chem.*, 2011, **13**, 1960–1979.
- [5] C.-H. (Clayton) Zhou, J. N. Beltramini, Y.-X. Fan and G. Q. (Max) Lu, Chemoselective catalytic conversion of glycerol as a biorenewable source to valuable commodity chemicals, *Chem. Soc. Rev.*, 2008, **37**, 527–549.
- [6] M. Pagliaro, R. Ciriminna, H. Kimura, M. Rossi and C. D. Pina, From glycerol to value-added products, *Angew. Chem. Int. Ed.*, 2007, **46**, 4434–4440.
- [7] R. F. Stockel, Method of treating dermatological conditions. U.S. Patent 2007/086 977 A1, April 19, 2007.
- [8] S. K. Gupta, Novel hydroxyl acid complexes for antiaging and skin renovation. U.S. Patent 2007/092 461 A1, April 26, 2007.

- [9] A. Behr, J. Eilting, K. Irawadi, J. Leschinski and F. Lindner, Improved utilisation of renewable resources: new important derivatives of glycerol, *Green Chem.*, 2008, **10**, 13–30.
- [10] Y. Nakagawa and K. Tomishige, Catalyst development for the hydrogenolysis of biomass-derived chemicals to value-added ones, *Catal. Surv. Asia*, 2011, **15**, 111–116.
- [11] G. L. Brett, P. J. Miedziak, N. Dimitratos, J. A. Lopez-Sanchez, N. F. Dummer, R. Tiruvalam, C. J. Kiely, D. W. Knight, S. H. Taylor, D. J. Morgan, A. F. Carley and G. J. Hutchings, Oxidative esterification of 1,2-propanediol using gold and gold-palladium supported nanoparticles, *Catal. Sci. Technol.*, 2012, **2**, 97–104.
- [12] R. Datta and M. Henry, Lactic acid: recent advances in products, processes and technologies — a review, *J. Chem. Technol. Biotechnol.*, 2006, **81**, 1119–1129.
- [13] S. Lux, P. Stehring and M. Siebenhofer, Lactic acid production as a new approach for exploitation of glycerol, *Separ. Sci. Technol.*, 2010, **45**, 1921–1927.
- [14] N. Dimitratos, J. A. Lopez-Sanchez, S. Meenakshisundaram, J. M. Anthonykutti, G. Brett, A. F. Carley, S. H. Taylor, D. W. Knight and G. J. Hutchings, Selective formation of lactate by oxidation of 1,2-propanediol using gold palladium alloy supported nanocrystals, *Green Chem.*, 2009, **11**, 1209–1216.

- [15] Z. Huang, F. Li, B. Chen, F. Xue, Y. Yuan, G. Chen and G. Yuan, Efficient and recyclable catalysts for selective oxidation of polyols in H₂O with molecular oxygen, *Green Chem.*, 2011, **13**, 3414–3422.
- [16] C. Bianchi, F. Porta, L. Prati and M. Rossi, Selective liquid phase oxidation using gold catalysts, *Top. Catal.*, 2000, **13**, 231–236.
- [17] S. Demirel, P. Kern, M. Lucas, P. Claus, Oxidation of mono- and polyalcohols with gold: comparison of carbon and ceria supported catalysts, *Catal. Today*, 2007, **122**, 292–300.
- [18] E. Taarning, A. T. Madsen, J. M. Marchetti, K. Egeblad and C. H. Christensen, Oxidation of glycerol and propanediols in methanol over heterogeneous gold catalysts, *Green Chem.*, 2008, **10**, 408–414.
- [19] S. Sugiyama, H. Tanaka, T. Bando, K. Nakagawa, K.-I. Sotowa, Y. Katou, T. Mori, T. Yasukawa and W. Ninomiya, Liquid-phase oxidation of propylene glycol using heavy-metal-free Pd/C under pressurized oxygen, *Catal. Today*, 2013, **203**, 116–121.
- [20] D. Wang, A. Villa, F. Porta, D. Su and L. Prati, Single-phase bimetallic system for the selective oxidation of glycerol to glycerate, *Chem. Commun.*, 2006, 1956–1958.
- [21] C. L. Bianchi, P. Canton, N. Dimitratos, F. Porta and L. Prati, Selective oxidation of glycerol with oxygen using mono and bimetallic catalysts based on Au, Pd and Pt metals. *Catal. Today*, 2005, **102–103**, 203–212.
- [22] N. Dimitratos, F. Porta and L. Prati, Au, Pd (mono and bimetallic) catalysts supported on graphite using the immobilisation method: synthesis and catalytic

- testing for liquid phase oxidation of glycerol, *Appl. Catal. A-Gen.*, 2005, **291**, 210–214.
- [23] L. Prati, F. Porta, D. Wang and A. Villa, Ru modified Au catalysts for the selective oxidation of aliphatic alcohols, *Catal. Sci. Technol.*, 2011, **1**, 1624–1629.
- [24] W. Hu, D. Knight, B. Lowry and A. Varma, Selective oxidation of glycerol to dihydroxyacetone over Pt–Bi/C catalyst: optimization of catalyst and reaction conditions, *Ind. Eng. Chem. Res.*, 2010, **49**, 10876–10882.
- [25] P. Maity, C. S. Gopinath, S. Bhaduri and G. K. Lahiri, Applications of a high performance platinum nanocatalyst for the oxidation of alcohols in water, *Green Chem.*, 2009, **11**, 554–561.
- [26] H. Zhang and N. Toshima, Glucose oxidation using Au-containing bimetallic and trimetallic nanoparticles, *Catal. Sci. Technol.*, 2013, **3**, 268–278.
- [27] D. Liang, J. Gao, J. Wang, P. Chen, Z. Hou and X. Zheng, Selective oxidation of glycerol in a base-free aqueous solution over different sized Pt catalysts, *Catal. Commun.*, 2009, **10**, 1586–1590.
- [28] R. Nie, D. Liang, L. Shen, J. Gao, P. Chen and Z. Hou, Selective oxidation of glycerol with oxygen in base-free solution over MWCNTs supported PtSb alloy nanoparticles, *Appl. Catal. B-Environ*, 2012, **127**, 212–220.
- [29] D. Liang, J. Gao, J. Wang, P. Chen, Y. Wei and Z. Hou, Bimetallic Pt—Cu catalysts for glycerol oxidation with oxygen in a base-free aqueous solution, *Catal. Commun.*, 2011, **12**, 1059–1062.

- [30] S. Hirasawa, Y. Nakagawa and K. Tomishige, Selective oxidation of glycerol to dihydroxyacetone over a Pd–Ag catalyst, *Catal. Sci. Technol.*, 2012, **2**, 1150–1152.
- [31] D. Tongsakul, S. Nishimura, C. Thammacharoen, S. Ekgasit and K. Ebitani, Hydrotalcite-supported platinum nanoparticles prepared by a green synthesis method for selective oxidation of glycerol in water using molecular oxygen, *Ind. Eng. Chem. Res.*, 2012, **51**, 16182–16187.
- [32] A. Tsuji, K. T. V. Rao, S. Nishimura, A. Takagaki and K. Ebitani, Selective oxidation of glycerol by using a hydrotalcite-supported platinum catalyst under atmospheric oxygen pressure in water, *ChemSusChem*, 2011, **4**, 542–548.
- [33] D. Tongsakul, K. Wongravee, C. Thammacharoen and S. Ekgasit, Enhancement of the reduction efficiency of soluble starch for platinum nanoparticles synthesis, *Carbohydr. Res.*, 2012, **357**, 90–97.
- [34] K. Kaneda, K. Ebitani, T. Mizugaki and K. Mori, Design of high-performance heterogeneous metal catalysts for green and sustainable chemistry, *Bull. Chem. Soc. Jpn.*, 2006, **79**, 981–1016.
- [35] S. Nishimura, A. Takagaki and K. Ebitani, Characterization, synthesis and catalysis of hydrotalcite-related materials for highly efficient materials transformations, *Green Chem.*, 2013, **15**, 2026–2042.
- [36] H. Lorenz, S. Penner, W. Jochum, C. Rameshan and B. Klötzer, Pd/Ga₂O₃ methanol steam reforming catalysts: Part II. catalytic selectivity, *Appl. Catal. A-Gen.*, 2009, **358**, 203–210.

- [37] G. L. Brett, Q. He, C. Hammond, P. J. Miedziak, N. Dimitratos, M. Sankar, A. A. Herzing, M. Conte, J. A. Lopez-Sanchez, C. J. Kiely, D. W. Knight, S. H. Taylor and G. J. Hutchings, Selective oxidation of glycerol by highly active bimetallic catalysts at ambient temperature under base-free conditions, *Angew. Chem. Int. Ed.*, 2011, **50**, 10136–10139.
- [38] C. Shang and Z.-P. Liu, Origin and activity of gold nanoparticles as aerobic oxidation catalysts in aqueous solution, *J. Am. Chem. Soc.*, 2011, **133**, 9938–9947.
- [39] B. N. Zope, D. D. Hibbitts and M. Neurock, R. J. Davis, Reactivity of the gold/water interface during selective oxidation catalysis, *Science*, 2010, **330**, 74–78.
- [40] F. Porta and L. Prati, Selective oxidation of glycerol to sodium glycerate with gold-on-carbon catalyst: an insight into reaction selectivity, *J. Catal.*, 2004, **224**, 397–403.
- [41] W. C. Ketchie, M. Murayama and R. J. Davis, Promotional effect of hydroxyl on the aqueous phase oxidation of carbon monoxide and glycerol over supported Au catalyst, *Top. Catal.*, 2007, **44**, 307–317.
- [42] L. Prati, P. Spontoni and A. Gaiassi, From renewable to fine chemicals through selective oxidation: the case of glycerol, *Top. Catal.*, 2009, **52**, 288–296.
- [43] C.-W. Chen and M. Akashi, Synthesis, characterization, and catalytic properties of colloidal platinum nanoparticles protected by poly(*N*-isopropylacrylamide), *Langmuir*, 1997, **13**, 6465–6472.

- [44] Z. Peng and H. Yang, PtAu bimetallic heteronanostructures made by post-synthesis modification of Pt-on-Au nanoparticles, *Nano. Res.*, 2009, **2**, 406–415.
- [45] E. Antolini, J. R. C. Salgado, R. M. da Silva and E. R. Gonzalez, Preparation of carbon supported binary Pt–M alloy catalysts (M = first row transition metals) by low/medium temperature methods, *Mater. Chem. Phys.*, 2007, **101**, 395–403.
- [46] M.-L. Wu, D.-H. Chen and T.-C. Huang, Preparation of Au/Pt bimetallic nanoparticles in water-in-oil microemulsions, *Chem. Mater.*, 2001, **13**, 599–606.
- [47] S. Carrettin, P. McMorn, P. Johnston, K. Griffin, C. J. Kiely and G. J. Hutchings, Oxidation of glycerol using supported Pt, Pd and Au catalysts, *Chem. Chem. Phys.*, 2003, **5**, 1329–1336.
- [48] G.-R. Zhang and B.-Q. Xu, Surprisingly strong effect of stabilizer on the properties of Au nanoparticles and Pt⁺Au nanostructures in electrocatalysis, *Nanoscale*, 2010, **2**, 2798–2894.
- [49] Y. Borodko, S. E. Habas, M. Koebel, P. Yang, H. Frei and G. A. Somorjai, Probing the interaction of poly(vinylpyrrolidone) with platinum nanocrystals by UV-Raman and FTIR, *J. Phys. Chem. B*, 2006, **110**, 23052–23059.
- [50] G.-R. Zhang and B.-Q. Xu, Surprisingly strong effect of stabilizer on the properties of Au nanoparticles and Pt⁺Au nanostructures in electrocatalysis, *Nanoscale*, 2010, **2**, 2798–2804.

- [51] P. Raveendran, J. Fu and S. L. Wallen, Completely “green” synthesis and stabilization of metal nanoparticles, *J. Am. Chem. Soc.*, 2003, **125**, 13940–13941.
- [52] N. Vigneshwaran, R. P. Nachane, R. H. Balasubramanya, P. V. Varadarajan, A novel one-pot ‘green’ synthesis of stable silver nanoparticles using soluble starch, *Carbohydr. Res.*, 2006, **341**, 2012–2018.
- [53] Further study in chapter 4 currently under investigation to clarify this point.
- [54] I. E. Beck, V. V. Kriventsov, D. P. Ivanov, V. I. Zaikovsky and V. I. Bukhtiyarov, XAFS study of Pt/Al₂O₃ nanosystem with metal-oxide active component, *Nucl. Instrum. Meth. A*, 2009, **603**, 108–110.
- [55] P. Zhang and T. K. Sham, Tuning the electronic behavior of Au nanoparticles with capping molecules, *Appl. Phys. Lett.*, 2002, **81**, 736–738.
- [56] S. Nishimura, Y. Yakita, M. Katayama, K. Higashimine and K. Ebitani, The role of negatively charged Au states in aerobic oxidation of alcohols over hydrotalcite supported AuPd nanoclusters, *Catal. Sci. Technol.*, 2013, **3**, 351–359.
- [57] H. Tsunoyama, H. Sakurai, Y. Negishi and T. Tsukuda, Size-specific catalytic activity of polymer-stabilized gold nanoclusters for aerobic alcohol oxidation in water, *J. Am. Chem. Soc.*, 2005, **127**, 9374–9375.
- [58] J. A. van Bokhoven and J. T. Miller, d Electron density and reactivity of the d band as a function of particle size in supported gold catalysts, *J. Phys. Chem. C*, 2007, **111**, 9245–9249.

- [59] J. Zeng, J. Yang, J. Y. Lee and W. J. Zhou, Preparation of carbon-supported core-shell Au-Pt nanoparticles for methanol oxidation reaction: the promotional effect of the Au core, *Phys. Chem. B*, 2006, **110**, 24606–24611.
- [60] L. B. Ortiz-Soto, O. S. Alexeev and M. D. Amiridis, Low temperature oxidation of CO over cluster-derived platinum-gold catalysts, *Langmuir*, 2006, **22**, 3112–3117.
- [61] L. Qiu, F. Liu, L. Zhao, W. Yang and J. Yao, Evidence of a unique electron donor-acceptor property for platinum nanoparticles as studied by XPS, *Langmuir*, 2006, **22**, 4480–4482.
- [62] H. Tsunoyama, N. Ichikuni, H. Sakurai and T. Tsukuda, Effect of electronic structures of Au clusters stabilized by poly(*N*-vinyl-2-pyrrolidone) on aerobic oxidation catalysis. *J. Am. Chem. Soc.*, 2009, **131**, 7086–7093.
- [63] M. Chen, D. Kumar, C.-W. Yi and D. W. Goodman, The promotional effect of gold in catalysis by palladium-gold, *Science*, 2005, **310**, 291–293.
- [64] S. N. Rashkeev, A. R. Lupini, S. H. Overbury, S. J. Pennycook and S. T. Pantelides, Role of the nanoscale in catalytic CO oxidation by supported Au and Pt nanostructures, *Phys. Rev. B*, 2007, **76**, 035438-1–035438-7.
- [65] D. Mott, J. Luo, P. N. Njoki, Y. Lin, L. Wang and C.-J. Zhong, Synergistic activity of gold-platinum alloy nanoparticle catalysts, *Catal. Today*, 2007, **122**, 378–385.
- [66] L. Prati, A. Villa, C. Campione and P. Spontoni, Effect of gold addition on Pt and Pd catalysts in liquid phase oxidations, *Top. Catal.*, 2007, **44**, 319–324.

- [67] N. K. Chaki, H. Tsunoyama, Y. Negishi, H. Sakurai and T. Tsukuda, Effect of Ag-doping on the catalytic activity of polymer-stabilized Au clusters in aerobic oxidation of alcohol, *J. Phys. Chem. C*, 2007, **111**, 4885–4888.
- [68] M. Okumura, Y. Kitagawa, M. Haruta and K. Yamaguchi, The interaction of neutral and charged Au clusters with O₂, CO and H₂, *Appl. Catal. A-Gen.*, 2005, **291**, 37–44.
- [69] K. Gustafsson and S. Andersson, Infrared spectroscopy of physisorbed and chemisorbed O₂ on Pt(111), *J. Chem. Phys.*, 2004, **120**, 7750–7754.
- [70] Y. S. Kim, A. Bostwick, E. Rotenberg, P. N. Ross, S. C. Hong and B. S. Mun, The study of oxygen molecules on Pt (111) surface with high resolution x-ray photoemission spectroscopy, *J. Chem. Phys.*, 2010, **133**, 034501-1–034501-4.

Chapter 5

GENERAL CONCLUSION

This thesis exploits highly active platinum (Pt)-based mono- and bimetallic nanoparticles (NPs), which is synthesized by green synthetic method using ligands. Hydrotalcite supported-Pt based NPs (Pt NPs/HT) is used as a heterogeneous catalyst in order to transform polyols selectivity to value-added chemicals by the aerobic oxidation in base-free aqueous solution using atmospheric pressure of molecular oxygen at room temperature.

Chapter 1 reviews the environmentally benign and sustainable chemistry and methodologies for the development of Pt-based mono- and bimetallic heterogeneous catalyst using novel green synthetic method. This research emphasizes on the designation of synthetic method utilizing green chemicals or/and reducing toxic chemicals in order to produce effective and reusable catalyst which can transform abundant biomass industrial waste such as glycerol (GLY) and its derivative (1,2-propanediol, PG) to valued-added chemicals via oxidation reaction using green oxidant and solvent. In addition, the catalysis for the oxidation reaction of polyols strongly depends on the basicity of the reaction medium. However, the salt of the products was formed when a homogeneous base was used, and then the obtained products required an additional neutralization or acidification. Hence, this research

choices the smart material which functional groups contain the basicity on the surface as the support for the fabrication of green catalyst. Finally, I also summarize the recent progresses in nanotechnology which facilitates the development of nanocatalyst by controllable the metal structures, e.g., size, shape, composition, stability and electronic state.

Description in Chapter 2 is the development of a simple and efficient technique for the preparation of starch stabilized-Pt NPs/HT heterogeneous catalysts using a “Green” synthesis approach, and investigation on the catalytic activity for the GLY oxidation in base-free aqueous solution using an atmospheric pressure of molecular oxygen. The catalysts show the high activity for GLY conversion under moderate reaction conditions in base-free aqueous solution leading to form salt-free products. These findings conduct to the green process for utilization of the wasted GLY which can be escaped from the additional neutralization or acidification process. Furthermore, the catalysts could be reused up to three times with a high selectivity.

Chapter 3 exploits the effect of stabilizing agent on the Pt surface and alteration of the catalytic activity of Pt NPs/HT by tuning the electronic properties with stabilizers (i.e., soluble starch, poly (vinyl pyrrolidone) (PVP) and poly (vinyl alcohol) (PVA)) with same particle size. Starch is found to be a suitable ligand for creating negative charge on Pt surface atoms with better wettability of active Pt surface atoms for water solvent leading to high catalytic activity for PG oxidation under at under atmospheric pressure of molecular oxygen in base-free aqueous solution. Therefore, the catalytic oxidation of PG could be enhanced. These

exploration guides to the selection of stabilizing agent, which may influence catalysis or determine the electronic state of NPs, and thus modify catalytic properties.

Explanation in Chapter 4 is the modification of the developed method which brings about the exploration of the highly efficient starch-stabilized Pt/Au heterogeneous catalyst for the selective oxidation of polyols (GLY and PG) in base-free aqueous solution under atmospheric pressure of molecular oxygen at room temperature. Pt_xAu_y NPs formed as alloy structure and their d -spacing being change from individual metals. In addition, the electronic structure investigation of Pt_xAu_y NPs/HT indicated that negative charge on both Au and Pt atoms, in which starch ligand donates electrons, and the excess charge on Au atoms can also transfer to Pt atoms. Therefore, the geometric and electronic changes of the catalytically active Pt sites by adjacent Au atoms and the starch ligand lead to improvement of the activity and selectivity to target products. The finding leads to the preparation of the effective catalyst for utilization of the wasted GLY under atmospheric conditions.

Overall, I can conclude that this research successfully develops technique for the improvement of catalysis of Pt NPs tuned by second metal and ligand. Modification of electronic state of Pt NPs is crucial to improve their catalysis for polyol oxidation. The catalysts effectively transform GLY and PG into the corresponding value-added chemicals via the aerobic oxidation reaction in base-free aqueous solution under an atmospheric pressure of molecular oxygen at room temperature. This research provides a noble route to converting wasted polyols into chemical sources through well-tuned catalytic methodology.

Scope of the research

1. Exploration the strategy in the development of simple and high effective technique based on green method for the preparation of heterogeneous catalyst, will provide a change for sustainable development of catalyst. The findings may lead to the application for the different type of mono- and heterometallic heterogeneous catalysts including further methodology using other kinds of biomass as a green reagent. Another notable strategy is the developed method for the fabrication of active catalyst in water media for the aerobic oxidation of polyols.
2. The evolution of the developed technique based on green method results in discovery of highly efficient catalyst tuning by metal and ligand. The catalytic oxidation of polyols can proceed under atmospheric conditions in base-free aqueous solution as mention in Chapters 2 and 3. The discovery is expected to employ for the preparation of other metal catalysts, and cover to apply catalyst for transformation of biomass materials by other chemical reactions to the corresponding value-added chemicals. In addition, the results bring about sustainable development by the enhancement of catalytic efficiency, and the reduction of energy used and chemical waste generation.
3. Well-understanding of the crucial action of stabilizing/capping agent causes the effective and economical way to improve the catalysis of metal nanoparticles. As stated in Chapter 4, the stabilizing agent may play a crucial role not only control particle formation in small size but also tune the catalytic and electronic properties of metal. Thus, the proper consideration in the selection of stabilizing/capping

agent for the preparation of metal catalyst may tune or avoid the reduction in catalytic activity.

ACHIEVEMENTS

PUBLICATIONS

1. **D. Tongsakul**, S. Nishimura, C. Thammacharoen, S. Ekgasit and K. Ebitani,
Hydrotalcite-supported platinum nanoparticles prepared by a green synthesis
method for selective oxidation of glycerol in water using molecular oxygen,
Ind. Eng. Chem. Res., **2012**, *51*, 16182–16187.
2. **D. Tongsakul**, S. Nishimura and K. Ebitani,
Platinum/gold alloy nanoparticles-supported hydrotalcite catalyst for selective
aerobic oxidation of polyols in base-free aqueous solution at room temperature,
ACS Catal., **2013**, *3*, 2199–2207.
3. **D. Tongsakul**, S. Nishimura and K. Ebitani,
Effect of stabilizing polymers on catalysis of hydrotalcite-supported platinum
nanoparticles for aerobic oxidation of 1,2-propanediol in aqueous solution at
room temperature,
J. Phy. Chem. C, **2014**, *118*, 11723–11730.

PRESENTATIONS

INTERNATIONAL CONFERENCE

1. **D. Tongsakul**, K. Ebitani and S. Ekgasit,
Green synthesis of platinum nanoparticles by using polysaccharide as a reducing agent and stabilizer,
Joint Conference of 7th ISAMAP and NT2010, Nomi, Japan, September 30, **2010**. [Poster]
2. **D. Tongsakul**, S. Nishimura, C. Thammacharoen, S. Ekgasit and K. Ebitani,
Pt/Au Bimetallic nanoparticles supported onto hydrotalcite surface as heterogeneous catalyst for selective oxidation of glycerol synthesized via green chemistry,
14th Asian Chemical Congress 2011, Bangkok, Thailand, September 5, **2011**.
[Poster]
3. **D. Tongsakul**, S. Nishimura, C. Thammacharoen, S. Ekgasit and K. Ebitani,
Green synthesis of platinum/gold bimetallic nanoparticles supported onto hydrotalcite surface as heterogeneous catalyst for selective oxidation of glycerol,
2011 AIChE Annual Meeting, Catalysis and Reaction Engineering Division,
Paper ID = 228567, Minnesota, USA, October 17, **2011**. [Oral]

DOMESTIC CONFERENCE

1. **D. Tongsakul**, S. Nishimura, S. Ekgasit and Kohki Ebitani,
Green synthesis of platinum mono- and bimetallic supported on hydrotalcite
catalysts for selective oxidation of glycerol,
The 91th annual meeting of Chem. Soc. Jpn., Kanagawa, Japan, March 27, **2011**.
[Oral]
2. **D. Tongsakul**, S. Nishimura and Kohki Ebitani,
High selectivity of hydrotalcite supported-platinum/gold alloy nanoparticle
catalysts for aerobic oxidation of polyols under base-free and atmospheric
conditions,
The 93th annual meeting of Chem. Soc. Jpn., Kyoto, Japan, March 23, **2013**.
[Oral]

AWARD

“Young Chemist awards” supported by IUPAC, RSC, and Bangkok Bank from
the 14th Asian Chemical Congress 2011, 14th Asian Chemical Congress 2011(14
ACC), Bangkok, Thailand, September 5, **2011**. [Poster]

RELATED WORK

D. Tongsakul, K. Wongravee, C. Thammacharoen, S. Ekgasit,

Enhancement of the reduction efficiency of soluble starch for platinum nanoparticles synthesis,

Carbohydr. Res., **2012**, 357, 90–97.

ENHANCEMENT OF THE REDUCTION EFFICIENCY OF SOLUBLE STARCH FOR PLATINUM NANOPARTICLES SYNTHESIS

Student Number 1040013

Duangta Tongsakul

1. Introduction

Green chemistry involves a reduction or elimination of the use or generation of hazardous substances. It plays an important role in nanotechnology research.^[1] The green synthesis of metal nanoparticles could take advantage of green chemistry principles by employing green reagents (e.g., solvent, reducing agent, stabilizing agent) under mild reaction conditions.^{[1][2]} The nanoparticles (NPs) of noble metals such as silver (Ag), palladium (Pd), gold (Au) and platinum (Pt) synthesized using green reagents such as a reducing/stabilizing agent have been reported. For instance, Raveendran *et al.* synthesized Ag NPs using β -D-glucose as a reducing agent and soluble starch as a protecting agent,^[3] Huang and Yang^[4] synthesized gold nanoparticles using chitosan as both reducing/protecting agent, Adlim *et al.*^[5] used methanol or NaBH₄ as a reducing agent and chitosan as a stabilizing agent for synthesizing Pt NPs and Pd NPs and Mallikarjuna and Rajender used vitamin-B₂ as a reducing agent for the synthesis of Pt NPs with ethylene glycol, acetic acid, N-

methylpyrrolidinone, isopropanol and acetonitrile as solvents.^[2] Moreover, other green reagents such as amino-terminated ionic liquid (1-(3-aminopropyl)-methylimidazolium bromide, IL-NH₂),^[6] dextran,^[7] β -D-glucose,^[8] and aminodextran^[9] have been employed in the synthesis of different platinum nanostructures. To produce metal nanoparticles (e.g., Ag NPs) with well-defined size and shape, polysaccharides (i.e., starch and cellulosic material) were employed either as a protecting agent or stabilizing agent.^{[10][11]} Soluble starch was also used in the synthesis of Ag NPs where the reaction was carried out in an autoclave at 15 psi and 121°C for 5 min.^[12] Carboxymethyl cellulose obtained from the alkaline and perborate treatment of cotton,^[13] and hydroxypropyl cellulose prepared by etherification reaction with propylene oxide^[14] were exploited for the synthesis of silver nanoparticles. It has been reported that functional groups with reducing potential (aldehyde and α -hydroxy ketone) can be obtained from the degradation of polysaccharides under alkaline conditions.^{[15][16]} Soluble starch is a linear polysaccharide with α -(1 \rightarrow 4) linkages between D-glucose units. The alkaline degradation is expected to generate more reducing end groups or reducing species.^[12] The hydroxyl group in the starch structure complexes with the metal ion and prevents aggregation or precipitation of metal nanoparticles.^{[8][12]} Although soluble starch has been employed for the synthesis of Ag NPs, the reaction was carried out in caustic conditions. In addition, the detailed reduction mechanism has not been reported. Platinum metal has been widely used in many applications, for example, catalysts,^[17] fuel cells,^{[17][19]} electro-optical devices,^[20] and magnetic devices.^{[20][21]} The properties of Pt NPs depend strongly on the particle size, shape, composition and

structure.^{[19][21].[23]} There are numerous reports concerning the synthesis of shape-controlled Pt NPs. However, they require extreme conditions (e.g., high pressure and high temperature) and extra reducing agents. In this paper, we reveal a green approach for a 'one pot' synthesis of Pt NPs using soluble starch as an efficient reducing and protecting agent. Our results indicated that the alkaline degradation of starch molecule is the key for the synthesis of Pt NPs without aggregation. Under an optimized condition, soluble starch could be degraded while simultaneously generating reducing species that convert Pt ions into Pt NPs. The partially degraded starch molecule could also stabilize the generated metal nanoparticles.

2. Experimental

2.1 Chemicals and materials

Soluble starch, sodium hydroxide (NaOH) and hydrochloric acid (HCl, 37% w/v) were purchased from Merck (Thailand). All chemicals were analytical grade and were used without any additional purification. De-ionized water was used as a solvent. All glassware and magnetic bars were cleaned with detergent and rinsed with de-ionized water followed by aqua regia and finally rinsed again with de-ionized water before using.

2.2 Synthesis of platinum nanoparticles (Pt NPs)

Pt NPs were synthesized by chemical reduction using soluble starch as both stabilizer and reducing agent. Briefly, a 20 mM platinum salt solution was prepared from hexachloroplatinic acid. The pH of the solution was adjusted to neutral with 1 M

NaOH. Separately, 5 mL fractions of the solution was again individually pH adjusted to acidic, neutral and alkaline conditions, respectively, with an equal volume of 2×10^{-5} – 2×10^{-6} M HCl, water and 2×10^{-6} – 2×10^{-2} M NaOH. A 4% w/v soluble starch solution was prepared by dissolving 4 g of soluble starch in hot water (100 mL). After cooling down, 5 mL fractions of starch solution were mixed with an equal volume of 2×10^{-5} – 2×10^{-6} M HCl, water and 2×10^{-6} – 2×10^{-2} M NaOH. The platinum solutions and the starch solutions with the same acidic/alkaline treatment were heated at 100°C for 20 min before mixing under a vigorous stirring. The mixed solution was kept at the controlled temperature for another 20 min before cooling down to room temperature. The total volume was kept constant at 20 mL by an addition of de-ionized water at the same temperature. In addition, time-dependent studies on the generation of Pt NPs were conducted at 1, 3, 5, 10, 15, 30 and 40 min incubation time.

2.3 Characterization

2.3.1 UV/vis spectroscopy (UV/vis)

The product with 5 mM Pt NPs was investigated by UV/vis spectroscopy to confirm the formation of Pt NPs. The absorption spectra of Pt ion and the colloidal Pt NPs were measured with a portable fiber optics UV/vis spectrometer (USB4000 Ocean Optics) equipped with a deuterium/halogen lamp light source (DH-2000, Micropack). The solutions of platinum salt and colloidal Pt NPs were diluted to 0.05 mM with deionized water before analysis.

2.3.2 Attenuated Total Reflection Fourier Transform Infrared spectroscopy (ATR FT-IR)

A Nicolet 6700 FT-IR spectrometer attached to the ‘Continuum infrared microscope’ equipped with a mercury–cadmium–telluride (MCT) detector and a built-in 15X Schwarzschild-Cassegrain infrared objective was used for all infrared spectral acquisitions. A slide-on Ge μ ATR accessory with a cone shaped Ge μ IRE was employed as the sampling probe.^[24] To acquire an infrared spectrum, starch solution and starch-stabilized Pt NPs colloid were dropped onto a glass slide and dried under an ambient condition. The dried film on the glass slide was mounted onto the sample stage beneath the infrared objective. The spectral acquisition at a defined position was conducted by raising the sample stage until the film on the glass slide comes in contact with the tip of Ge μ IRE. The degree of contact was monitored and controlled by a built-in pressure sensor. All ATR spectra were collected at 4 cm^{-1} with 128 co-addition scans.

2.3.3 Transmission electron microscopy (TEM)

The colloidal Pt NPs were diluted to 0.25 mM and dropped onto a carbon-coated copper grid. The excess liquid was removed by a lint-free paper. The specimen was dried overnight in a desiccator. The morphology of Pt NPs was captured by a transmission electron microscope (H-7650, Hitachi High-Technologies Corporation) operated at 100 kV accelerating voltage.

3 Result and discussion

3.1 Synthesis of platinum nanoparticles (Pt NPs)

Platinum solution (hexachloroplatinic acid, H_2PtCl_6) has an orange-yellow color with a strong absorption in UV/vis region at 263 nm, as shown in Figure 1.^[7] Figures 1A and 1B show digital images of platinum salt in the presence of 1% w/v starch under various acid/alkaline treatments. The absorption at 263 nm shows a significant decrease with an increase of alkalinity. The change is more pronounced than that observed in the system without starch. The decrease of peak intensity is expected to be due to the changes of Pt complex ion. Pt salt is known to undergo hydrolysis from $[\text{PtCl}_6]^{2-}$ to $[\text{PtCl}_5(\text{H}_2\text{O})]^-$ and $[\text{PtCl}_4(\text{H}_2\text{O})_2]$ with a gradual increase in alkalinity.^[25] An indication of the reduction of platinum ions platinum ionsto Pt NPs was observed as the color of the solution changed from yellow to black colloid at 0.01 M NaOH. The existence of Pt NPs was confirmed by the baseline shift of UV/vis spectra (Figures 1C) and TEM images, as shown in Figures 1D–1E. However, under stronger alkaline treatments (0.1 and 1 M), the Pt NPs aggregated and precipitated within a few minutes. This observed phenomenon suggests that the platinum ion could be reduced by *in situ* generated reducing species under an alkaline degradation of starch.

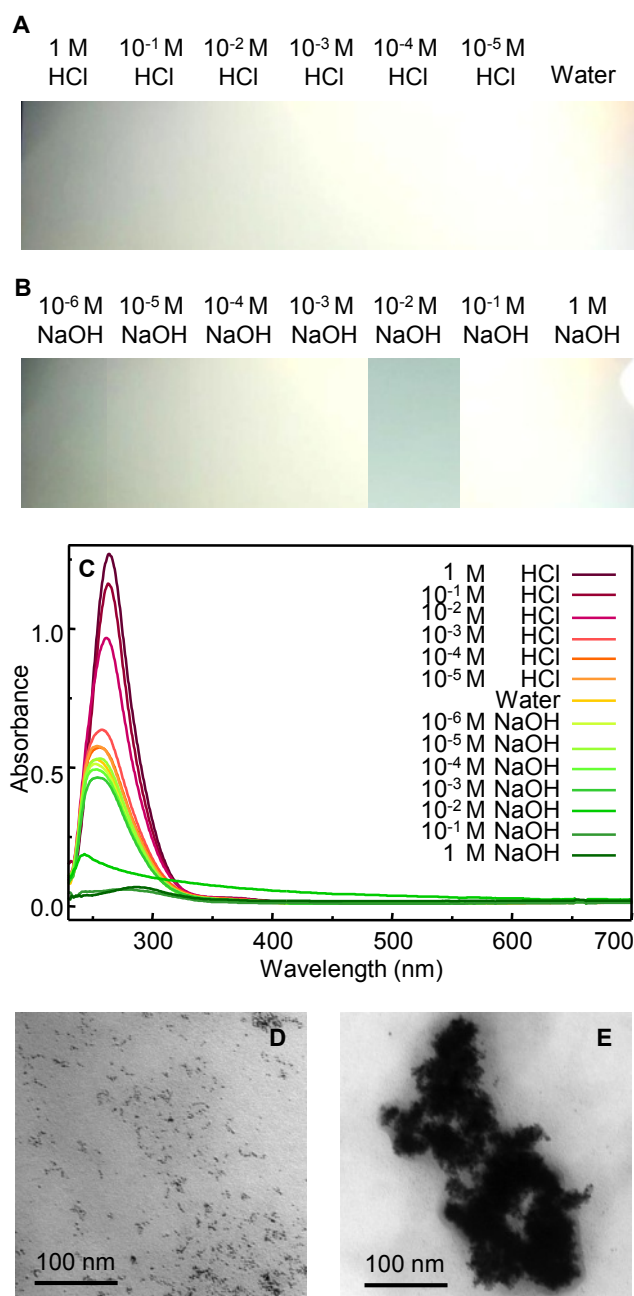
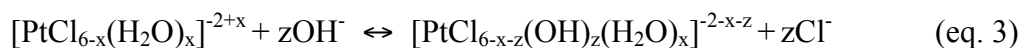
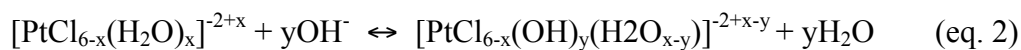
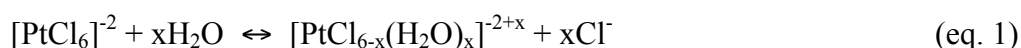


Figure 1 (A) Digital image of platinum solution in acidic condition adjusted by addition of HCl (1–10⁻⁵ M) and water, (B) digital image of platinum solution in alkaline condition, (C) UV/vis spectra of platinum solution at various acidic-alkaline conditions after reduction, (D) TEM image of platinum solution at 10⁻² M and (E) TEM image of platinum solution at 10⁻¹ M.

3.2 Influence of acidic-alkaline treatment for platinum complex

In order to gain an insight understanding on the influence of acidic-alkaline treatment for platinum complex, the platinum salt (H_2PtCl_6) adjusted at different alkalinity were performed. In our work, the initial H_2PtCl_6 (20 mM, pH \sim 1) was pH adjusted with NaOH until the solution became neutral (pH 7) and used as a stock solution. The UV/vis absorption at 260 nm, presenting to $[\text{PtCl}_5(\text{H}_2\text{O})]^{-1}$ or $[\text{PtCl}_4(\text{H}_2\text{O})_2]$ was observed.^{[25][26]} Under acidic treatment, the stock solution was adjusted to the difference pH by using HCl solution (10^{-5} –1 M). The UV/vis spectra reveal the peak maxima blue shift to 263 nm as the HCl concentration increased to 1 M. These phenomena represented to the aquo ligand exchange chloride to form H_2PtCl_6 .

Similarly with alkaline treatment, the platinum stock solutions were pH adjusted by using NaOH solution (10^{-6} –1 M). The UV/vis spectra showed the peak maxima red shift. These phenomena explained by the hydroxide ion ligand exchange of chloride and aquo ligand leading to the formation platinum hydroxo complex (i.e., $[\text{PtCl}_4(\text{OH})_2]^{-2}$). However, result in Figure 2 shows the peak maxima shift to nearly 263 nm while the peak intensity lowers than the initial solution instead of the appearance of the platinum aquo complex. It is due to the initial hydrolysis reaction of aquo ligand exchange (eq. 1) of chloride and aquo are fast and reversible (eq. 2–3) while the hydroxide ion ligand exchange of chloride and aquo ligand are relatively slow.^[25] Spieker *et al.*^[25] reports that H_2PtCl_6 is a strong acid which undergoes rapid and extensive hydrolysis. The set of reactions are as follows:



In our work, platinum nanoparticles were formed in the alkaline treatment when platinum ions and starch solution were adjusted with NaOH over 0.01 M. However, the precipitated Pt NPS were found when those solutions over 0.05 M NaOH. Hence, the proper alkaline condition for the formation of platinum nanoparticles in the range of 10^{-2} M to 10^{-1} M NaOH was investigated. Although, the UV/vis result in Figure 2 confirmed that the alkalinity had an influence on the platinum complex and Yu *et al.* reported that the product of $\text{H}_2\text{O}/\text{Cl}^-$ ligand exchange could be more easily reduced than PtCl_6^{2-} for the synthesis of platinum nanocrystals by reduction with H_2 .^[27]

However, under the window of the observation (in the range of 10^{-2} M to 10^{-1} M NaOH) the UV/vis spectra no significantly changed both of peak maximum and intensity. It means that the initial platinum complex adjusted with above alkaline concentrations seem to be the same.

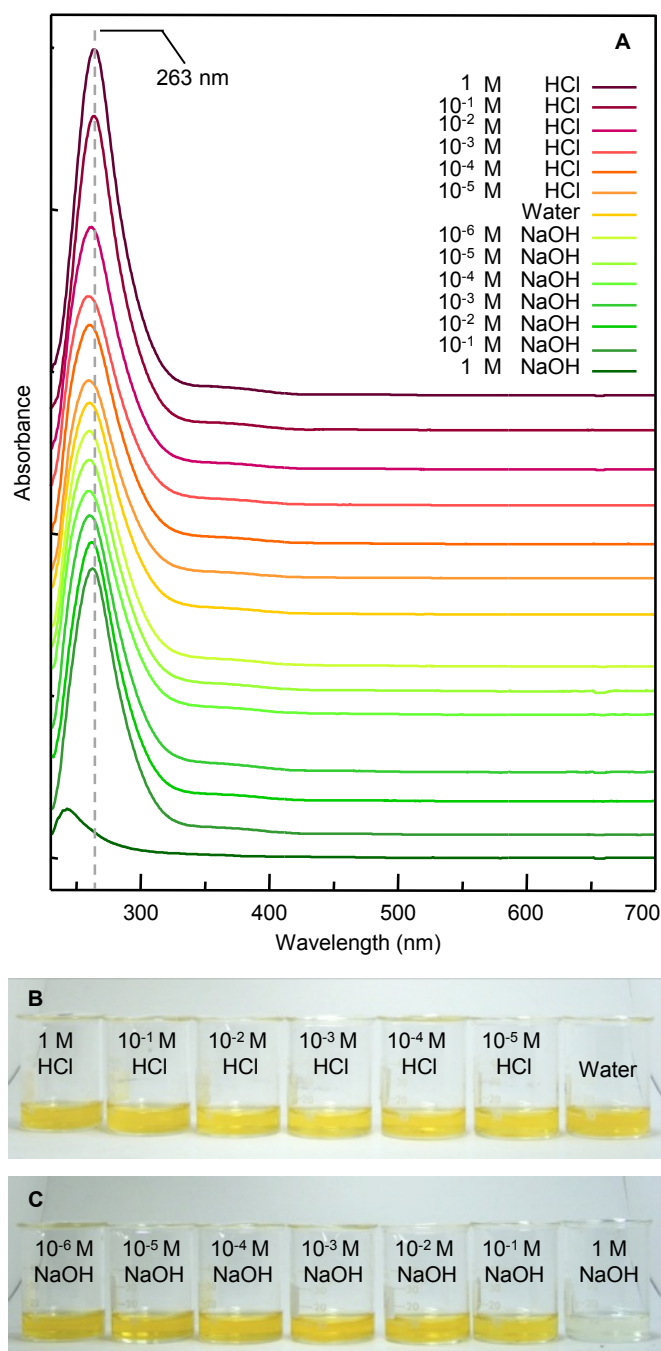


Figure 2 (A) UV/vis spectra of platinum at various acidic-alkaline conditions after reduction, (B) digital image of platinum solution in acidic condition adjusted by addition of HCl (1–10⁻⁵ M) and water and (C) digital image of platinum solution in alkaline condition.

3.3 Investigation of starch degradation under an alkaline treatment

It is well-known that starch molecules are degraded and broken down to small organic acid (e.g., formic acid, acetic acid, glycolic acid and lactic acid) under an alkaline treatment.^[28] Since, the organic acid possesses no reducing potential, the degraded intermediates are expected to be responsible for the reduction of platinum ions to Pt NPs.

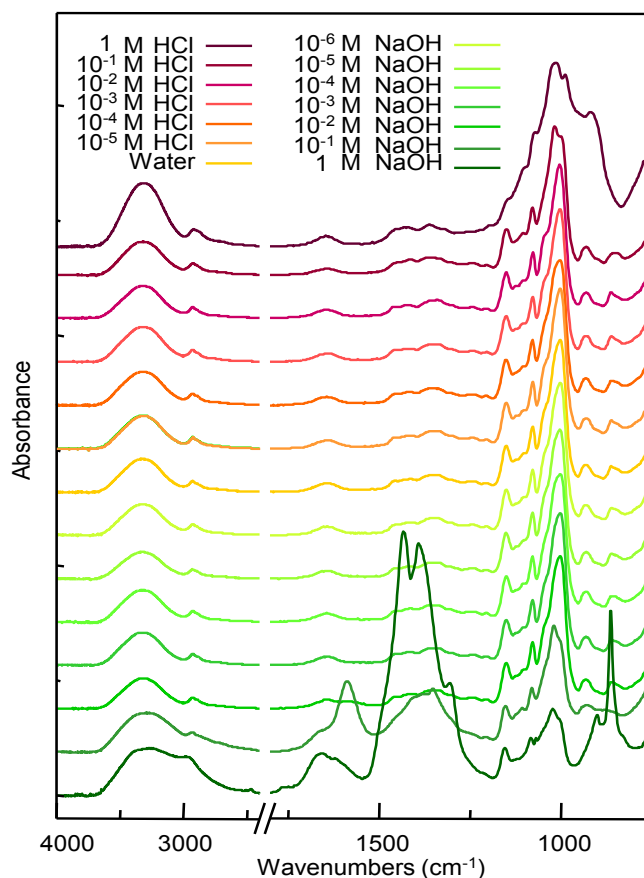


Figure 3 Normalized ATR FT-IR stack spectra of soluble starch at various acidic-alkaline conditions adjusted by HCl, water and NaOH solutions.

Aldehyde and α -hydroxy ketone in alkaline media are well-known function as efficient reducing species. There are reports indicating that the degraded species of glucose and cellulose under alkaline condition contain aldehyde, ketone and acid moiety.^{[16][28]} Figure 3 shows attenuated total reflection Fourier transform infrared (ATR FT-IR) spectra of products obtained after the acidic/alkaline treatments of soluble starch.

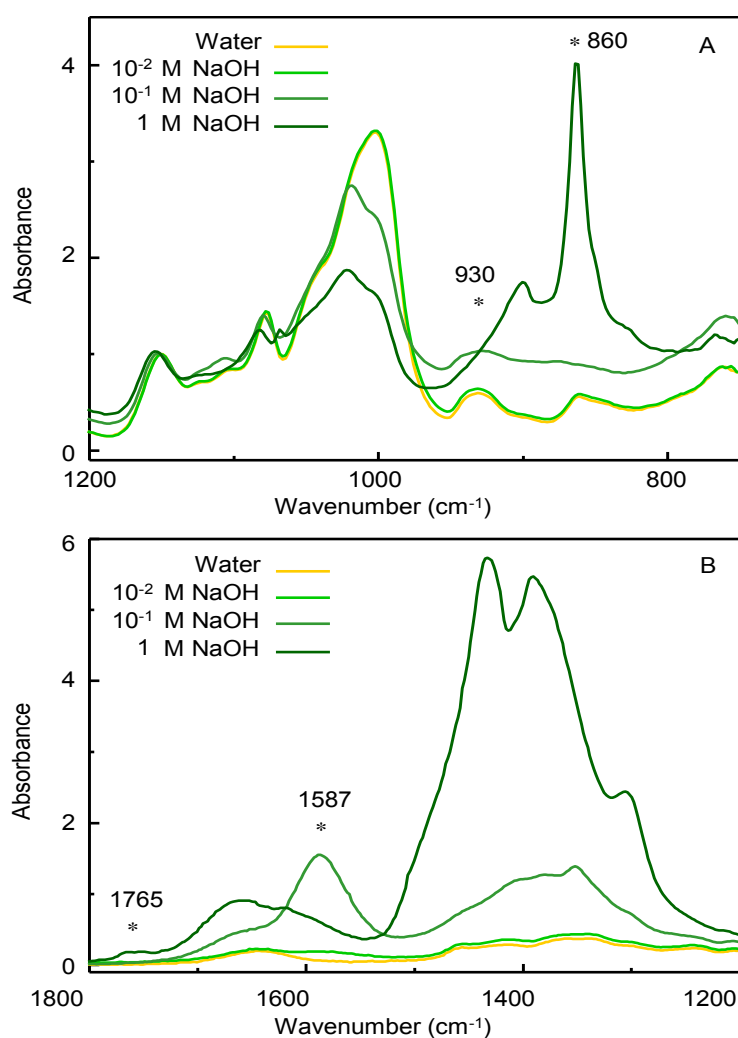


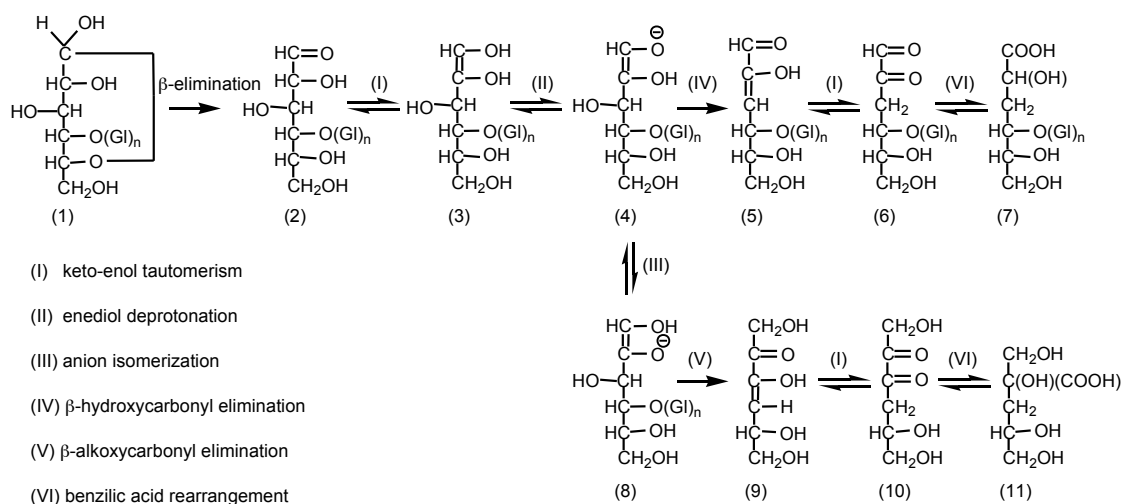
Figure 4 Normalized ATR FT-IR stack spectra of soluble starch at 10⁻²–1 M NaOH in the region of (A) 1200–750 cm⁻¹ and (B) 1800–1200 cm⁻¹.

The spectra show a significant break down of glycosidic linkage of starch bridge β C¹-O-C⁴ in the region 1200–900 cm⁻¹ (i.e., C-O, C-C stretching (1163 cm⁻¹), C-O-H bending (1094 cm⁻¹), C¹-H bending (1067 cm⁻¹) and skeleton mode vibration of α -1,4 glycosidic linkage, C-O-C (930 cm⁻¹)) under alkalinity greater than 0.01 M as the absorption was significantly decreased.^{[29],[31]} In fact at 0.01 M a slight degradation was observed. At a greater alkalinity (0.1 M), an indication for the generation of the carboxylate group is observed at 1587 cm⁻¹.

At an extremely high alkaline condition (1 M), the extensive destruction of starch molecule and evolution of collective carbonyl group (e.g., carboxylic acid and aldehyde) were indicated by a development of a broad absorption band at 1770–1550 cm⁻¹, as shown in Figure 4.^[32] The observed infrared spectra demonstrate the formation of carbonyl species after an alkaline treatment. These species are expected to be responsible for the formation of Pt NPs observed in Figure 1D–1E. The detail infrared band assignment is shown in Table 1.^{[29],[32]}

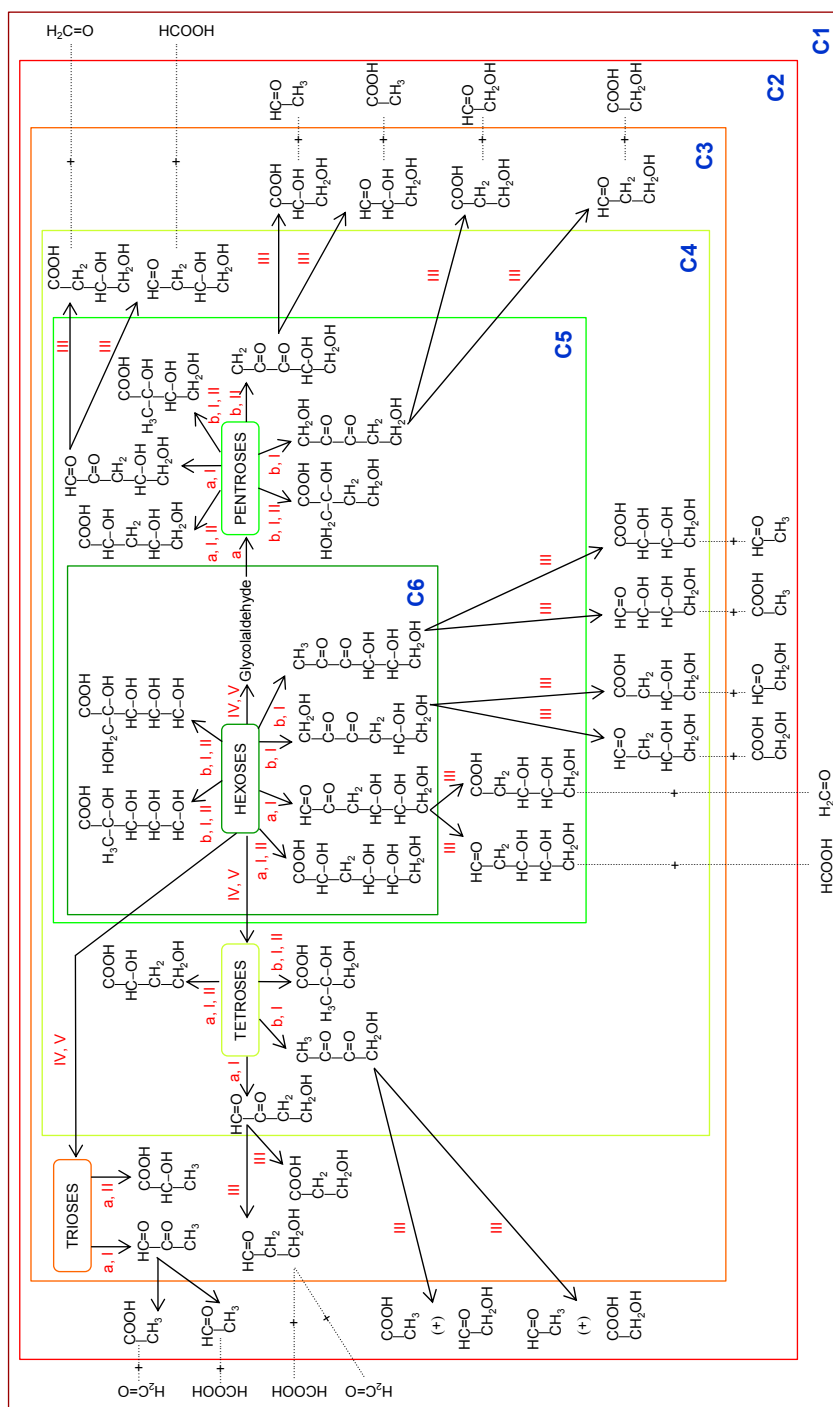
Table 1 Infrared bands assignment of starch.

Infrared band (cm ⁻¹)	Infrared band assignment
860	CH ₂ deformation
930	Skeleton mode vibration of α-1,4 glycosidic linkage (C-O-C)
1200 - 900	Bridge β C ¹ -O-C ⁴ stretching
1500 - 1300	Vibration band related to the carbon and hydrogen atoms
1610 – 1550/1420-1300	COO ⁻ stretching vibration (carboxylic acid salt)
1642	Water adsorbed in the amorphous region of starch
1765	C=O stretching vibration of carboxylic acid
3000 - 2800	C-H stretching
3600 - 3100	O-H stretching

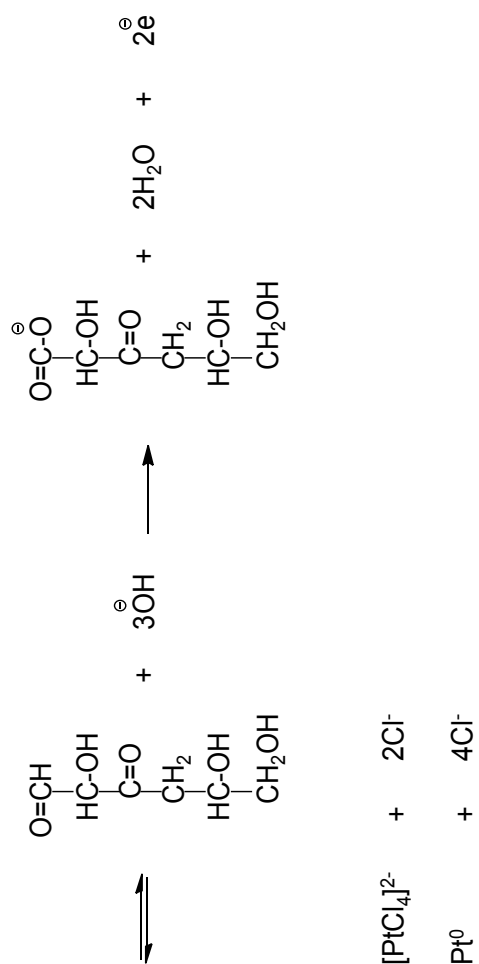


Scheme 1 The possible process of starch under alkaline degradation to generate reducing end groups adapted from Nef-Isbell mechanism.

The observed infrared spectral changes are in good agreement with the alkaline degradation of polysaccharide given by the Nef-Isbell mechanism.^[15] In this work, soluble starch, a linear polymer of glucose units, was used as both the reducing and the stabilizing agent. The degradation of starch under alkaline treatment involves a β -elimination reaction followed by a series of rearrangement before liberation of a glucose unit. A simplified mechanism of starch degradation is shown in Scheme 1.^{[15][16][28],[33].[35]} The glucose unit undergoes further degradations before breaking down to smaller organic species containing carbonyl moiety. Previous works show that the final products of starch/polysaccharide degradation are small organic acid.^[26] However, the intermediates involve the formation of organic species with reducing potential containing carbonyl species (i.e., aldehyde and α -hydroxy ketone). A simplification of starch degradation products with different carbon number are shown in Scheme 2.^{[15][16][28],[33].[35]} Some of the intermediates have aldehyde or α -hydroxy ketone moiety which can function as powerful reducing species under an alkaline condition. There are at least 17 reported reducing species of different carbon number (as shown in Table 2). Aldehyde and α -hydroxy ketone can be efficient reducing specie under the employed alkaline condition (Scheme 3A). As a result, platinum ions could be reduced to Pt NPs as indicated by Scheme 3B.



Scheme 2 The reaction pathways of monosaccharide under alkaline degradation. Classification of the degraded products based on carbon number was simplified (adapted from references [15],[16],[28],[33]–[35]). Some of the degradation intermediates contain functional groups with reduction potential (i.e., aldehyde and α -hydroxy ketone moieties).



Scheme 3 (A) Example of reducing species (C₆) from starch degraded intermediates and (B) reduction of platinum ions into Pt NPs.

Table 2 The possible degradation products of starch in alkaline solution those act as reducing species. ^{[15][16][28],[33],[35]}

Numbers of Carbon	Structure	Product name
6	$ \begin{array}{c} \text{HC=O} \\ \\ \text{C=O} \\ \\ \text{CH}_2 \\ \\ \text{HC-OH} \\ \\ \text{HC-OH} \\ \\ \text{CH}_2\text{OH} \end{array} $	4,5,6-trihydroxy-2-oxohexanal
6	$ \begin{array}{c} \text{CH}_2\text{OH} \\ \\ \text{C=O} \\ \\ \text{C=O} \\ \\ \text{CH}_2 \\ \\ \text{HC-OH} \\ \\ \text{CH}_2\text{OH} \end{array} $	1,5,6-trihydroxyhexane-2,3-dione
6	$ \begin{array}{c} \text{CH}_3 \\ \\ \text{C=O} \\ \\ \text{C=O} \\ \\ \text{HC-OH} \\ \\ \text{HC-OH} \\ \\ \text{CH}_2\text{OH} \end{array} $	4,5,6-trihydroxyhexane-2,3-dione
5	$ \begin{array}{c} \text{HC=O} \\ \\ \text{C=O} \\ \\ \text{CH}_2 \\ \\ \text{HC-OH} \\ \\ \text{CH}_2\text{OH} \end{array} $	4,5-dihydroxy-2-oxopentanal
5	$ \begin{array}{c} \text{CH}_3 \\ \\ \text{C=O} \\ \\ \text{C=O} \\ \\ \text{HC-OH} \\ \\ \text{CH}_2\text{OH} \end{array} $	4,5-dihydroxypentane-2,3-dione
5	$ \begin{array}{c} \text{CH}_2\text{OH} \\ \\ \text{C=O} \\ \\ \text{C=O} \\ \\ \text{CH}_2 \\ \\ \text{CH}_2\text{OH} \end{array} $	1,5-dihydroxypentane-2,3-dione
5	$ \begin{array}{c} \text{HC=O} \\ \\ \text{CH}_2 \\ \\ \text{HC-OH} \\ \\ \text{HC-OH} \\ \\ \text{CH}_2\text{OH} \end{array} $	3,4,5-trihydroxypentanal

Table 2 (continue) The possible degradation products of starch in alkaline solution those act as reducing species. ^{[15][16][28],[33],[35]}

Numbers of Carbon	Structure	Product name
4	$\begin{array}{c} \text{HC=O} \\ \\ \text{C=O} \\ \\ \text{CH}_2 \\ \\ \text{CH}_2\text{OH} \end{array}$	4-hydroxy-2-oxobutanal
4	$\begin{array}{c} \text{CH}_3 \\ \\ \text{C=O} \\ \\ \text{C=O} \\ \\ \text{CH}_2\text{OH} \end{array}$	1-hydroxybutane-2,3-dione
4	$\begin{array}{c} \text{HC=O} \\ \\ \text{CH}_2 \\ \\ \text{HC-OH} \\ \\ \text{CH}_2\text{OH} \end{array}$	3,4-dihydroxybutanal
4	$\begin{array}{c} \text{HC=O} \\ \\ \text{HC-OH} \\ \\ \text{HC-OH} \\ \\ \text{CH}_2\text{OH} \end{array}$	2,3,4-trihydroxybutanal
3	$\begin{array}{c} \text{HC=O} \\ \\ \text{HC-OH} \\ \\ \text{CH}_2\text{OH} \end{array}$	2,3-dihydroxypropanal
3	$\begin{array}{c} \text{HC=O} \\ \\ \text{CH}_2 \\ \\ \text{CH}_2\text{OH} \end{array}$	3-hydroxypropanal
3	$\begin{array}{c} \text{HC=O} \\ \\ \text{C=O} \\ \\ \text{CH}_3 \end{array}$	2-oxopropanal
2	$\begin{array}{c} \text{HC=O} \\ \\ \text{CH}_2\text{OH} \end{array}$	2-hydroxyacetaldehyde
2	$\begin{array}{c} \text{HC=O} \\ \\ \text{CH}_3 \end{array}$	Acetaldehyde
1	$\text{H}_2\text{C=O}$	formaldehyde

3.4 Investigation of stabilization power of starch

According to the observed phenomena in Figure 1, an onset of efficient reduction was observed at an alkaline concentration greater than 0.01 M. It is imperative to gain an in-depth understanding of the influences of alkalinity on the formation of reducing species and Pt NPs with NaOH concentration in the range of 0.01–0.1 M. The obtained Pt NPs were investigated by TEM and the results are shown in Figure 5. Spherical Pt NPs with an average size of 2–4 nm were generated under all examined conditions. The particle size does not significantly change with increased NaOH concentration (Figure 5A–5E). However, when NaOH solution with a concentration greater than 0.05 M was used, large aggregations of primary particles were observed. Those aggregated particles with a domain size of 20–80 nm could be disaggregated into primary particles by ultrasonic treatment (Figure 5D2 and 5E2). The observed phenomena suggest that small Pt NPs were formed and stabilized at the early stage of the reduction process. Those primary particles do not grow bigger due to starch stabilization. The complete reduction of Pt ions to Pt NPs occurs before the aggregation. The aggregation of Pt NPs at a higher alkaline concentration (Figure 5C2–5E2) results in precipitation within a few minutes. The prolonged reaction breaks down glycosidic linkages and diminishes the stabilization potential of starch at stronger alkaline conditions. The breakdown of glycosidic linkages shortens the starch chain and triggers precipitation.

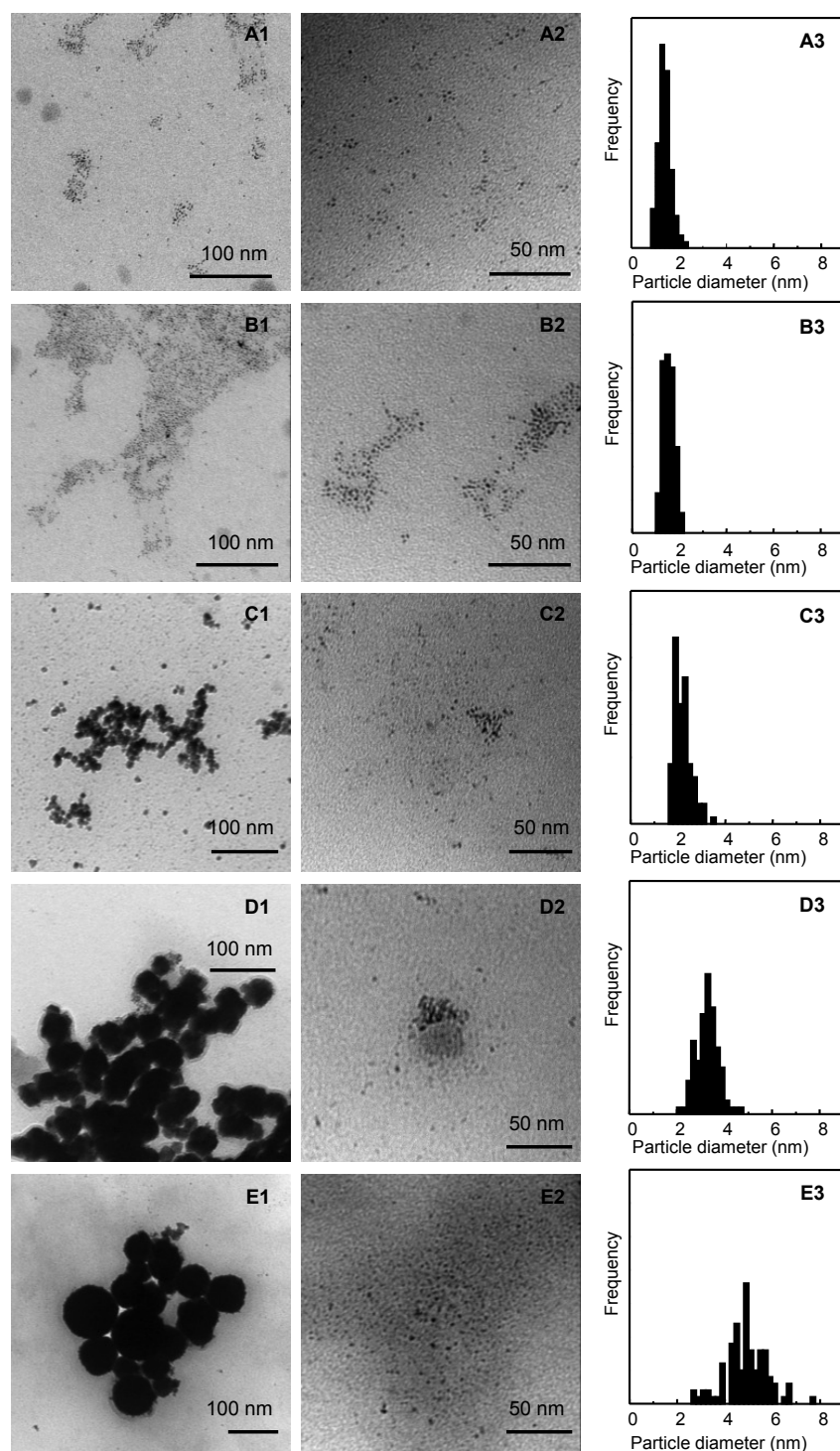


Figure 5 TEM images and their particle size distribution of synthesized Pt NPs at various concentrations of NaOH solution (A) 0.01, (B) 0.025, (C) 0.05, (D) 0.075 and (E) 0.1 M. The particle size distribution was measured from the non-aggregate particles.

Based on the observed phenomena, the reducing and stabilizing potential of starch was investigated by the ATR FT-IR spectroscopy. Figure 6 shows overall changes associated with starch degradation under 0.01–0.1 M NaOH treatment. Increase of the carbonyl absorption at 1770–1550 cm^{-1} indicates the extensive decomposition of glucose unit which imply the increasing of reducing species. A rapid reduction was observed at high alkaline concentration. At the same time, a decrease in the absorption of glycosidic linkage (bridge β C¹-O-C⁴ stretching) in the region 1200–900 cm^{-1} indicates the progressive break down of the starch skeleton. As a result, stabilization via steric hindrance was drastically decreased after the glycosidic linkage breakdown. The observed phenomena are in good agreement with previously reported works that the extensive number of hydroxyl groups present in soluble starch can facilitate the complexation of metal ion to molecular matrix.^{[3][12]} Platinum ions were reduced on the starch chain and were stabilized. Steric hindrance imposed by starch molecules prevents Pt NPs aggregation and result in a small size (2–4 nm) and narrow size distribution. However, when starch chain was later damaged, the shorter chain cannot provide an adequate stabilization of Pt NPs. Particles aggregate without further fusion or particles grow as platinum ions were completely consumed.

3.5 Efficiency of the *in situ* reducing species

In order to investigate the reducing efficiency of the *in situ* generated species, a time dependent UV/vis experiment was conducted and the results are shown in Figure 7. Since, the quantitative analysis of generated Pt NPs is commonly monitored

through the baseline shift at 500 nm, a plot of time dependent baseline shift is shown in Figure 8.^[36] The reduction profile show sigmoidal shape. An increasing absorbance in the first period corresponded to the seed nucleation, followed by a rapid particle growth (as suggested by LaMer^[37] in colloidal growth mechanism). In our case, due to the high efficiency of the *in situ* generated species, the nucleation is very fast and the reaction was completed within 5 min. As a result, very small particles with narrow size distribution (2–4 nm) were obtained.

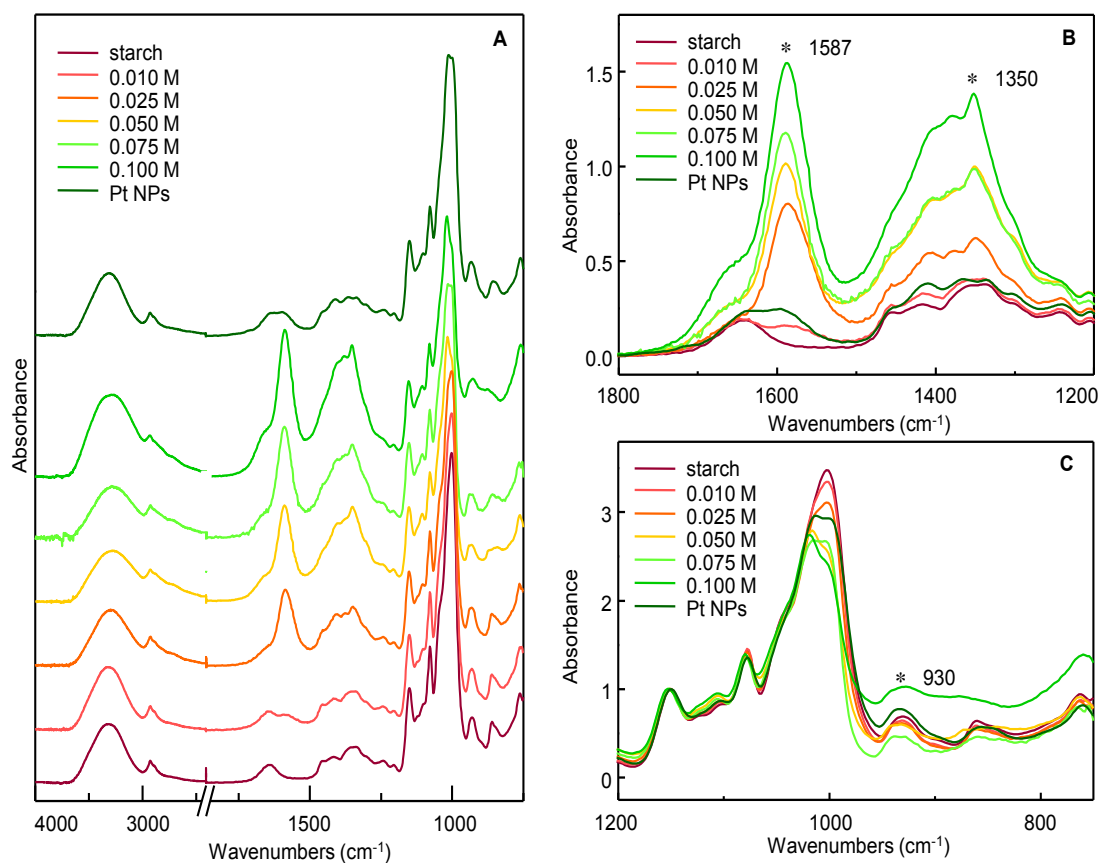


Figure 6 Normalized ATR FT-IR (A) stack spectra, (B) overlay spectra in the region of 1800–1200 cm^{-1} , and (C) overlay spectra in the region of 1200–750 cm^{-1} of soluble starch after a 20 min incubation with 0.01–0.1 M NaOH.

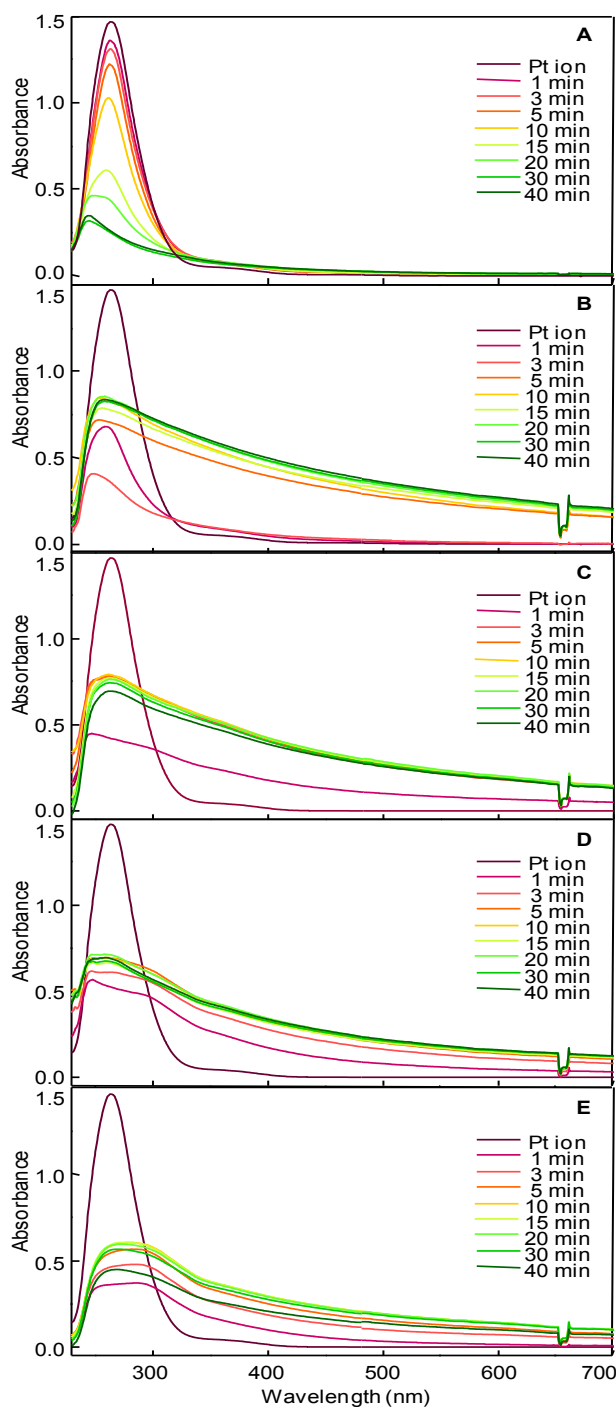


Figure 7 Time-resolved UV/vis spectra of synthesized platinum nanoparticles with (A) 0.01 M NaOH, (B) 0.025 M NaOH, (C) 0.50 M NaOH, (D) 0.075 NaOH and (E) 0.10 NaOH.

The synthesized Pt NPs using appropriate (0.025 M) NaOH concentration can be stabilized in the solution for 3 months without any sign of aggregation. The complete reduction was confirmed by a NaBH₄ test, results are shown in Figure 9. A complete reduction of platinum ions is signified by an insignificant spectral change after an addition of NaBH₄.

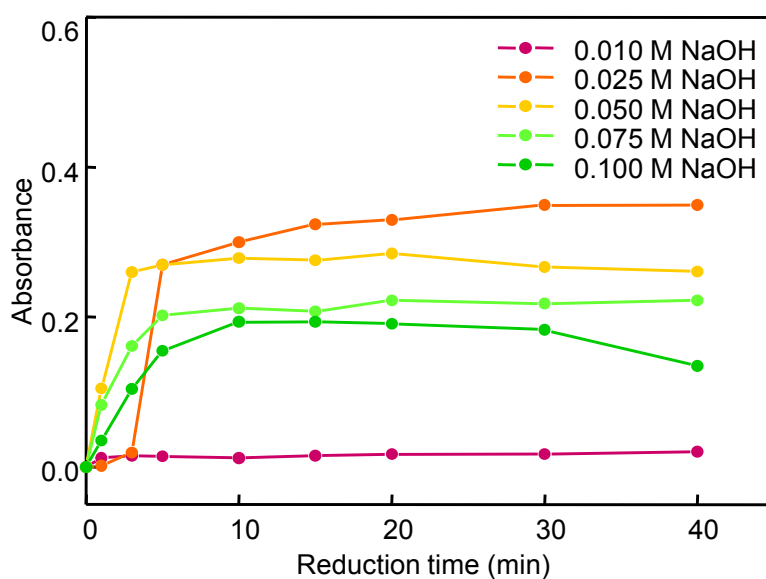


Figure 8 Time-dependent baseline shift at 500 nm of colloidal platinum nanoparticles after treatment under various alkaline conditions.

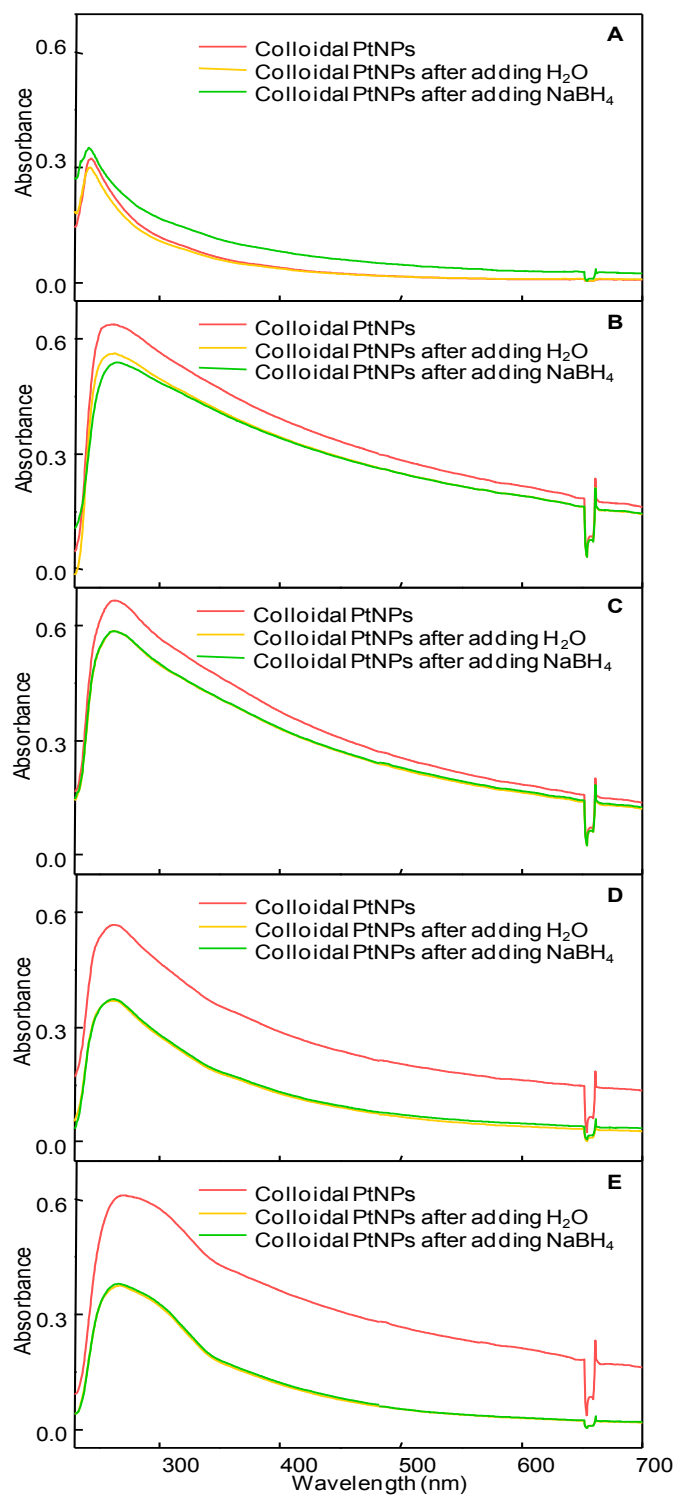


Figure 9 UV/vis spectra of colloidal Pt NPs at (A) 0.01 M NaOH, (B) 0.025 M NaOH, (C) 0.05 M NaOH, (D) 0.075 M NaOH and (E) 0.10 M NaOH before and after checking the completely of the reduction with NaBH_4 .

4. Conclusion

I have successfully synthesized Pt NPs via a “Green” synthesis approach using starch as the reducing and stabilizing agent. Uniform spherical Pt NPs (2–4 nm) were obtained. The reduction efficiency of the soluble starch was enhanced by an alkaline treatment. The active reducing species were expected to be the degraded intermediates containing aldehyde and α -hydroxy ketone moiety. The system is rapid and very efficient as all platinum ions (20 mM) were completely reduced to Pt NPs within 5 min. The obtained Pt NPs are expected to have a good catalytic activity. The ongoing glycerol oxidation by this green Pt NPs is being investigated

5. References

- [1] J. A. Dahl, B. L. S. Maddux and J. E. Hutchison, *Chem. Rev.*, 2009, **107**, 2228.
- [2] N. N. Mallikarjuna and S. V. Rajender, *Green Chem.*, 2006, **8**, 516.
- [3] P. Raveendran and J. Fu, S. L. Wallen, *J. Am. Chem. Soc.*, 2003, **125**, 13940.
- [4] H. Huang and X. Yang, *Carbohydr. Res.*, 2004, **339**, 2627.
- [5] M. Adlim, M. A. Baker, K. Y. Liew and J. Ismail, *J. Mol. Catal. A: Chem.*, 2004, **212**, 141.
- [6] W. Yang, Y. Ma, J. Tang and X. Yang, *Colloids Surf., A*, 2007, **302**, 628.
- [7] W. Yang, C. Yang, M. Sun, F. Yang, Y. Ma, Z. Zhang and X. Yang, *Talanta*, 2009, **78**, 557.
- [8] Y. Shin, I.-T. Bae and G. J. Exarhos, *Colloids Surf., A*, 2009, **348**, 191.
- [9] F. Li, F. Li, J. Song, J. Song, D. Han and L. Niu, *Electrochem. Commun.*, 2009, **11**, 351.
- [10] M. Singh, I. Sinha and R. K. Mandal, *Mater. Lett.*, 2009, **63**, 425.
- [11] Z. Shervani and Y. Yamamoto, *Carbohydr. Res.*, 2011, **346**, 651.
- [12] N. Vigneshwaran, R. P. Nachane, R. H. Balasubramanya and P. V. Varadarajan, *Carbohydr. Res.*, 2006, **341**, 2012.
- [13] A. A. Hebeish, M. H. El-Rafie, F. A. Abdel-Mohdy, E. S. Abdel-Halim and H. E. Eman, *Carbohydr. Polym.*, 2010, **82**, 933.
- [14] E. S. Abdel-Halim and S. S. Al-Deyab, *Carbohydr. Polym.*, 2011, **86**, 1615.
- [15] C. J. Knill and J. F. Kennedy, *Carbohydr. Polym.*, 2003, **51**, 281.
- [16] M. A. Clarke, L. A. Edye and G. Eggleston, *Advances in Carbohydrate Chemistry and Biochemistry*; Academic Press, **1997**; Vol. 52, 449.

- [17] X. Feng, Q. Kong, X. Chen and J. Hu, *Mater. Lett.*, 2009, **63**, 2171.
- [18] Z. Shen, M. Yamada and M. Miyake, *Chem. Commun.*, 2007, **47**, 245.
- [19] Z. Liu, Z. Q. Tian and S. P. Jiang, *Electrochim. Acta.*, 2006, **52**, 1213.
- [20] J. M. Petroski, Z. L. Wang, T. C. Green and M. A. El-Sayed, *J. Phys. Chem. B.*, 1998, **102**, 3316.
- [21] Z. Tang, D. Geng and G. Lu, *Mater. Lett.*, 2005, **59**, 1567.
- [22] C.-W. Chen, T. Takezako, K. Yamamoto, T. Serizawa and M. Akashi, *Colloids Surf., A.*, 2000, **169**, 107.
- [23] E. P. Lee, Z. Peng, D. M. Cate, H. Yang, C. T. Campbell and Y. Xia, *J. Am. Chem. Soc.*, 2007, **129**, 10634.
- [24] S. Ekgasit, N. Pattayakorn, D. Tongsakul, C. Thammacharoen and T. Kongyou, *Anal. Sci.*, 2007, **23**, 863.
- [25] W. A. Spieker, J. Liu, J. T. Miller, A. J. Kropf and J. R. Regalbuto, *Appl. Catal., A*, 2002, **232**, 219.
- [26] B. Shelimov, J.-F. Lambert, M. Che and B. Didillon, *J. Catal.*, 1999, **185**, 462.
- [27] Y.-T. Yu, J. Wang, J.-H. Zhang, H.-J. Yang, B.-Q. Xu and J.-C. Sun, *J. Phys. Chem. C*, 2007, **111**, 18563.
- [28] E. Sjöström, *Biomass Bioenergy*, 1991, **1**, 61.
- [29] L. G. Thygesen, M. M. Lokke, E. Micklander and S. B. Engelsen, *Trends Food Sci. Technol.*, **2003**, 14, 50.
- [30] R. Kizil, J. Irudauraj and K. Seetharaman, *J. Agric. Food Chem.*, 2002, **50**, 3912.

- [31] M. Sekkal, V. Dincq, P. Legrand and J. P. Huvenne, *J. Mol. Struct.*, 1995, **349**, 349.
- [32] J. Coated, *Encyclopedia of Analytical Chemistry*; John Wiley & Sons: Chichester, USA, **2000**, 10815.
- [33] M. I. Sinnott, *Carbohydrate Chemistry and Biochemistry*; The Royal Society of Chemistry, **2007**, 492.
- [34] M. Reintjes and G. K. Coope, *Ind. Eng. Chem. Prod. Res. Dev.*, 1984, **23**, 70.
- [35] M. A. Glaus, L. R. Van Loon, S. Achatz, A. Chodura and K. Fischer, *Anal. Chim. Acta*, 1999, **398**, 111.
- [36] C.-W. Chen and M. Akashi, *Langmuir*, 1997, 13, 6465.
- [37] C.-H. Yu, K. Tam and E. S. C. Tsang, *Handbook of Metal Physics*; Elsevier, **2009**, 113.

CURRICULUM VITAE

Miss Duangta Tongsakul was born on May 2, 1983 in Kanchanaburi, Thailand. She graduated with Bachelor of Engineering Degree in Petrochemistry and Polymeric Materials from Faculty of Engineering and Industrial Technology, Silpakorn University in 2004 and Master of Science Degree in Program in Petrochemistry and Polymer Science, Faculty of Science, Chulalongkorn University in 2006. She continued studying Doctor of Philosophy in Program in Petrochemistry at Faculty of Science, Chulalongkorn University in 2007, and joined the Dual Ph.D Program between Chulalongkorn University and Japan Advanced Institute of Science and Technology (JAIST), Japan in 2010 and completed dual-degree in September 2014. She was awarded the “Young Chemist awards” supported by IUPAC, RSC and Bangkok Bank from the 14th Asian Chemical Congress 2011 (14 ACC). Presently, she joins in the Public Service Executive Development Program, Office of the Public Sector Development Commission, THAILAND.